RPG-XCH-DP Instrument Manual

X Frequency, Dual Polarized Radiometers
(1.4 / 6.925 / 10.65 / 18.70 (21.00) / 36.50 (90.0) GHz h/v)
(45.0 / 90.0 GHz L/R circular polarized)

Version 8.01 (6.7.2015)

Version A (heavy duty, 4 modules max.)

Version B (light weight, 2 modules max.)

(www.radiometer-physics.com)

Document Change Log

Date	Issue/Rev	Change
07.07.2011	00/01	Work
20.07.2011	01/01	Release
20.12.2011	01/02	description of new 2 line fibre connector system added (2.7.4)
23.03.2015	01/03	TCP-IP communication with radiometer added

Table of Contents

1. Unpacking and Radiometer Assembly

1.1 Radiometer Modules and Positioner

The instrument is delivered in a single box with the frequency modules packed in flight cases. If an L-Band (1.4 GHz), S-Band (6.925 GHz) or X-Band (10.65 GHz) module is part of the delivery, a parabola reflector (S-Band or X-Band) with a diameter of 85 cm and / or a patch antenna array (L-Band) is included, which is disassembled from the positioner for transportation. These antennas have to be mounted to a special frame structure integrated into the module base frame.

Fig.1.1a: Two radiometer system versions: Left: Version A for heavy duty applications holding a maximum of 4 modules. Right: Version B with light weight positioner (portable) for a maximum of 2 frequency modules.

RPG's polarized radiometer models can be subdivided into two types shown in Fig.1.1a: Version A comprising a heavy duty positioner that can handle up to four frequency modules, and a light weight positioner version B for up to two frequency modules. The stand and Elevation / Azimuth drive of version B are dismountable (described in the next section), so that the system can be hand carried by two people. This makes it very easy to install version B at locations which are difficult to access by cranes or fork lifters.

Fig.1.1b: Parabola antenna mount structure used for 6.925 / 10.7 GHz combination modules.

1.1.1 Disassembly of Version B Radiometer Type

Fig.1.1.1a: Turn off the radiometer power first (if radiometer is turned on).

Fig.1.1.1b: Unplug the frequency modules' data and power cables.

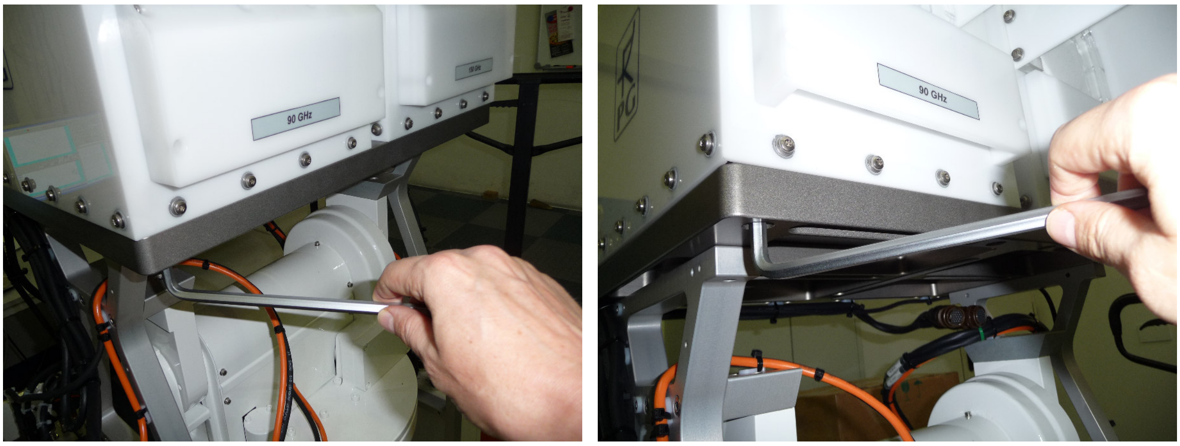

Fig.1.1.1c: Unscrew the frequency modules from the top mounting frame.

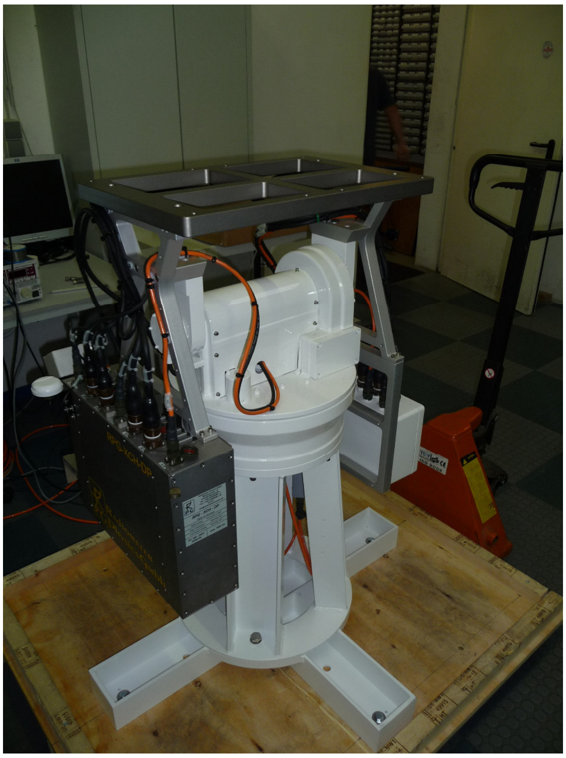

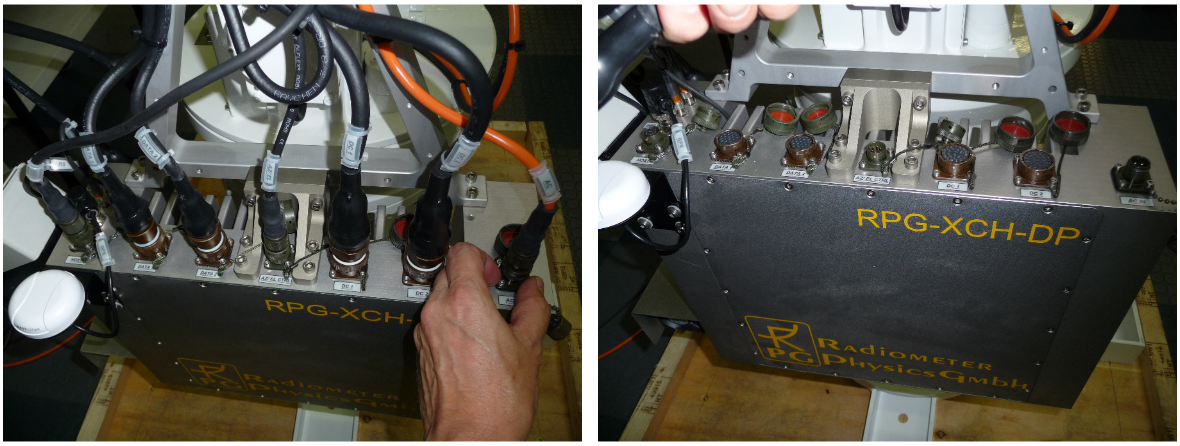

Fig.1.1.1d: On the right side, unplug the following connectors from the main control unit: HOST, DATA1, DATA2, AZ / EL CTRL, DC1, DC2, AC.

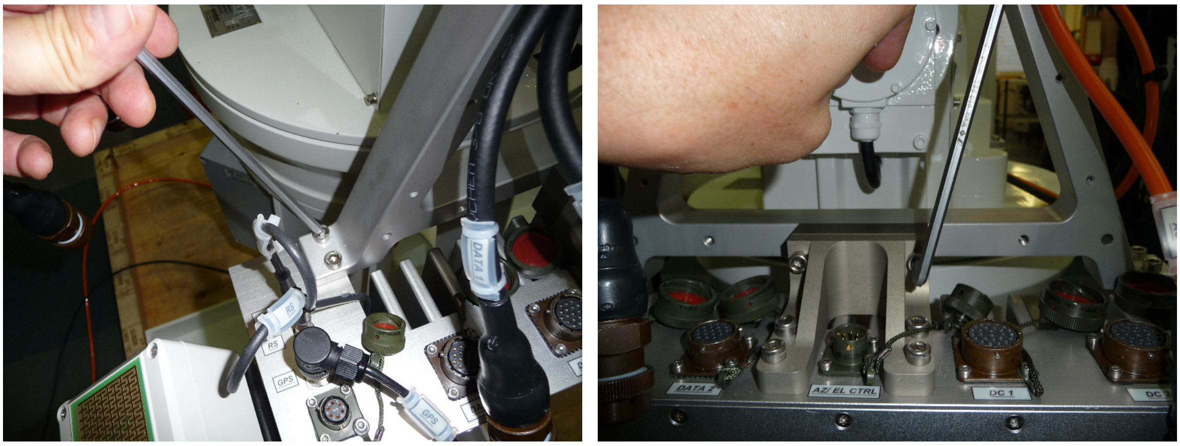

Fig.1.1.1e: Unscrew the main control unit from the holding frame.

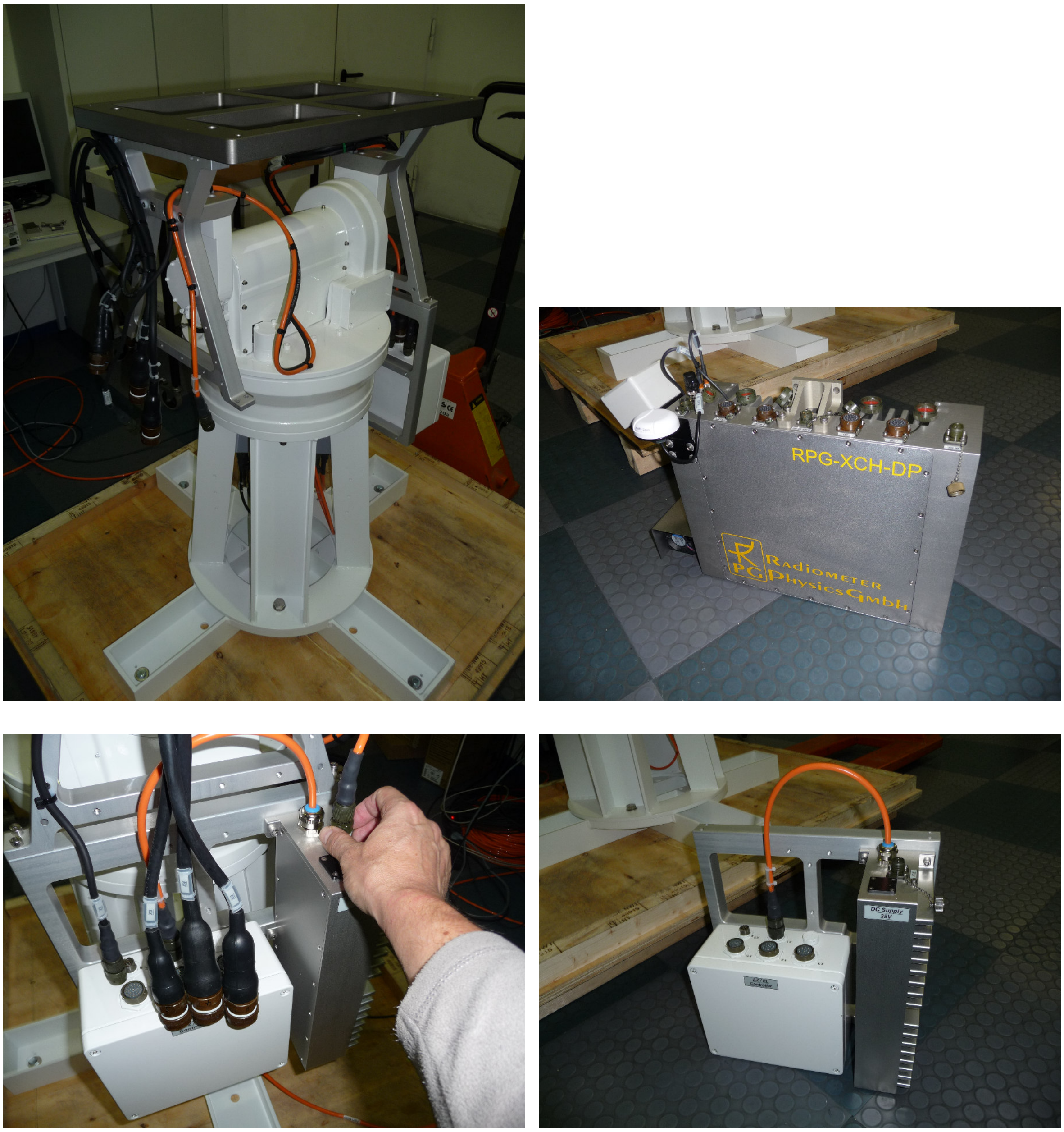

Fig.1.1.1f: On the left side, unplug the following connectors from the El / Az controller unit: X2, X3, X4, X5, AC IN. Then unscrew the unit.

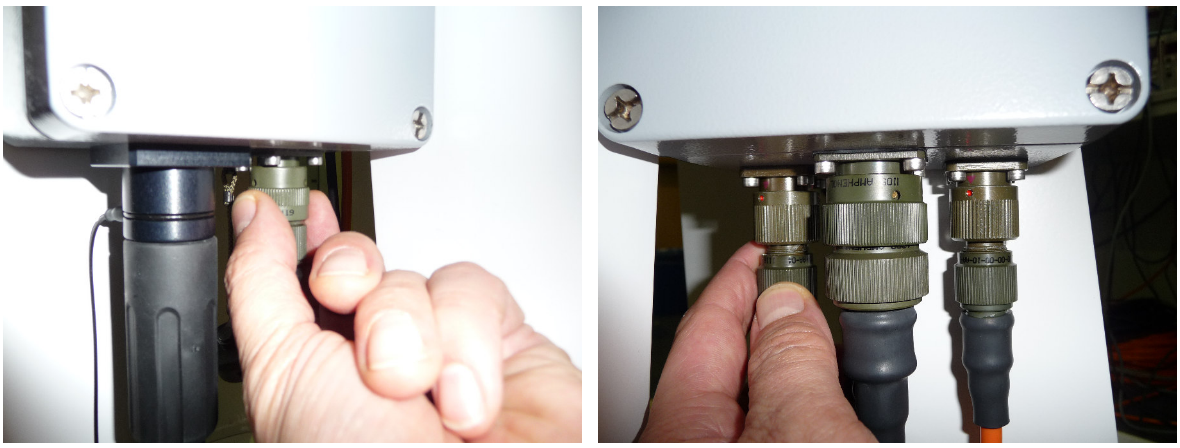

Fig.1.1.1g: Unplug the data and two power cables from the converter and power distribution boxes.

Fig.1.1.1h: Unscrew the azimuth drive from the positioner`s stand.

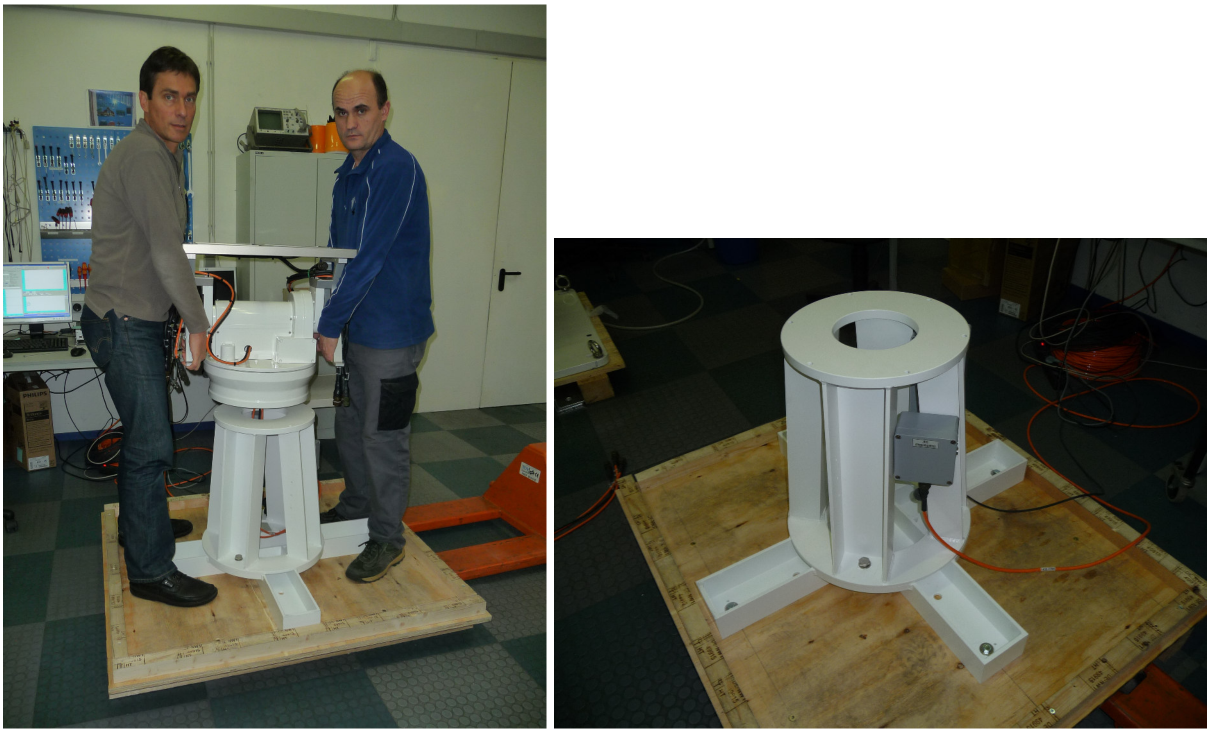

Fig.1.1.1i: Take off the El / Az driver from the stand.

The remaining parts can be hand carried to any site location and assembled in the reverse order as described above.

1.2 Electrical Connections

Each frequency module has two electrical connecting cables. The first is directed towards one of the two power supplies (Fig.1.5) while the second is connected to the data acquisition unit. All frequency modules provide identical power and data interfaces. Therefore, their

power cables can be plugged into any of the four available sockets on the rear side of the two power supplies. Also the data cable socket (located on the rear side of the data acquisition unit), used for the connection of the module's data cable, can be arbitrarily selected from one of the four available sockets (see Fig.1.2, Fig.1.3). This is possible because each module is sending an ID-code to the radiometer software during the boot-up sequence, so that the software 'knows', which frequency module is connected to each socket.
Due to different pin numbers on power and data sockets, an erroneous interchanging of power and data cables is not possible.

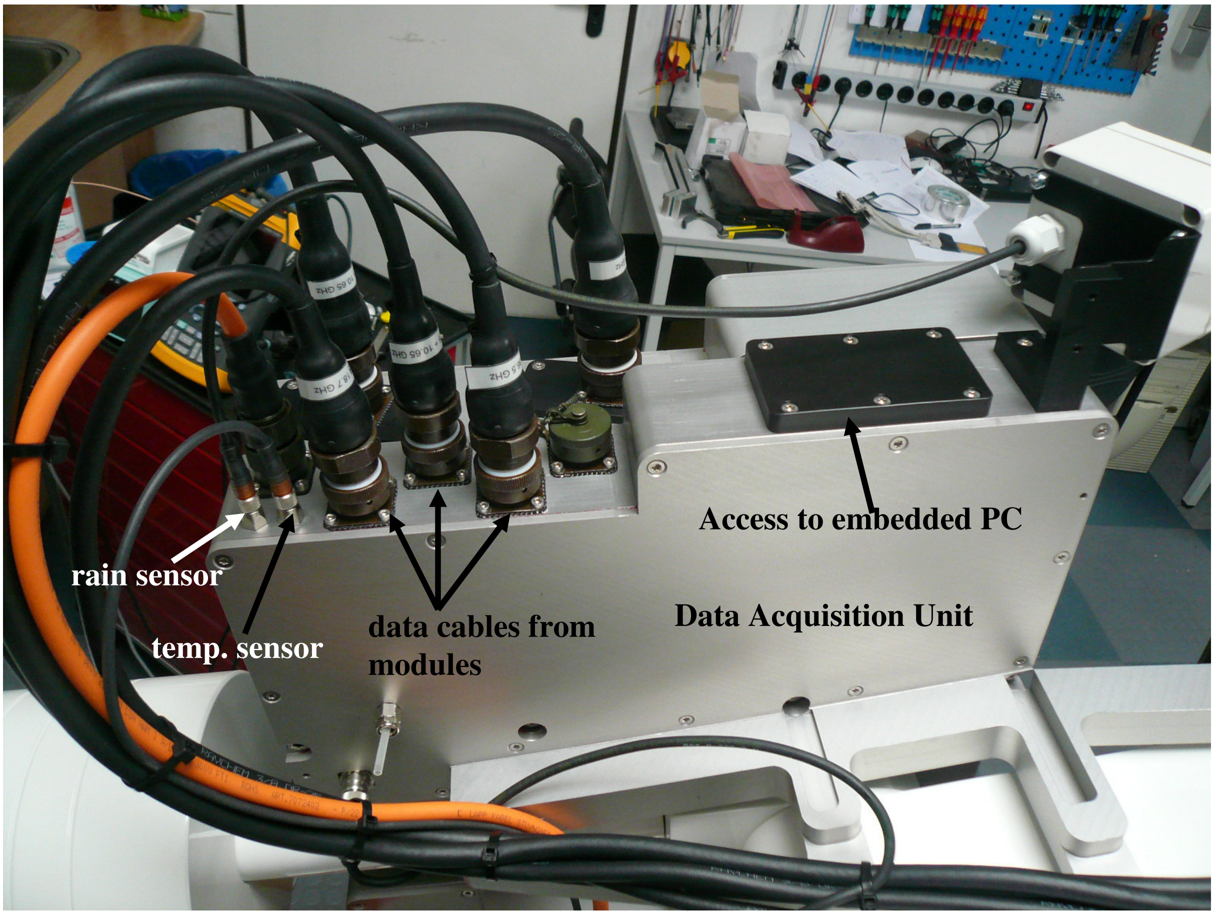

Fig.1.2: View from data acquisition side (Version A).

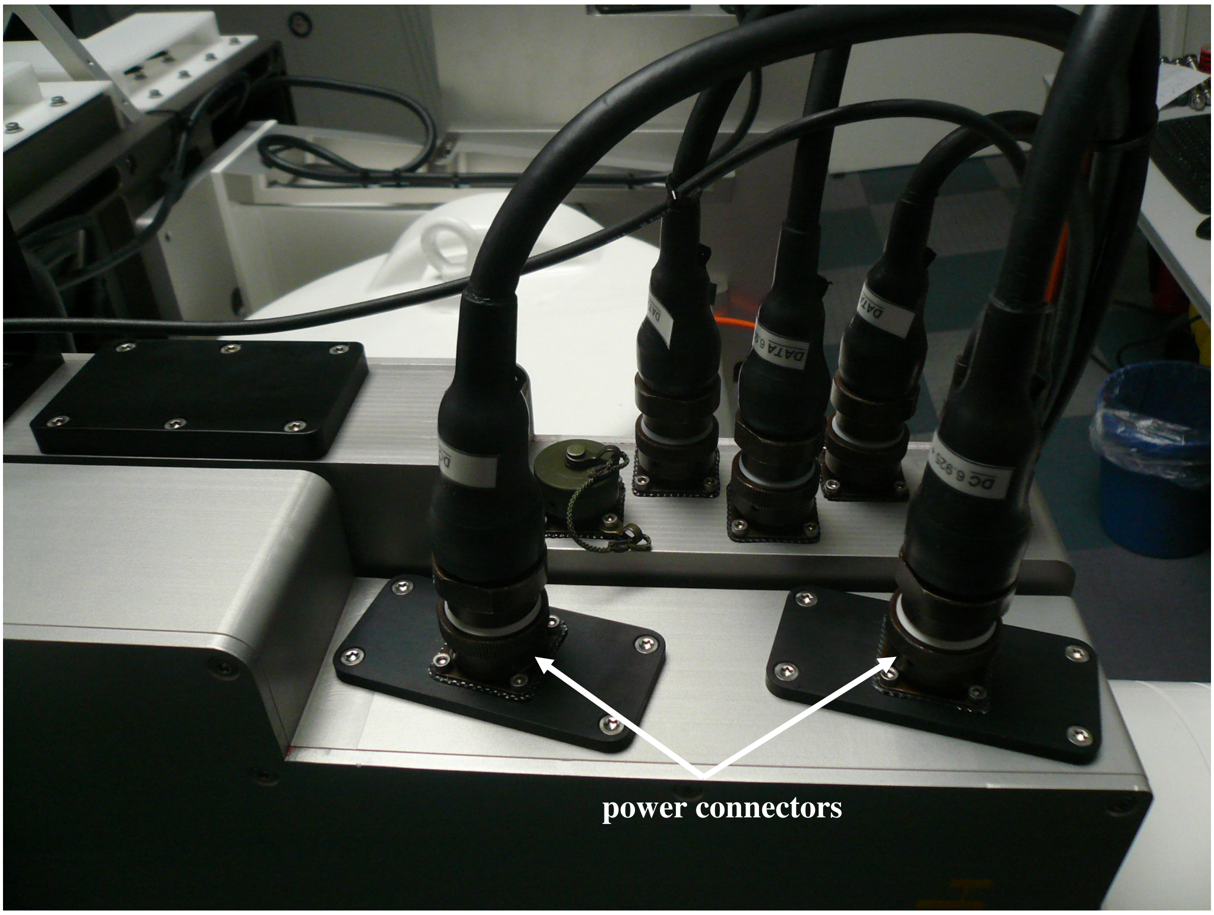

Fig.1.3: View from power supply side.

Fig.1.4: Example of rear side of assembled instrument (version A).

1.2.1 Fibre Data Cable Connections

All radiometers shipped in 2011 or later are equipped with 2 line fibre optics data cables.

Fig.1.2.1a: 2 line fibre optics connector socket.

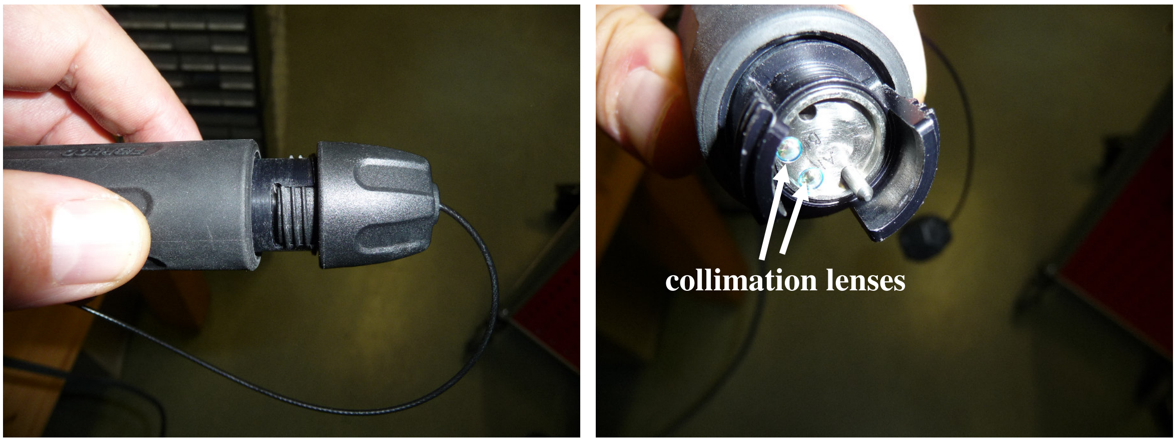

Fig.1.2.1b:2 line fibre optics connector plug.

Fig.1.2.1c: Plug in 2 line fibre optics connector.

The new system comprises collimation lenses on both fibre ends which prevent de-focussing and connection loss under cold environmental conditions. The connector can be used for temperatures down to -60°C.

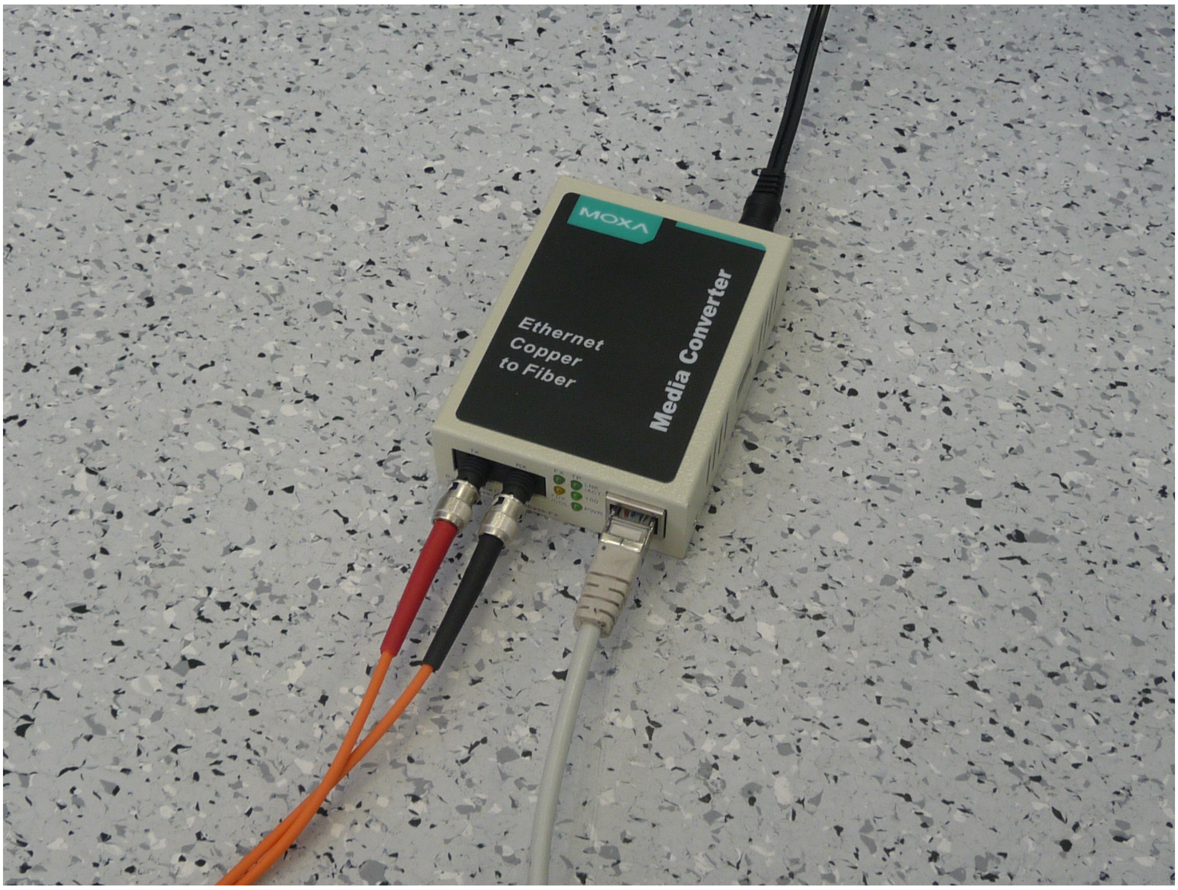

Fig.1.2.1d: 2 line fibre optics to Ethernet converter.

The other end of the 2 line fibre cable is connected to a MOXA Fibre-to-Ethernet converter as indicated in Fig.2.7.8d. The converter's power cable has a USB plug. Please plug this into one of the Host PC's USB sockets. Make sure the TX fibre line (red) gets connected to the TX converter output and the RX fibre line (black) to the RX converter input.

1.3 Powering up the Radiometer

After all mechanical and electrical connections have been established, the radiometer can be turned on. The embedded PC takes about two minutes to boot and to start the radiometer software (Windows®7 Embedded OS). This software auto-detects all peripherals like surface sensors, positioner interface, GPS clock and rain detector. Wait at least 30 minutes for warm-up at operating temperatures >10°C and 45 minutes warm-up time at lower environmental temperatures. The stabilization process is indicated in the radiometer status box on the host software's main window.
During warming up, the system actively heats the receivers with a total power consumption of 500 Watts. Once the receivers are thermally stabilized, the power consumption drops down to less than 300 Watts.

2. Instrument Hardware

2.1 General Radiometer Configuration

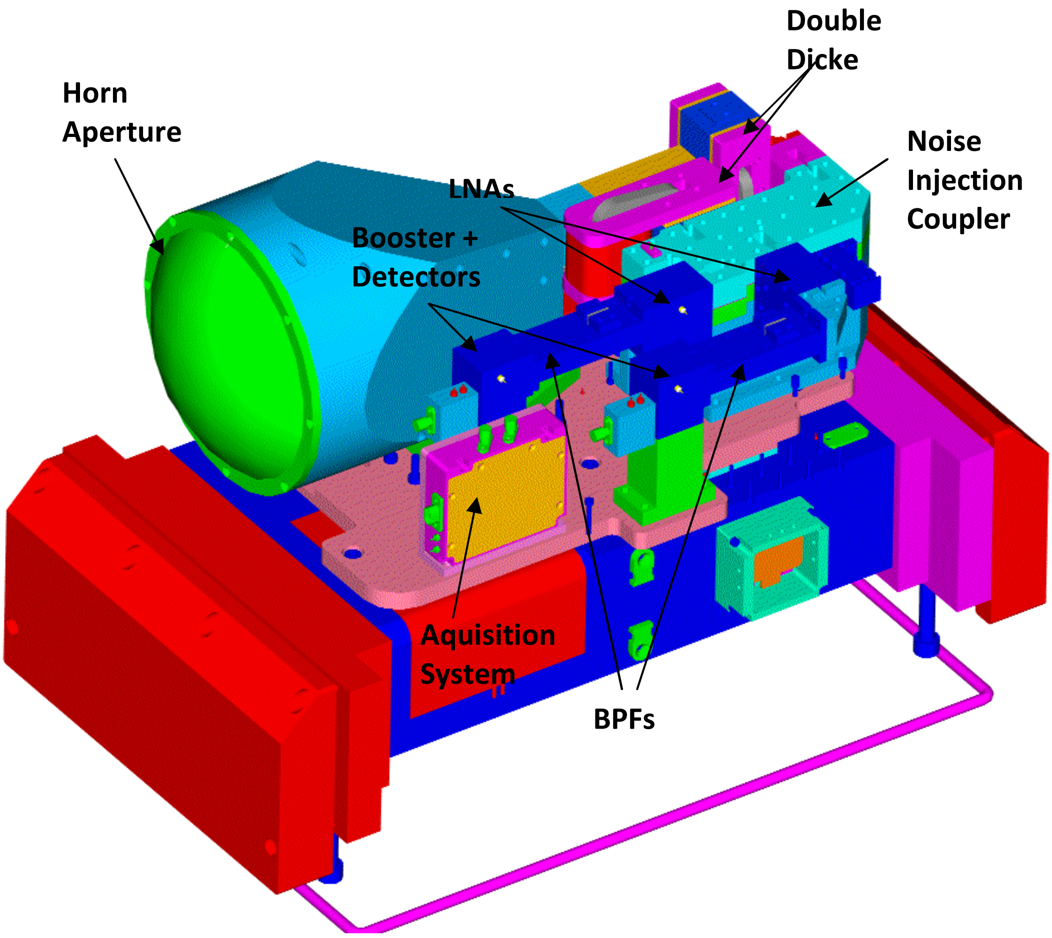

Fig.2.1 shows a drawing of one of the internal receivers, illustrated as an example for the 18.7 GHz radiometer. The following functional blocks can be identified:

- Receiver optics comprising corrugated feed horn with aperture lens (encapsulated in thermal insulation)
- OMT (Ortho Mode Transducer) for splitting the signal into vertical and horizontal polarization channels.
- Calibration system comprising a double Dicke switch (system noise temperature calibration) and noise injection section (gain calibration).
- Signal processing components like isolators, LNAs, BPFs (band pass filters) and detectors.
- The instrument electronics sections
- Data aquisition system

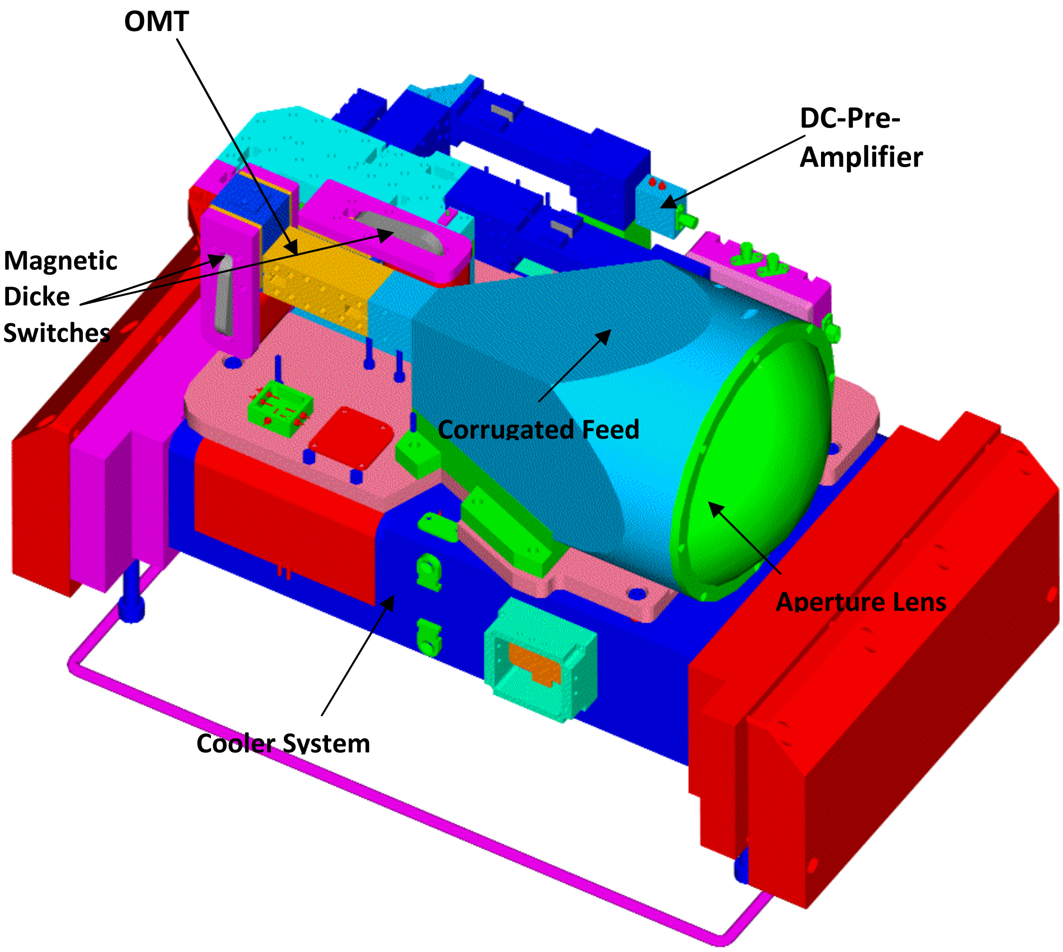

Fig. 2.1: Radiometer configuration (18.70 GHz radiometer).

The optical section is optimized for a beam of approximately 5.0° HPBW for all channels. At 6.925 GHz and 10.65 GHz the beam is formed by a combination of corrugated feed horn and off-axis parabola antenna while at 18.7 and 36.5 GHz a corrugated feed with aperture lens is sufficient to achieve the desired beam width. The corrugated feed horn offers a low cross polarization level and a rotationally symmetric beam pattern.

The receivers are integrated together with their feeds and lenses and are thermally insulated to achieve a high thermal stability.

2.3 Receivers

The RPG-XCH-DP (X stands for 4, 6, 8 or 10) receiver concept is motivated by the following design goals:

- The design of the receiver section focuses on maximum thermal and electrical stability, a compact layout with a minimum of connectors and thermally drifting components, an integrated RF design, low power consumption and weight.
- The receivers comprise a reliable calibration system with precision secondary standards and Dicke switches. The accuracy of calibration target temperature sensors and the minimization of thermal gradients are critical items to achieve an absolute brightness temperature accuracy of 1K.
- A high temporal resolution in the order of seconds is achieved. The minimum integration time for each channel is 1 second.

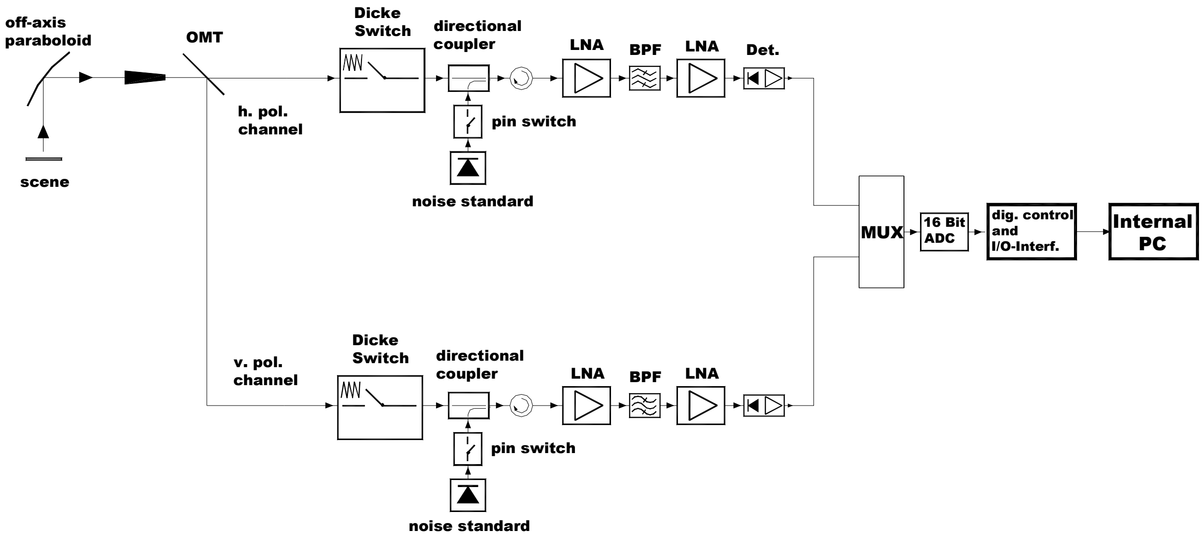

Fig.2.3: RPG-XCH-DP schematic receiver layout. All radiometers are direct detection systems without the need for local oscillators and mixers.

Fig.2.3 shows a schematic of the receiver system. At the receiver inputs a Dicke Switch periodically switches the receiver inputs to an internal black body with well know brightness temperature. It is used to continuously determine the system noise temperature of the radiometers. The Dicke Switch is followed by a directional coupler which allows for the injection of a precision noise signal generated by an on/off switching calibrated noise source.

This noise signal is used to determine system nonlinearities (four point method, described in section 'Calibration') and system gain drifts during measurements.
A 40 dB low noise amplifier (LNA) boosts the input signal before it is filtered and again boosted by another 20 dB amplifier. The waveguide bandpass filters' (BPF) bandwidths and centre frequencies are listed in table 2.1. In the host software, the different receiver modules are numbered 1-4:

f_c[GHz]	**1.40**	**6.925**	**10.65**	**18.70**	**21.00**	**36.50**	**45.00**	**90.0 (lin.p)**	**90.0 (circ.p**
b[MHz]	20	400	400	400	400	400	6000	2000	8000

Table 2.1: RPG-XCH-DP possible channel centre frequencies and corresponding bandwidths.

Each channel has its own detector diode. This allows for a parallel detection and integration of all channels. The detector outputs are amplified by an ultra low drift operational amplifier chain and multiplexed to a 16 bit AD converter for each of the four frequency modules.

The receivers are based on the direct detection technique without using mixers and local oscillators for signal down conversion. Instead the input signal is directly amplified, filtered and detected. The advantages over a heterodyne system are the following:

- No mixers and local oscillators required (cost reduction)
- Local oscillator drifts in amplitude and frequency avoided (stability improvement)
- Mixer sideband filtering not required (cost reduction)
- Reduced sensitivity to interfering external signals (mobile phones etc.) due to avoidance of frequency down conversion
-

A high integration level is achieved due to the use of state of the art low noise amplifier MMICs, which offer superior sensitivity performance compared to mixers.
The total power consumption of each receiver package is < 4 Watts. This includes biasing of RF- and DC- amplifiers, noise diodes, Dicke switch drives, ADCs and digital control circuits. The low consumption simplifies the thermal receiver stabilization with an accuracy of < 0.05 K over the whole operating temperature range (-40°C to +45°C).

3. Detailed Description of Receiver Components

3.1 Antenna Performance

To meet the optical requirements of minimum reflection losses and compactness, a corrugated feed horn is an optimal choice. It offers a wide bandwidth, low cross polarization level and a rotationally symmetric beam. Corrugated feed horns can be designed for a great variety of beam parameters. The horn should be as small as possible to reduce weight and costs.
In order to generate a beam with the desired divergence (6.0° HPBW) a focussing element is needed at 6.925 GHz and 10.65 GHz. An off axis parabola antenna has negligible losses.

The side-lobe levels produced by the feed horn/parabola system is below -30 dBc so that brightness temperature errors can be kept < 0.2 K in the case that the side-lobe crosses the sun.

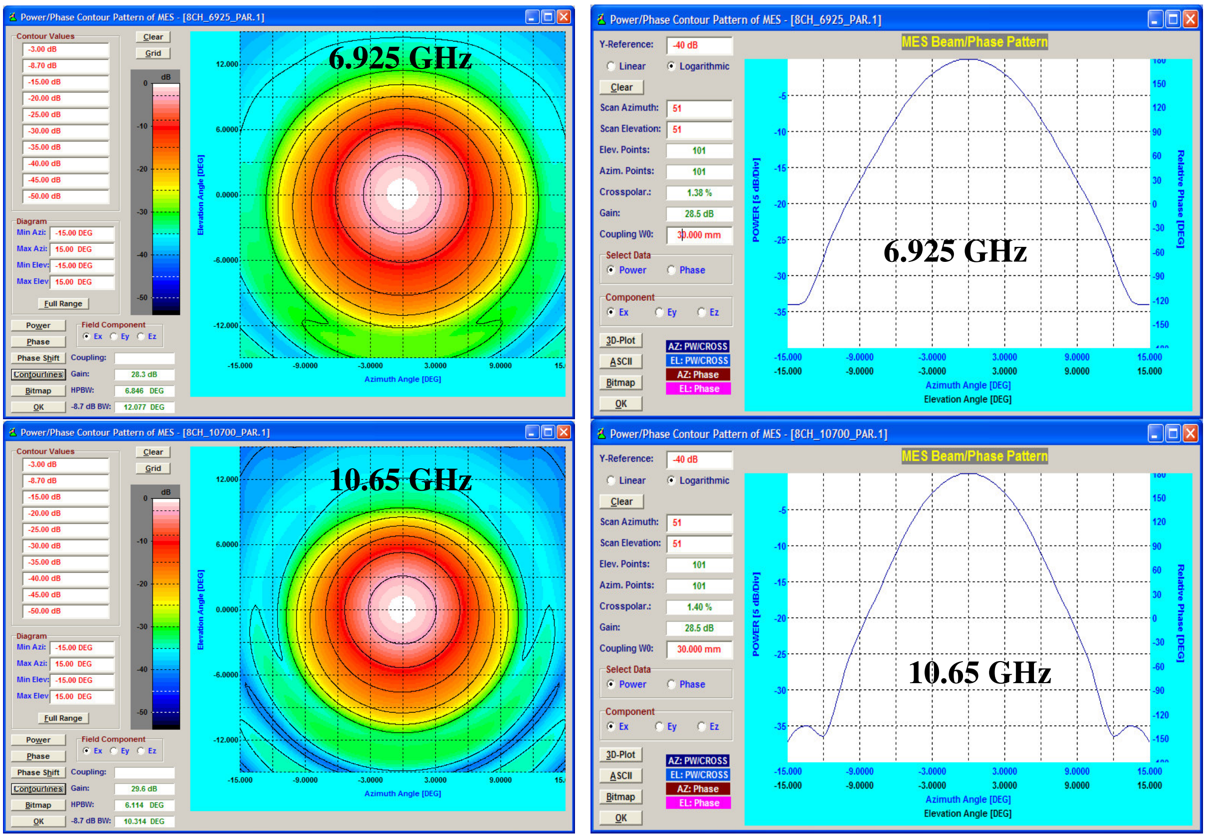

Fig.3.1: Left: 2d amplitude distributions of the parabola/corrugated feed @ 6.925 and 10.65 GHz and H-and E-plane cuts on the right. H/E plane cuts of the corrugated feed/lens system @ 18.70 and 36.5 GHz.

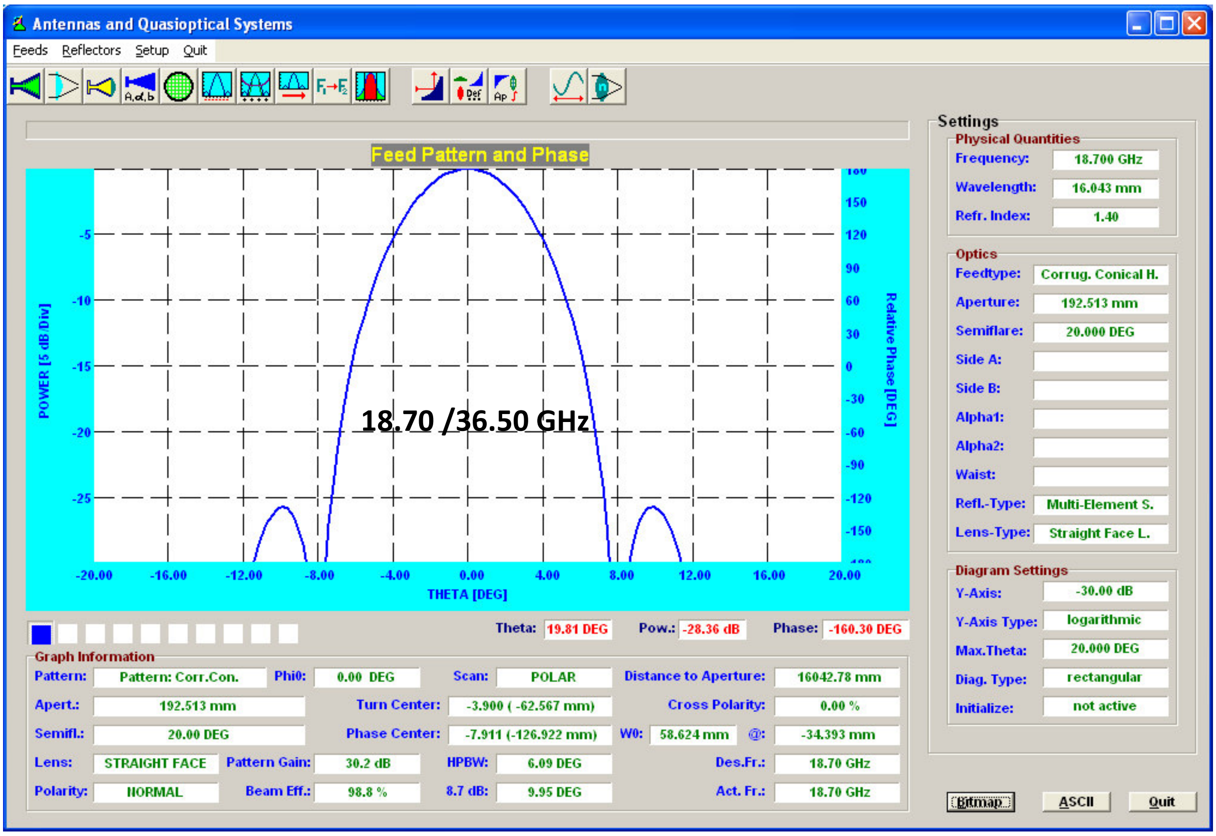

Frequency [GHz]	6.925	10.65	18.70	36.50
sidelobe level [dBc]	<-30	<-35	<-40	<-40
directivity [dB]	28.3	29.6	30.2	30.2
HPBW [°]	6.85	6.11	6.09	6.09
Aperture Diameter [mm]	450	330	192.0	86.0

Table 3.1: Optical antenna performance of corrugated feed / off-axis parabola systems.

3.2 Noise Diodes

The noise diode is one of the most critical receiver components because the system's brightness temperature critically depends on the calibration reliability. For this reason a careful circuit design and component selection is essential. The noise diode meets MIL-STD202, is hermetically sealed and has been burned in for 170 hours in order to achieve a precisely constant symmetrical white Gaussian noise level. The waveguide circuit layout including a -25 dB directional coupler guarantees the required mechanical stability needed to operate the calibration standard for several month without recalibration. The thermally stabilized diode is biased by a self adjusting current source. The directional coupler offers an isolation of >30 dB to the input signal path so that the noise injection does not significantly affect the antenna temperature. The equivalent noise temperature injected by the noise diode is in the range 150K-300K at the isolator input.

3.3 RF-Amplifiers

The advances in MMIC technology during recent years have led to low noise amplifiers up to 220 GHz. A key feature of this technology is the possibility of integrating the receiver into a compact planar structure without the need for bulky waveguide designs. In the frequency range between 7 and 40 GHz noise figures of 3.5 dB and bandwidth of 20 GHz are available. Each amplifier comprises a thermal compensation circuit to reduce gain drifts. The amplifier inputs are equipped with isolators to ensure a proper matching between successive stages. Assuming a 3.5 dB noise figure for the first amplifier and additional 1.0 dB for losses in the feed horn, isolator and directional coupler results in a system noise temperature of 450 K. With a scene temperature of 300 K the overall RMS noise, assuming a 400 MHz bandwidth and 1 second integration time) is 0.2 K in Dicke switch operation mode.

3.4 Bandpass Filters

The receiver channel bandwidths are determined by waveguide bandpass filters. The 3 pole Chebychev-type filters with 0.2 dB bandpass ripple and 1.0 dB typical transmission loss have a cutoff slope of 20 dB/200 MHz. The high Q design (2.0% rel. bandwidth) is realized by waveguide cavity resonators.

3.5 Detector, Video Amplifier, ADC

The zero bias highly doped GaAs Schottky detector diodes can handle frequencies up to 170 GHz with a virtually flat detection sensitivity from 7 GHz to 40 GHz. In addition, the detector diode offers superior thermal stability when compared to silicon zero bias Schottky diodes.
The rectified DC-signal enters an ultra stable OP-Amp circuit with internal analogue integrator. The utilized OP-Amps offer a thermal drift stability of 0.03 µV/°C which is roughly equivalent to a brightness temperature drift of 10 mK/°C assuming a broadband detector with a sensitivity of 1 mV/µW. The long term stability is 0.2 µV/month.
The 16 bit AD-converter is part of the video amplifier's circuit board to avoid noise from connecting cable pickup. It is optimized for low power dissipation (10 mW) and the high resolution makes a variable offset- and gain-control of the video amplifier superfluous.
The detector, video amplifier and ADC are integrated within a single hermetically shielded unit which is part of the receiver block (thermally stabilized to <0.03K).

3.6 Additional Sensors

Apart from the microwave receivers the RPG-XCH-DP radiometers are equipped with the following additional sensors:
Environmental Temperature Sensor: Accuracy: ±0.3°C, used to estimate T_{mr} (mean atmospheric temperature) needed for sky tipping calibration procedure.

Barometric Pressure Sensor: Accuracy: ±1 mbar, used to estimate T_{mr} (mean atmospheric temperature) needed for sky tipping calibration procedure and for the determination of liquid nitrogen boiling temperature (absolute calibration).

Rain Sensor: The rain flag is used as an additional parameter in measurement files and for triggering the elevation threshold feature (microwave window protection), see section 5.9.

GPS antenna: In some polarized radiometer models, a GPS receiver is added for solar tracking purposes (e.g. Solar Patrollers).

All meteorological sensors are calibrated without the need for further recalibration.

3.7 Other Radiometer Details

In order to fulfil the requirement of low maintenance regarding absolute calibrations, the instrument is equipped with a two-stage thermal control system for all receivers with an accuracy of ±0.05 K over the full operating temperature range. Due to this extraordinary high stability, the receivers can run freely without any calibration (not even the automatic gain calibration) for 20 minutes while maintaining an absolute brightness temperature accuracy of ±0.5 K. Each receiver is equipped with a precision noise standard (long term stability) at its signal input which replaces the external cold target in the internal absolute calibration procedure.
The system performs many automatic tasks like data interfacing with the external host, data acquisition of all housekeeping channels and detector signals, controlling of azimuth/elevation positioner, backup storage of measurement data, automatic and absolute calibration procedures etc. These tasks are handled by a build in embedded PC with 10.0 Gbyte flash memory for data storage. This PC is designed for operating temperatures from –40°C to +60 °C and is therefore ideal for remote application. The software running on this PC can easily be updated by a password protected file transfer procedure between host and embedded PC.
The host computer software operates under Windows NT4.0, Windows 2000, Windows XP, Windows Vista and Windows 7. A complete host software description is given in chapter 5.

3.8 Instrument Specifications

(All Modules, except for L-Band, 1.40 GHz)

Parameter	Specification
System noise temperatures	<900 K typical for all receiver (including calibration frontend, <1400 K at 90 GHz
Radiometric resolution	0.2 RMS @ 1.0 sec integration time
Channel bandwidth	400 MHz, 2000 MHz at 90 GHz for linear pol. systems, 6000 MHz at 45 GHz, 8000 MHz at

	90 GHz for circular pol. systems (solar patrollers)
Absolute system stability	1.0 K
Radiometric range	0-350 K
Absolute calibration	with internal Dicke switch & external cold load, automatic sky tipping
Internal calibration	gain: with internal Dicke Switch + noise standard automatic abs. cal.: sky tipping calibration
Receiver and antenna thermal stabilization	Accuracy <0.05 K
Gain nonlinearity error correction	Automatic, four point method
Brightness calculation	based on exact Planck radiation law
Integration time	>=1 second for each channel, standard measurements, 10 ms during solar tracking
Data interface	RS-232, 115 kBaud
Data rate	8.5 kByte/sec., RS-232
Instrument control	Industrial PC, Pentium based
Housekeeping	all system parameters, history documentation
Optical resolution	HPBW: 6.0°
Sidelobe level	<-30dBc
Pointing speed	elevation: 3°/sec, azimuth: 5°/sec
Operating temperature range	-40°C to +45°C
Power consumption	<350 Watts average, 500 Watts peak
Input voltage	100-230 V AC, 50 to 60 Hz
Weight	105 kg for receiver modules, 300 kg for positioner

3.9 L-Band Module (1.40 GHz)

The design of the L-Band module and its antenna differs significantly from those of all other direct detection modules. This is why it is described here in a separate section.

Typical combination: L-band (front view, left) and 6.925/10.65 GHz packages (front view, right).

3.9.1 Antenna Performance

Parameter	Specification
Geometry	Planar 64 square patch array
Antenna dimensions	1200 x 1200 x 65 mm³
HPBW (half power beam width)	11°
Antenna gain	24.9 dB
Main beam efficiency	99.4% (same envelope as dual-mode horn)
Side lobe level	<30 dB
Minimum observation distance	5 m
Mass	36 kg
Operating temperature range	-40° to +50°

Parameter	Specification
Operating humidity range	0-100% (rain protected)

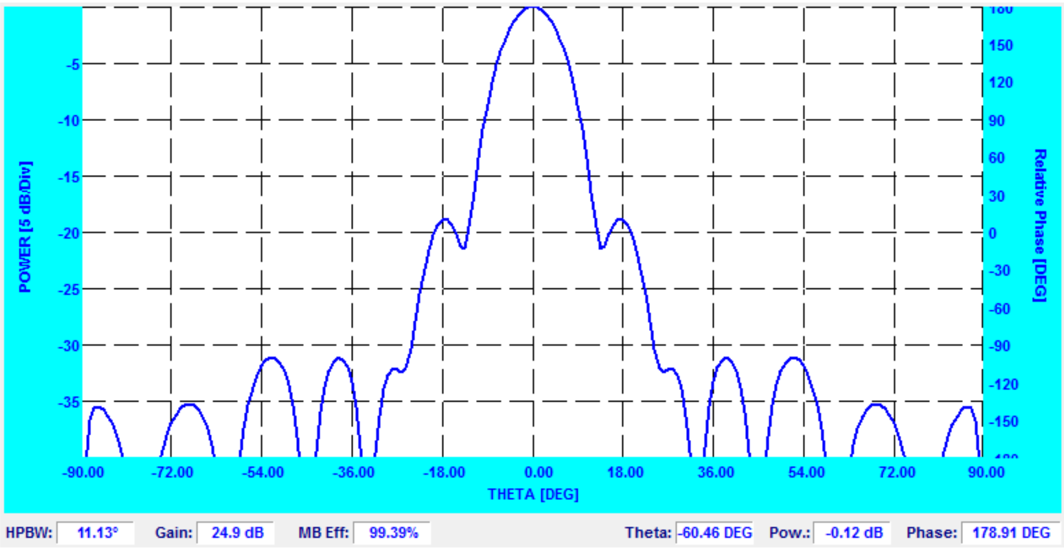

Calculated L-Band antenna pattern.

3.9.2 Receiver Performance

The receiver package continuously performs internal automatic calibration cycles for complete radiometric calibrations. The internal calibration standards are regularly compared to absolute standards by sky tipping procedures.

Parameter	Specification
Calibration	Dicke switch (internal ambient target), cold FET cold target, pin switch (1p3t) for antenna, cold target, ambient target
Ambient calibration temperature	315 (typical)
Cold calibration temperature	55 K (typical, cold FET)
Receiver system noise	<200 K (typical)
Calibration switch leakage	<0.01%
Detection bandwidth	20 MHz, 1.40 to 1.42 GHz
Out-of-band rejection	-50 dB @ 1.39 / 1.43 GHz
Polarization	Horizontal and vertical
Total system noise	500 K (typical, including patch antenna array)
Brightness temperature range	0 K to 800 K
Accuracy	1 K typ. for sky observations, 0.5 K typ. for soil moisture / ocean salinity observations
Radiometric noise	<0.15 K RMS
Thermal receiver stability	<30 mK over full environmental temperature range

Parameter	Specification
Operating temperature range	-40° to +50°
Operating humidity range	0-100% (rain protected)

3.9.3 Filter Characteristic

Super steep filter function with out-of-band rejection of -50 dB @ 10 MHz off band. The 1.40 to 1.42 GHz band is protected.

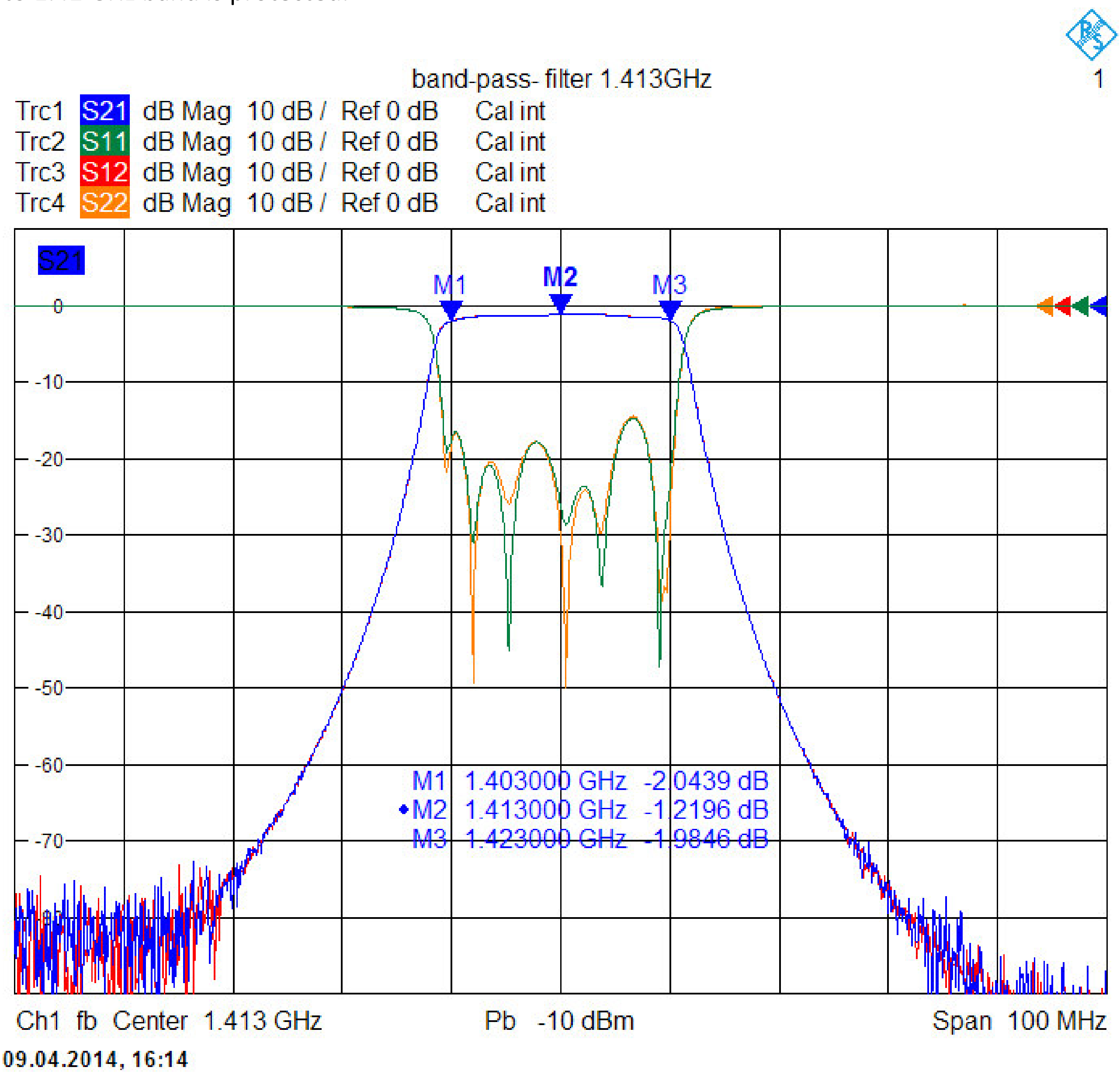

Sweep range: 1.36 GHz to 1.46 GHz.

3.9.4 L-Band Receiver Calibration

Because of the low L-band frequency (1.4 GHz) the antenna is a huge object of 1.2 x 1.2 m^2. The antenna is therefore located outside of the L-band receiver module, connected to it by semi-rigid cables (one for each polarization). This setup has certain implications on the calibration algorithm due to antenna losses.

In a first step the receiver is calibrated without the antenna by terminating the receiver inputs with two 50 Ohm terminations that can be cooled with liquid nitrogen. This standard hot / cold calibration determines the internal brightness temperatures of the Dicke switch T_{DS} and the cold FET brightness temperature T_{CF}. Also the system noise temperature of the receiver alone (T_1) is determined.

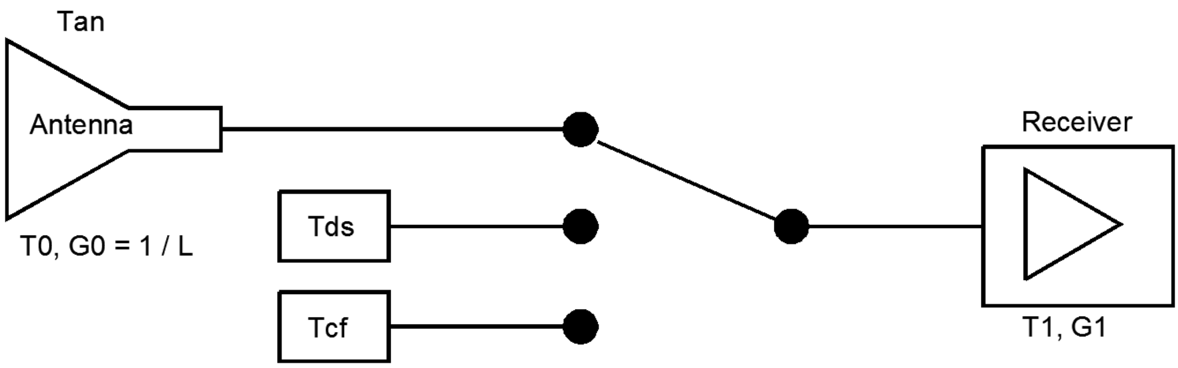

The antenna brightness temperature T_0 is given by:

$$T_0 = T_{an}(L-1)$$

T_{an} is the physical antenna temperature and L the antenna losses.

The total Gain G_{sys} of the combined system (Antenna + Receiver) is given as:

$$G_{sys} = G_0 G_1 = \frac{G_1}{L}$$

The total system noise temperature of the combined system is:

$$T_{sys} = T_0 + L \cdot T_1 \Leftrightarrow L = \frac{T_{sys} + T_{an}}{T_1 + T_{an}}, \quad (1)$$

When pointing to the 6.5 K celestial north point during the sky tipping calibration procedure (see section 4.4), the detector voltages on the Dicke Switch U_{DS} and on the sky (calibration switch on antenna position) U_{sky} are measured:

$$Y \equiv \frac{U_{DS}}{U_{sky}} = \frac{G_1(T_1 + T_{DS})}{G_{sys}(T_{sys} + T_{sky})} = L\frac{T_1 + T_{DS}}{T_{sys} + T_{sky}} \Leftrightarrow L = \frac{Y(T_{sys} + T_{sky})}{T_1 + T_{DS}}, \quad (2)$$

From (1) and (2) it follows:

$$T_{sys} = \frac{T_{an} - Y \cdot A \cdot T_{sky}}{Y \cdot A - 1} \; with \quad A \equiv \frac{T_1 + T_{an}}{T_1 + T_{DS}}$$

And L follows from (1).
During a calibration cycle in a running measurement, the two detector voltages on the Dicke Switch position (U_{DS}) and on the cold FET position (U_{CF}) are measured. Then

$$Y \equiv \frac{U_{DS}}{U_{CF}} = \frac{T_1 + T_{DS}}{T_1 + T_{CF}} \Leftrightarrow T_1 = \frac{T_{DS} - Y \cdot T_{CF}}{Y - 1} \quad and \quad G_1 = \frac{U_{DS}}{T_1 + T_{DS}}$$

By knowing the antenna loss L from a celestial north point observation, we conclude:

$$G_{sys} = \frac{G_1}{L} \quad and \quad T_{sys} = L \cdot (T_1 + T_{an}) - T_{an}$$

From the detector voltage measured on the scene (U_{sc}), we can derive the calibrated brightness temperature of the scene:

$$T_{sc} = \frac{U_{sc}}{G_{sys}} - T_{sys} \quad or \quad T_{sc} = L \cdot (\frac{U_{sc}}{G_1} - T_1 - T_{an}) + T_{an}$$

4. Calibrations

Calibration errors are the major source of inaccuracies in radiometric measurements. The standard calibration procedure is to terminate the radiometer inputs with two absolute calibration targets which are assumed to be ideal targets, meaning their radiometric temperatures are equal to their physical temperature. This assumption is valid with reasonable accuracy as long as proper absorber materials are chosen for the frequency bands in use and barometric pressure corrections are applied to liquid coolants in the determination of their boiling temperature.

4.1 Absolute Calibrations

A calibration target is considered to be an absolute standard when it is not calibrated by another standard. The RPG-XCH-DP has been calibrated by absolute standards when shipped (liquid nitrogen (LN2) standard and external ambient temperature target). All other absolute calibrations are performed on the sky as **sky tipping calibrations**. Therefore, the user does not need to handle LN2 coolants and cold targets as part of the maintenance services. This is possible because all RPG dual polarized frequency modules are offered for frequency bands at which the atmosphere is transparent and the requirements for sky tipping are fulfilled.

4.1.1 The Internal Dicke Switch Calibration Target

The Dicke switch target (see Fig.2.2 and Fig.2.3) is one of the instrument's key components. The switch magnetically terminates the receiver inputs with an absorber target of well

known physical temperature (ON position). This absorber serves as a termination of the same brightness temperature and is thus equivalent to a quasi-optical target (of the same temperature) when positioned in front of the receiver. The Dicke switch is located behind the feed horn and cannot calibrate changes in the feed horn T_B. It is therefore essential to thermally stabilize the feed horn and lens of each receiver to keep this contribution constant. The switches are operated once per second and are used to adjust drifts in the system noise temperature. Of course it is important to measure the Dicke switch physical temperature as accurate as possible.
The main advantage of using a Dicke switch instead of a quasi-optical target for absolute calibration is that this calibration can be performed frequently (every second!) while the radiometers are pointing to the scene. The switches work in combination with the built-in noise injection (or cold FET in the case of L-Band) system which is used to calibrate gain drifts. In contrast to the Dicke switches (these are absolute standards), noise diodes and cold FETs are secondary standards that have to be calibrated by a hot/cold calibration with liquid nitrogen or by a tip curve calibration on the clear sky.

4.1.2 External Liquid Nitrogen Cooled Calibration Target

Another absolute calibration standard is the liquid nitrogen cooled target (see Fig.4.1). **This target is only used as a first start-up calibration at RPG labs**. The positioner's elevation axis is tilted down to -90° and the target is located underneath the receiver antenna of the module which is actually calibrated. The calibration is repeated for each modul. This standard - together with the internal Dicke switch standard - is used for the absolute calibration procedure.
The liquid nitrogen boiling temperature and therefore the cold load physical temperature depends on the barometric pressure p. The radiometer's pressure sensor is read during absolute calibration to determine the corrected boiling temperature T_C according to the equation:

$$\ln\left(\frac{p}{1013.25\cdot mbar}\right)=\frac{\Delta H}{R}\left(\frac{1}{77.35K}-\frac{1}{T_C}\right) \quad , \quad Clausius-Clapeyron$$

T_0 = 77.36 K is the boiling temperature at 1013.25 hPa, ΔH is the latent heat of liquid nitrogen and R is the universal gas constant.
The calibration error due to microwave reflections at the LN/air interface is automatically corrected by the calibration software (embedded PC).
The main issue of the manual absolute calibration is the determination of certain receiver parameters, as Dicke Switch leakage or Dicke Switch brightness temperatures which do not change over time. All other receiver parameters can be determined with good accuracy by sky tipping.

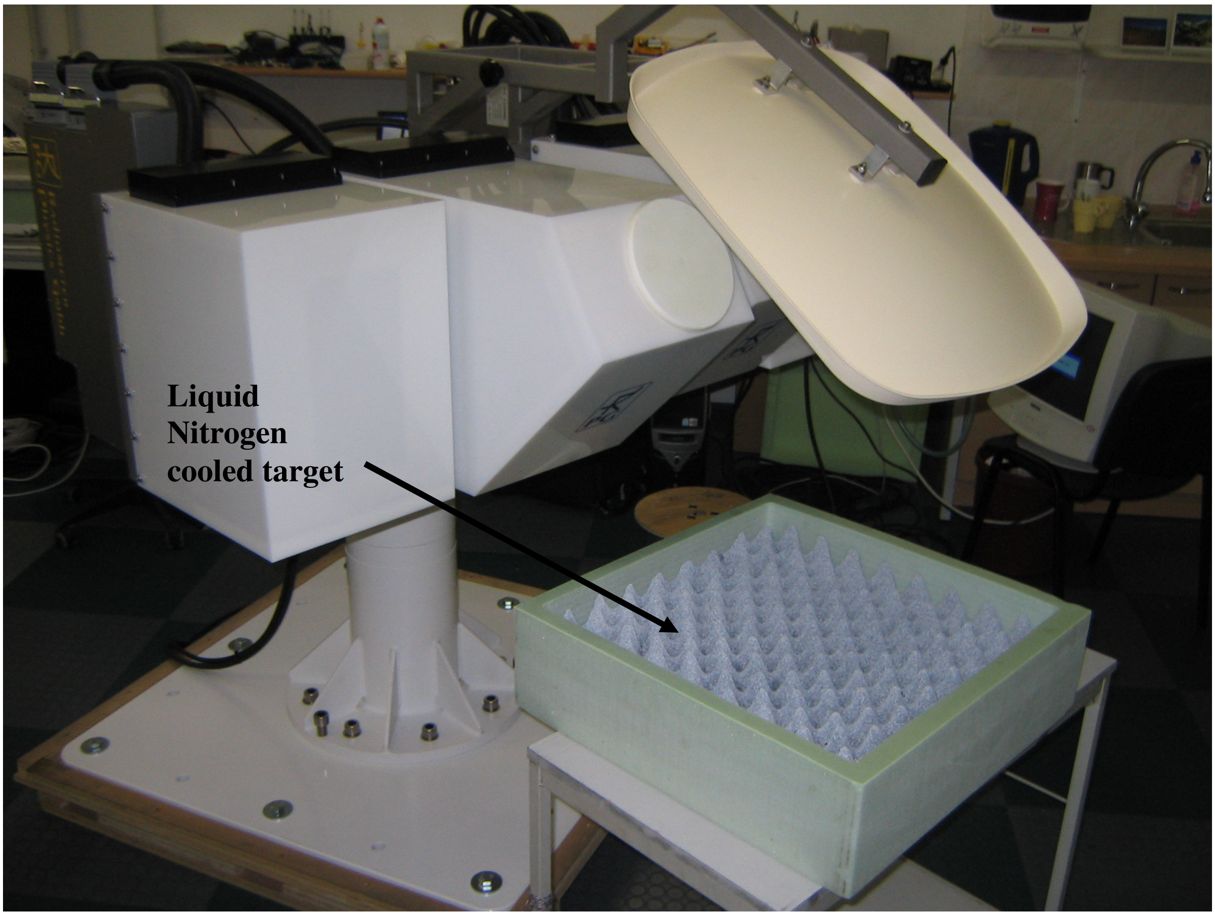

Fig.4.1: External cold load in front of the radiometer antenna.

It should be noted that the application of LN2 cooled calibration targets for L-Band radiometers (1.40 GHz) is not feasible because of the enormous required size and depth of a well suited target container (several thousand litres of LN2 would be needed). For L-Band modules, the sky calibration is definitely the only practical absolute calibration.

4.1.3 General Remarks on Absolute Calibrations

After the system has been turned on, at least 30 minutes are required for warming up and stabilization of all receiver components. To ensure accurate measurements, an absolute calibration should be performed only after completed warm-up.
The liquid nitrogen calibration was performed once at RPG to calibrate the noise standards. Usually it is not required to repeat this calibration when the radiometer regularly performs sky tipping calibrations. Sky tipping is the most accurate calibration method.

4.1.3.1 System Nonlinearity Correction

A common simplification in the design of calibration systems for total power receivers is the assumption of a linear radiometer response. In this case a simple two point calibration (hot/cold) is sufficient to determine the system noise equivalent temperature ($T_{sys,}$ offset noise) and system gain (G, slope of the linear response). Accurate noise injection measurements [2], [3] have shown that the assumption of linear system response is not valid in general. Calibration errors of 1-2 K have been observed at brightness temperatures in between the two calibration target temperatures. This system nonlinear behaviour is mainly caused by detector diodes [1] needed for total power detection. Even in the well defined square law operating regime (input power < -30 dBm) the detector diode is <u>not</u> an ideal element with perfect linearity. The noise injection calibration algorithm implemented in all RPG radiometers corrects for these nonlinearity effects.
The system nonlinearity is modelled by the following formula:

$$U = GP^{\alpha} \quad , \quad 0.9 \leq \alpha < 1 \qquad (1)$$

where *U* is the detector voltage, *G* is the receiver gain coefficient, α is a nonlinearity factor and *P* is the total noise power that is related to the radiometric brightness temperature T_R through the Planck radiation law:

$$P(T_R) \cong \frac{1}{e^{\frac{h\nu}{k_B T_R}} - 1}$$

(the proportionality factor is incorporated in G). T_R is the sum of the system noise temperature T_{sys} and the scene temperature T_{sc}.

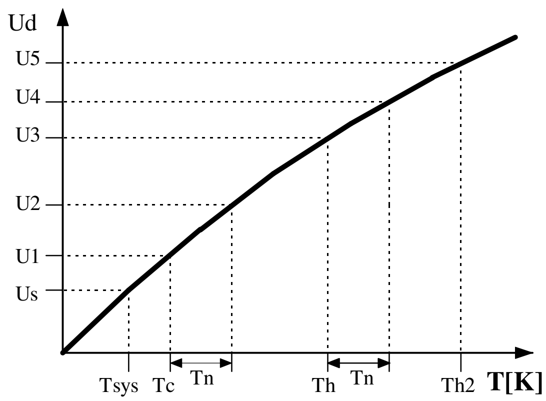

Fig.4.7: Detector response as a function of total noise temperature. T_{sys} is the system noise temperature, T_n the additionally injected noise, T_c the <u>total noise</u> when the radiometer is terminated with a cold load (e.g. liquid nitrogen cooled absorber) and T_h the corresponding noise temperatures for the ambient temperature load.

The problem is how to determine *G*, α and T_{sys} experimentally (three unknowns cannot be calculated from a measurement on two standards). A solution is to generate four temperature points by additional noise injection of temperature T_n which leads to four

independent equations with four unknowns (G, α, T_{sys} and T_n) The procedure is illustrated in Fig.4.7:
During the calibration cycle the elevation mirror automatically scans the two absolute targets.
The initial calibration is performed with absolute standards and leads to the voltages *U1* and *U3*. By injection of additional noise *U2* and *U4* are measured. For example *U2* is given by

$$U_2 = G(P(T_{sys}) + P(T_{cold}) + P(T_n))^{\alpha} \qquad (2)$$

where T_{cold} is the radiometric temperature of the cold target. The evaluation of the corresponding equations for *U1*, *U3* and *U4* results in the determination of T_{sys}, G, α and T_n. It is important to notice that the knowledge of the equivalent noise injection temperature T_n is not needed for the calibration algorithm. It is only assumed that T_n is constant during the measurement of U1 to U4.
After finishing the procedure the radiometer is calibrated. With the four point calibration method also the noise diode equivalent temperature T_n is determined. Assuming a high radiometric stability of the noise injection temperature, following calibrations can use this secondary standard (together with the built-in ambient temperature target) to recalibrate T_{sys} and G (considering α to be constant) without the need for liquid nitrogen.

References

[1] Cletus A. Hoer, Keith C. Roe, C. McKay Allred, 'Measuring and Minimizing Diode Detector Nonlinearity', IEEE Trans. on Instrumentation and Measurement, Vol. IM-25, No.4, Dec. 1976, page 324 pp.
[2] Sandy Weinreb, 'Square Law Detector Tests', Electronics Division Internal Report No. 214, National Radio Astronomy Observatory, Charlottesville, Virginia, May 1981
[3] Hvatum Hein, 'Detector Law' Electronics Division Internal Report No.6, National Radio Astronomy Observatory, Green Bank, West Virginia, Dec. 1962

4.2 Noise Injection Calibration

It is not convenient to use a liquid nitrogen cooled load for each calibration. For this reason the radiometer has four built-in noise sources (one for each receiver) that can be switched to the receiver inputs. The equivalent noise temperature T_n of the noise diode is determined by the radiometer after a calibration with two absolute standards (hot/cold or sky tipping) and is in the range 250 K to 1000 K. The noise diode is also used to correct for detector diode nonlinearity errors. The accuracy of a calibration carried out with this secondary standard and the Dicke Switches is comparable to the results obtained with a liquid nitrogen cooled load. The advantage of the secondary standard is obvious: A calibration can be automatically done at any time. All system parameters are recalibrated including system noise temperatures.
The noise diode is optimized for precision built-in test equipment (BITE) applications and meets MIL-STD202 standard with 170 hours burn-in. This process guarantees highest reliability and performance repeatability. The repeatability error is expected to be <0.1 K / month.

Due to the fact that only two calibration points are generated with this calibration type (T_a= Dicke Switch temperature, T_{a+n} = Dicke Switch temperature + noise standard), it has to be assumed that the non-linearity factor α does not change with time. This is a reasonable assumption because α is basically an intrinsic detector diode parameter.

4.3 Sky Tipping (Tip Curve)

Sky tipping (often referred to as tip curve calibration) is a calibration procedure suitable for those frequencies where the earth's atmosphere opacity is low (i.e. high transparency) but not close to zero as at L-Band frequencies (around 1.5 GHz), which means that the observed sky brightness temperature is influenced by the cosmic background radiation temperature of 2.7 K.

Sky tipping assumes a homogeneous, stratified atmosphere without clouds or variations in the water vapour distribution. If these requirements are fulfilled the following method is applicable:

The radiometer scans the atmosphere from zenith to around 14° in elevation and stores the corresponding detector readings for each frequency and angle. The path length for a given elevation angle α is 1/sin(α) times the zenith path length (defined as one "air mass"), thus the corresponding optical thickness should also be multiplied by this factor (if the atmosphere is stratified!).

When radiation of intensity Iv (v denotes a certain frequency) passes through an infinitely thin slice of gas, Iv is reduced by dIv given as

$$dI_\nu = -I_\nu \kappa_\nu ds$$

where κ_ν is the absorption coefficient and includes all processes implying a loss of photons on the way down to the radiometer. Integration over a finite sheet of gas leads to:

$$-\int \frac{dI_\nu}{I_\nu} = -\int d\ln(I_\nu) = \int \kappa_\nu ds \qquad \Rightarrow \qquad I_\nu = I_\nu^0 \cdot e^{-\int \kappa_\nu ds}$$

I^0_ν is the intensity before entering the sheet. The optical thickness is defined as:

$$\tau_\nu \equiv \int \kappa_\nu ds \qquad \Rightarrow \qquad I_\nu = I_\nu^0 \cdot e^{-\tau_\nu}$$

Spontaneous emission in the sheet increases the intensity. Atmospheric molecules perform rotational or vibrational transitions in the radiation field:

$$dI_\nu = \varepsilon_\nu ds$$

where ε_ν is the emission coefficient at frequency ν. The emission coefficient depends on pressure, temperature and chemical composition of the gas and has to be calculated quantum mechanically.

The total change of intensity for the infinitely thin gas sheet is then:

$$dI_\nu = \varepsilon_\nu ds - I_\nu \kappa_\nu ds \quad \Leftrightarrow \quad \frac{dI_\nu}{ds} = \varepsilon_\nu - I_\nu \kappa_\nu \quad or \quad \frac{dI_\nu}{d\tau_\nu} = \frac{\varepsilon_\nu}{\kappa_\nu} - I_\nu$$

We define the ratio ε / κ as the source function S. Then we get:

$$\left(\frac{dI_\nu}{d\tau_\nu} + I_\nu\right) \cdot e^{\tau_\nu} = S_\nu e^{\tau_\nu} \quad \Rightarrow \quad \frac{d}{d\tau_\nu}\left(I_\nu \cdot e^{\tau_\nu}\right) = S_\nu e^{\tau_\nu}$$

Integration leads to:

$$I_\nu(\tau_\nu) \cdot e^{\tau_\nu} - I_\nu^0 = \int_0^{\tau_\nu} S_\nu \cdot e^{\tau_\nu'} d\tau_\nu' \quad where \quad I_\nu^0 = I\left(\tau_\nu' = 0\right)$$

This is identical to the more common version of the radiative transfer equation:

$$I_\nu(\tau_\nu) = I_\nu^0 \cdot e^{-\tau_\nu} + \int_0^{\tau_\nu} S_\nu \cdot e^{-(\tau_\nu - \tau_\nu')} d\tau_\nu'$$

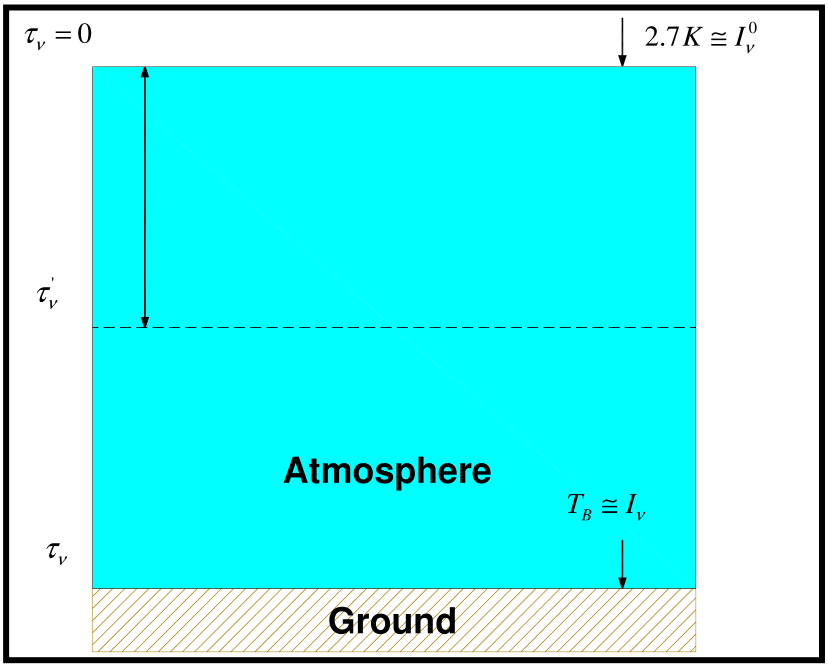

Fig.4.8: Radiative transfer geometry.

A sheet of optical thickness τ_ν absorbs a part of incident radiation I_ν^0 and emits radiation at each position, which is partly absorbed by (τ_ν-τ_ν'). In order to obtain the intensity on the ground, we have to compute the integral along the whole line of sight through the gas, τ_ν is the total optical thickness of the gas layer.

With the definition of the mean radiation temperature T_{mr} :

$$T_{mr} \equiv \frac{\int_0^{\tau_\nu} S_\nu \cdot e^{-\left(\tau_\nu - \tau_\nu^{'}\right)} d\tau_\nu^{'}}{1 - e^{-\tau_\nu}}$$

the optical thickness is related to the brightness temperature by the equation:

$$\tau_\nu = \ln\left(\frac{T_{mr} - T_{B0}}{T_{mr} - T_B}\right)$$

T_{mr} is a mean atmospheric temperature in the direction θ, T_{B0} is the 2.7 K background radiation temperature and T_B is the brightness temperature of the frequency channel.
The attenuation A in dB is related to τ_ν by the following formula:

$$\tau_\nu = A \cdot \frac{\ln 10}{10}$$

T_{mr} is a function of frequency and is usually derived from radiosonde data. A sufficiently accurate method is to relate T_{mr} with a quadratic equation of the surface temperature measured directly by the radiometer.

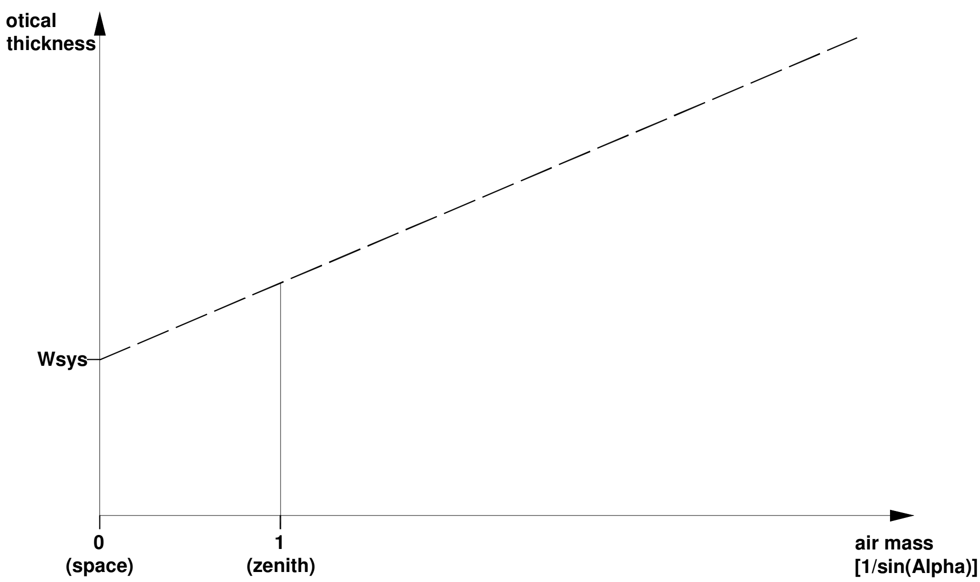

Fig.4.9: Extrapolation of tipping response to 2.7 K free space temperature.

The optical thickness as a function of air mass is a straight line (see Fig.4.9) which can be extrapolated to zero air mass. The detector reading U_{sys} at this point corresponds to a

radiometric temperature which equals to the system noise temperature plus 2.7 K: U_{sys} = G*(T_{sys} + 2.7 K). The proportionality factor (gain factor) G can be calculated when a second detector voltage is measured with the radiometer pointing to the ambient target with known radiometric temperature T_a. The sky tipping calibrates the system noise temperature and the gain factor for each frequency without using a liquid nitrogen cooled target.
The disadvantage of this method is that the assumption of a stratified atmosphere is often questionable even with clear sky conditions due to invisible inhomogeneous water vapour distributions (e.g. often observed close to coast lines). The built-in sky tipping algorithm investigates certain user selectable quality criteria to detect those atmospheric conditions that do not fulfil the calibration requirements. The most important criteria are:

- Linear correlation factor. This measures the correlation of the optical thickness samples (as a function of air mass) with a straight line. Typical linear correlation factor thresholds are >0.9995. The linear correlation factor is not sensitive for the noise of the optical thickness samples caused by clouds etc.
- χ^2-test. This measures the variance of the optical thickness samples relative to the straight line in Fig.4.9. Typical threshold values are <0.4 for a good quality calibration.

The tip curve calibration is considered to be the most accurate calibration method. The brightness temperatures acquired in the elevation scan are close to the scene temperatures measured during zenith observations.

4.4 L-Band (1.4 GHz) Sky Calibration

At L-Band the atmosphere is so transparent that a change in air mass will not significantly change the sky brightness temperature. An alternative sky calibration procedure has been suggested by Delahaye et al ('Calibration error of L-band sky looking ground based radiometers', Radio Science, Vol. 37, No. 1 1011, 2001):
Passive L-band radiometers are restricted to a relatively narrow protected frequency band, ranging from 1.400 GHz to 1.427 GHz. At this band, radio astronomers observe H_2 emissions of inter-stellar clouds located all over our galaxy due to the fine structure transition of neutral atomic hydrogen at 21 cm wavelength. Therefore, the sky brightness is mainly influenced by the observation direction. For instance, looking to the galactic center will lead to a significantly higher brightness temperature compared to a direction out of the galactic disc.

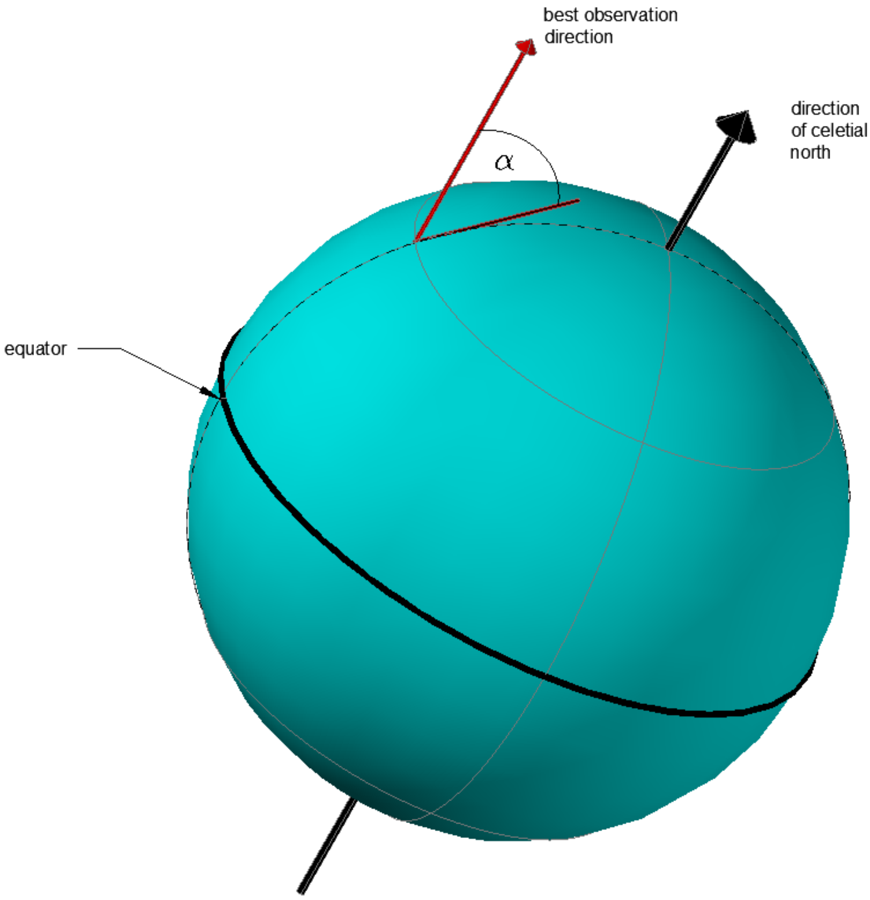

On the northern hemisphere exists a unique constant observation direction with low and well defined sky emission of about 6.5 K, which is pointing to the celestial north pole. This direction provides a stable L-band calibration temperature for all year observations, assuming a normal solar activity (no dramatic flares) and rain free conditions.
The pointing method is illustrated in the figure above. The direction to the celestial north is obtained by pointing the azimuth to north and setting the elevation angle α to the latitude of the radiometer's location.
In the host software, the L-band calibration is part of the general sky tipping procedure. But in contrary to the other modules, the L-band calibration is only using a single scanning point instead of a set of scan angles as required for the sky tipping algorithm. It is therefore possible to define different azimuth angles for the sky tip and for the L-band calibration point (which is always to the north). If the radiometer's azimuth zero is not aligned to north, the user should at least determine the radiometer's azimuth in north direction so that the radiometer software is able to find the celestial north even without the azimuth alignment.

5. Software Description

The following conventions are used in this software description:

- Messages generated by the program that have to be acknowledged are printed in red. Example: ***The specified port in 'R2CH.CFG' has no data cable connected to it!***
- Button labels are printed in green: ***Cancel***

- Messages that have to be answered by ***Yes*** or ***No*** are printed in light blue: ***Overwrite the existing file?***
- Labels produced by the software are printed in grey: *UTC*
- Names of group boxes are printed in blue. Example: ***Radiometer Status*** on the main screen.
- Names of tabs are printed in violet: ***Sky Tipping***
- Names of menus are printed in black: ***File Transfer***
- When a speed button shall be pressed this is indicated by its symbol:
- Hints to speed buttons are printed in brown: ***Define Serial Interface***
- Selections from list boxes are printed in magenta: ***Celsius***
- Selections from radio buttons are printed in dark green: ***COM1***
- File names are printed in orange: ***MyFileName***
- Directory names are printed in dark blue: ***C:\Programs\RPG-HATPRO***

5.1 Installation of Host Software

5.1.1 Hardware Requirements for Host PC

The hardware requirements for running the host software are:

- Pentium based PC, 2.0 GHz clock rate minimum
- 400 MB free RAM for software execution
- Ethernet interface

The host software XCHDP.EXE can be installed and run on any computer that fulfils the hardware requirements listed above.

5.1.2 Directory Tree

By clicking on the desktop icon the executable host program ***XCHDP.EXE*** is started (Windows XP, Windows Vista and Windows 7/8 systems). On pre-installed PCs this file is located in ***C:\RPG-XCH-DP\ or C:\RPG Solar Patrollers***. This directory path can be changed to any other path (in the following referred to as ***MY_DIRECTORY\RPG-XCH-DP***). Of course the corresponding desktop link has to be modified accordingly.

In the case that the user wants (or has) to install the software by himself, the following steps should be performed:

- Start your Windows operating system
- Start the Windows Explorer
- Insert the Radiometer CD-ROM or USB memory stick
- In Windows Explorer click on the CD-ROM drive or USB drive icon
- Click on the ***RPG-XCH-DP***-folder and drag the whole folder to ***MY_DIRECTORY*** (user selectable).
-

Example: If '***MY_DIRECTORY***' is the directory ***D:\Programs*** the complete tree should look like this:

D:
|---***Programs***
|---***RPG-XCH-DP***
| |---***CONFIG***
| |---***DATA***
| |---***MDF_MBF***
| |---***LICENSE***
| |---***LOG***
| |---***RETRIEVALS***
| |---***TEMP***

The different subdirectories are automatically created ***XCHDP.EXE*** when is executed for the first time.

The ***MDF_MBF*** directory is empty after installation and is intended for the Measurement Batch Files and Measurement Definition Files needed to initiate a measurement. ***DATA*** is reserved for measurement data files including user defined sub-directories. Of course the user can create any other directory for his data file storage.
Click into ***MY_DIRECTORY\RPG-XCH-DP***\ and locate ***XCHDP.EXE***. When clicking on this file with the right mouse button a list of actions is displayed. Select the 'Desktop (Create Shortcut)' option to generate an icon on the desktop.

5.2 Getting Started

When host program is started (***XCHDP.EXE***), it will automatically try to connect to a radiometer if the 'Auto-Connect' flag is set (see TCP-IP interfacing menu). Even if a connection try fails, the host software can still be used to inspect existing data files or calibration data.
On program start the screen looks like this:

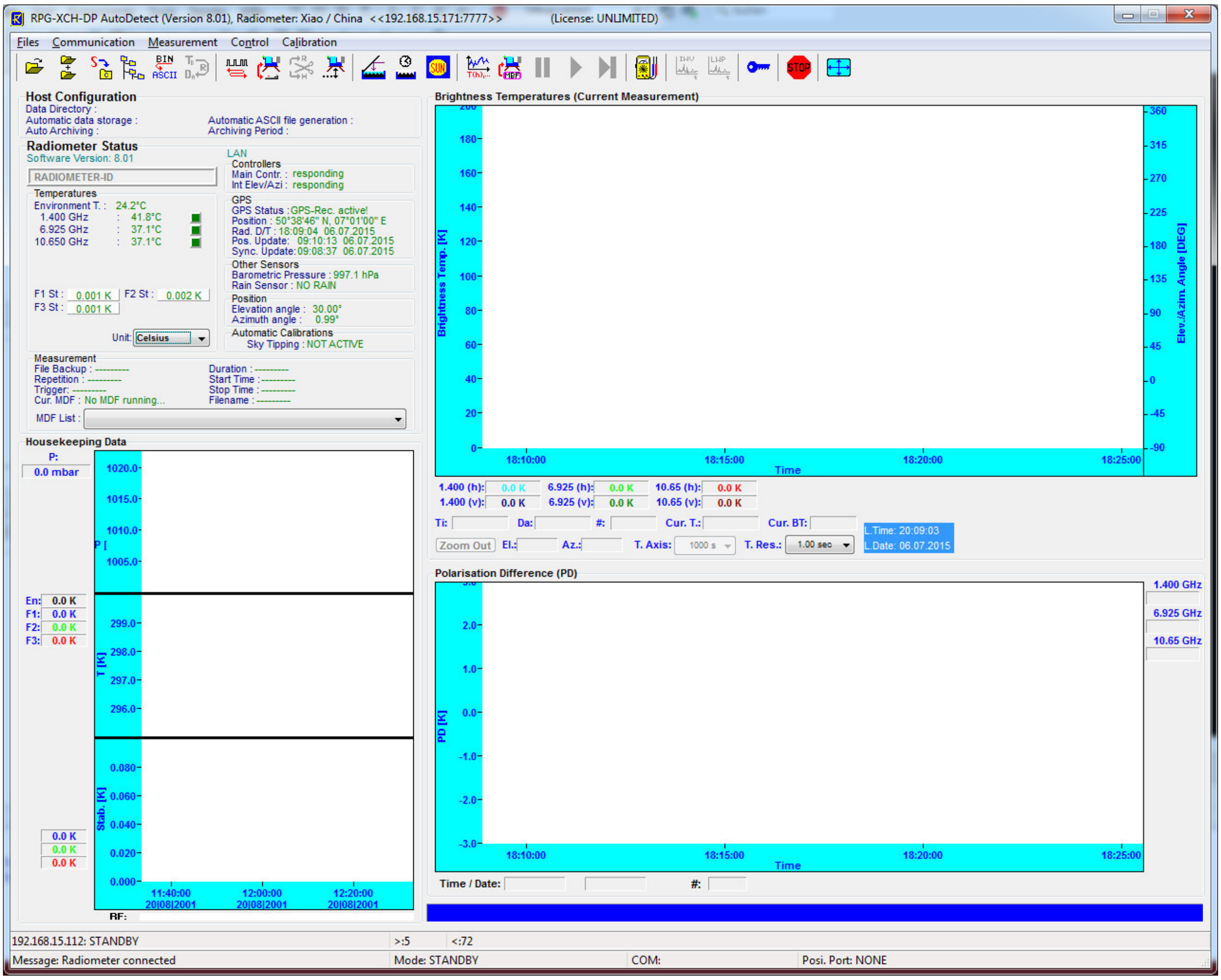

Fig.5.1: Starting the host software.

It is subdivided into:

- A set of short-cut commands on the top line for easy access of system menus
- A box with host PC configuration parameters, related to data storage, archiving, data directory settings and file conversion options
- The radiometer status box, containing information about the main controller and positioner status, environmental sensor readings, receiver temperatures and stability, the GPS updating, elevation and azimuth angles and measurement status parameters, as start / stop time, file backup and currently executed MDF.
- A box with a time series of housekeeping data (temperatures, pressure, receiver stability), which is updated only during measurements
- A brightness temperature display box showing the time series of channel brightness temperatures
- A display of a polarization difference time series

5.3 Interfacing via Ethernet

5.3.1 Setting up IPs

The RPG-XCH-DP radiometer communicates via a LAN (Ethernet) interface. In order to establish a connection to the instrument, the user clicks on to select the ***TCP-IP Interface*** menu. The configuration entry looks like this:

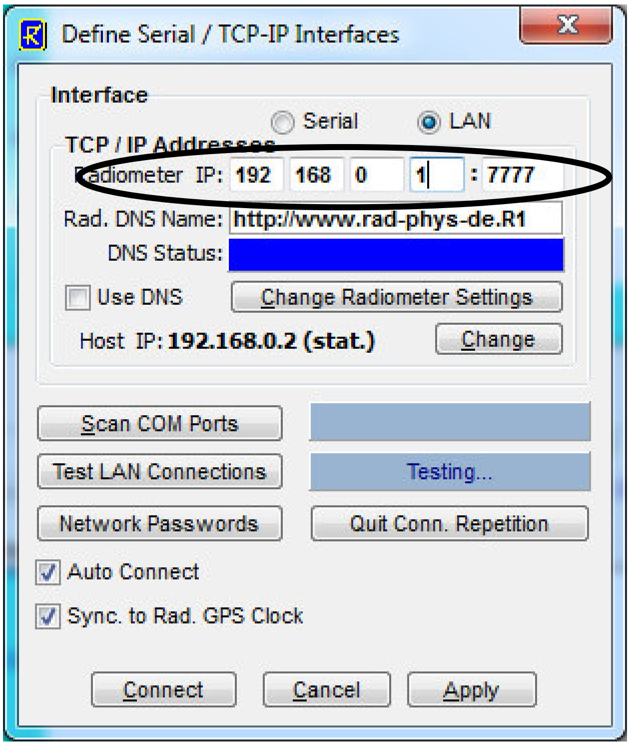

Fig.5.2: Definition of radiometer embedded PC's and host PC's TCP-IP interface parameters.

The radiometer PC (R-PC) is delivered with a fixed default IP address (default: 192.168.0.1, port no.:7777) which can be altered any time. For a fist connection the user should enter this IP to the edit fields right to ***Radiometer IP:*** (see encircled line above) and set the host PC (H-PC) IP address to the same subnet (e.g. 192.168.0.2) The radiometer Gateway is not required for a 'peer-to-peer' connection between the S-PC and the H-PC. A peer-to-peer connection is an Ethernet connection between two PCs without using a network in between. **In order to set up a peer-to-peer connection, the H-PC must have a fixed IP address.**

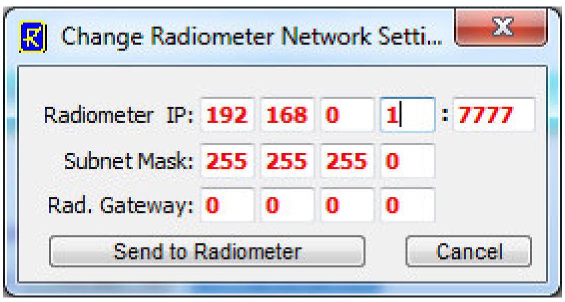

For changing the radiometer IP and gateway, e.g. when the radiometer shall be connected to a network, click ***Change Radiometer Settings*** (a new menu pops up) and edit the fields to the desired numbers.

The red IP / gateway settings are sent to the radiometer by clicking ***Send to Radiometer***. After new IPs have been successfully sent to the R-PC, it will be no longer accessible through the old IP / gateway addresses. In the case of a successful transfer of the new IP / gateway to the radiometer, the new IP is copied to the current IP fields automatically so that the H-PC can continue its connection to the radiometer. Then click ***Connect***.
You may test the connection with ***Test LAN Connections***. The H-PC will then try to get access to the R-PC via the specified IP address. If the connection is successful, 'STANDBY' is indicated in the blue panel, otherwise 'Failed to connect!'.

Example:
Consider a newly delivered radiometer with initial IP of 192.168.0.1, gateway of 0.0.0.0 and with port address 7777. Using this IP configuration the radiometer cannot be successfully connected to a network. In order to connect to it directly in a peer-to-peer connection, the MWS communication cable must be connected **DIRECTLY** (not via a network) to the Ethernet connector of the H-PC. Without limitation of generality, let us assume the H-PC IP to be 192.168.12.27. In order to tell the H-PC to directly listen to the LAN interface (NOT via a network gateway), its IP address should be in the same subnet as the radiometer, meaning its IP address should start with 192.168.0.xxx to establish a peer-to-peer connection.

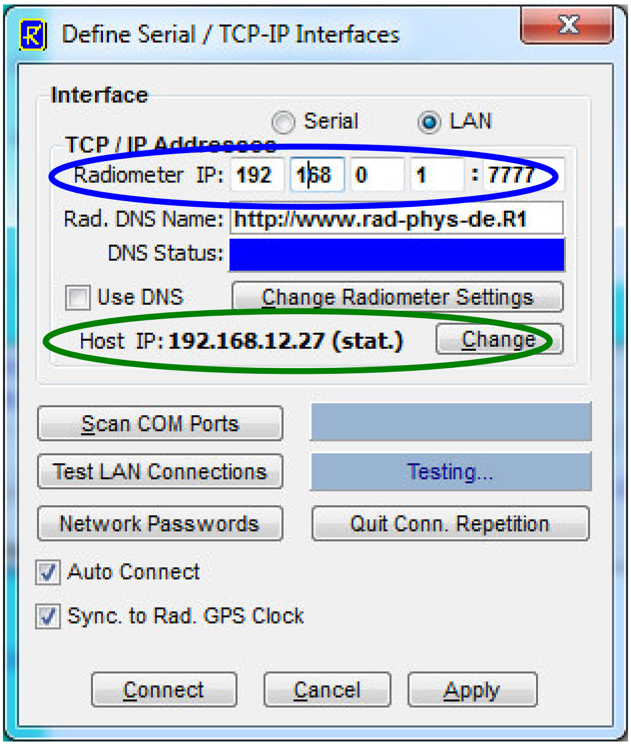

The blue ellipse marks the S-PC's default IP and the green ellipse marks the H-PC IP setting.

In order to modify the H-PC settings, click on the ***Change*** button and the following menu shows up (with possibly different settings):

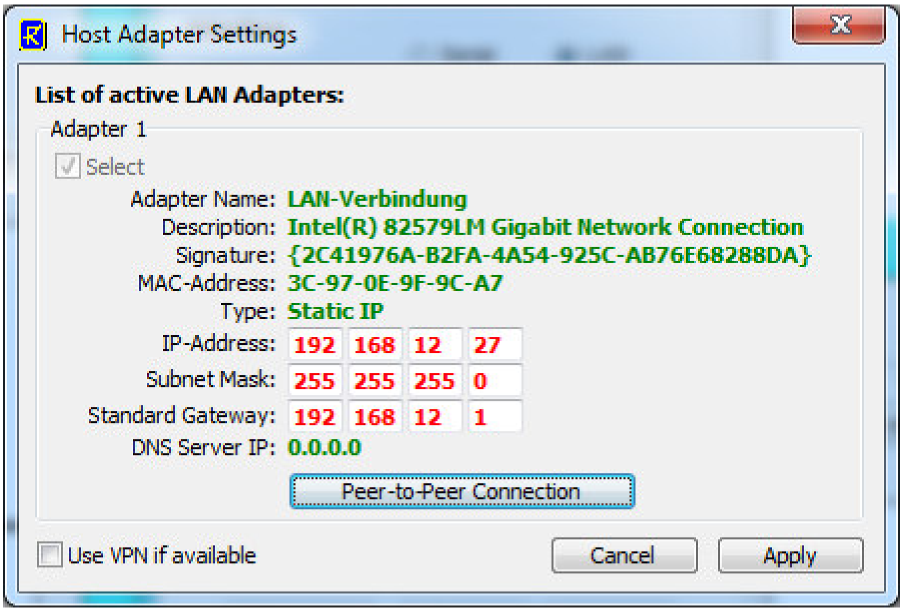

For establishing a peer-to-peer connection, modify the IP-address to be 192.168.0.xxx with 'xxx' being any number different from '1' .Click the ***Peer-to-Peer Connection*** button. The gateway address will be copied from the H-PC IP address. Then click ***Apply*** and the H-PC will be ready to connect to the radiometer. By clicking on ***Test LAN Connections***, the connection between H-PC and R-PC can be checked. If a connection can be established, the message **STANDBY** is shown in the blue field.
Let us now assume, the user's administrator wants to connect the radiometer to a network with the following network settings:

IP: 160.144.13.104
Standard Gateway: 160.144.11.1
Port Address: 6565

The way to send this new configuration to the R-PC is the following:
1. Click on ***Change Radiometer Network Settings***. The fields for the new radiometer IP and radiometer gateway are displayed in red. Edit these fields to the following settings:

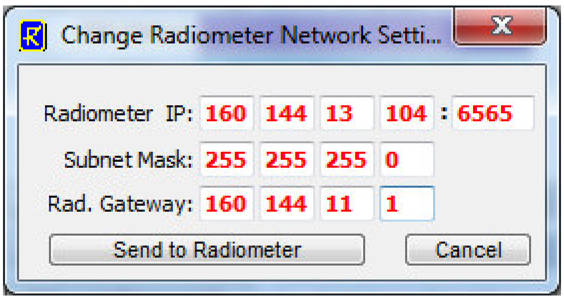

2. Then click on ***Send to Radiometer***. The settings in red are now transferred to the R-PC. If the radiometer has successfully changed its IP / gateway / port settings, a confirmation message is displayed.
After the IP / gateway / port numbers have been altered on the radiometer, it is not possible to connect to it through a peer-to-peer connection anymore. Therefore, connect the radiometer's communication line to the network.
3. Let us assume, the user's administrator has reserved the following network settings for the H-PC:

IP: 160.144.13.201
Standard Gateway: 160.144.11.1

Modify the H-PC TCP/IP settings by clicking ***Change*** and enter the new settings. Confirm your changes with ***Apply***. The H-PC then needs to be connected to the network as well.
Now both, the R-PC and the H-PC, are properly connected to the network with specific unique addresses and a connection between the two can be established over the network (e.g. click on ***Connect*** to verify this). Click ***Apply*** in the ***TCP-IP Interface*** menu to save the new settings.

5.3.2 VPN-Connections

If the H-PC is located far from the local network to which the radiometer is connected, the H-PC is typically using a VPN (Virtual Private Network) connection to the local network. This VPN connection is acting as a virtual adapter on the H-PC and can be inspected in the ***Host Adapter Settings*** menu. If you are not familiar of how to set up a VPN connection to a local network on your H-PC, please contact your network administrator.
The VPN service must be started on the Host-PC before it can be detected by the Host software. When checking the ***Use VPN if available*** box, you can ensure that the H-PC will always prefer the VPN connection over other active adapters on the system. For a long term installation the VPN connection should be configured with re-dial option for the case that the VPN connection is interrupted. The Host-PC will then automatically reconnect to the radiometer as soon as the VPN becomes operational again.

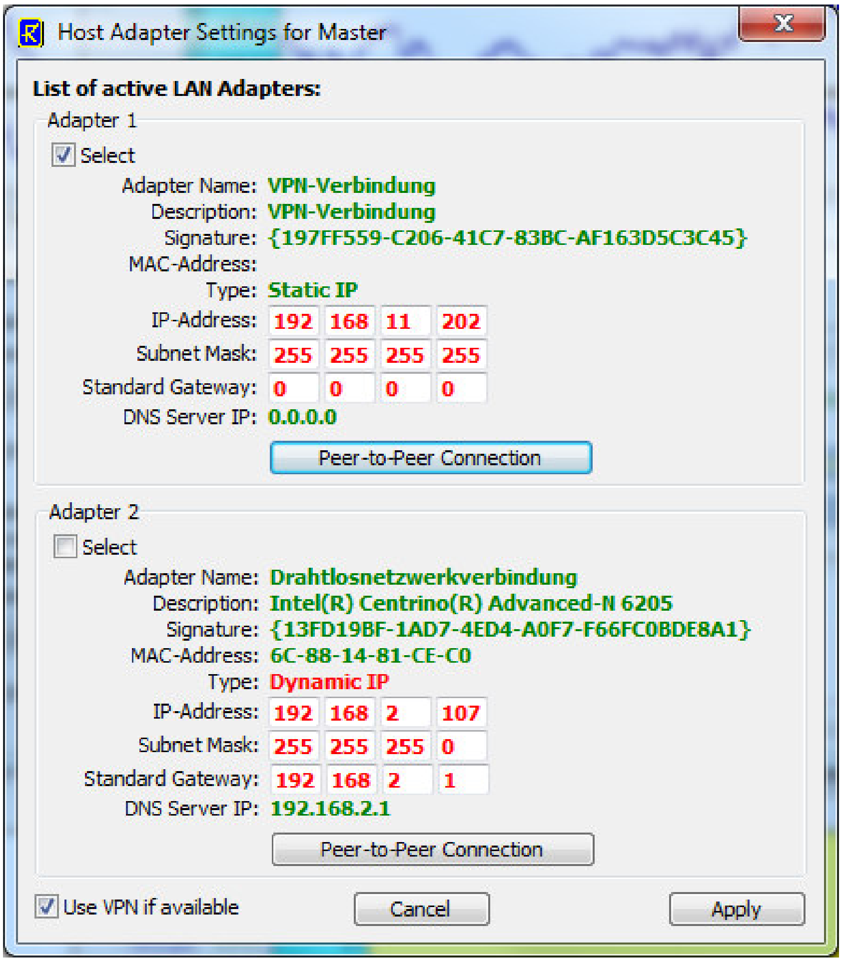

5.3.3 Multiple Clients

The R-PC connected to a H-PC is acting as a server, while the H-PC is the client. Every exchange of data packages is initiated by a H-PC request. The S-PC is permanently listening to its IP address and port for possible client requests. The H-PC is defined to be the *FIRST* client that connects to the radiometer. The radiometer then reserves its connection channel to this H-PC. Any other client requests from other IPs are rejected by the radiometer and a message is displayed to the new (secondary) client:

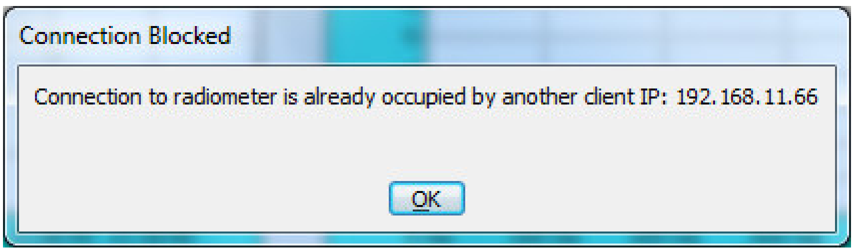

The secondary client is blocked from being connected to the radiometer.

5.3.4 Ethernet Passwords

When the radiometer becomes part of a network (not in a peer-to-peer connection), it acts as a server that will only allow one client (H-PC) to connect to it. In principle, any client, who uses a valid network address and who knows the radiometer IP address, can connect to the radiometer. Therefore, the radiometer is using a password control system in order to identify the access right of a particular client. This password is called a ***User Access Password (UAPW)*** and it is defined by a person with administrator rights, who should be a single IT person responsible for the network. Also the network administrator has a password called the ***Administrator Password (AMPW)***.
When clicking ***Ethernet Passwords*** from the TPC-IP interface menu, a new menu opens for defining such passwords.
The menu appears in the way shown below (left), if the AMPW is already defined. The fields to enter new passwords are disabled, until a valid AMPW is entered, which switches the menu to the status on the right. At radiometer delivery, the default AMPW is '***Administrator***'. The responsible network administrator should overwrite the AMPW as soon as possible when the radiometer has been assigned a valid IP address in a network. The network administrator is the only person who is authorized to set the UAPW and the password checking enable / disable.

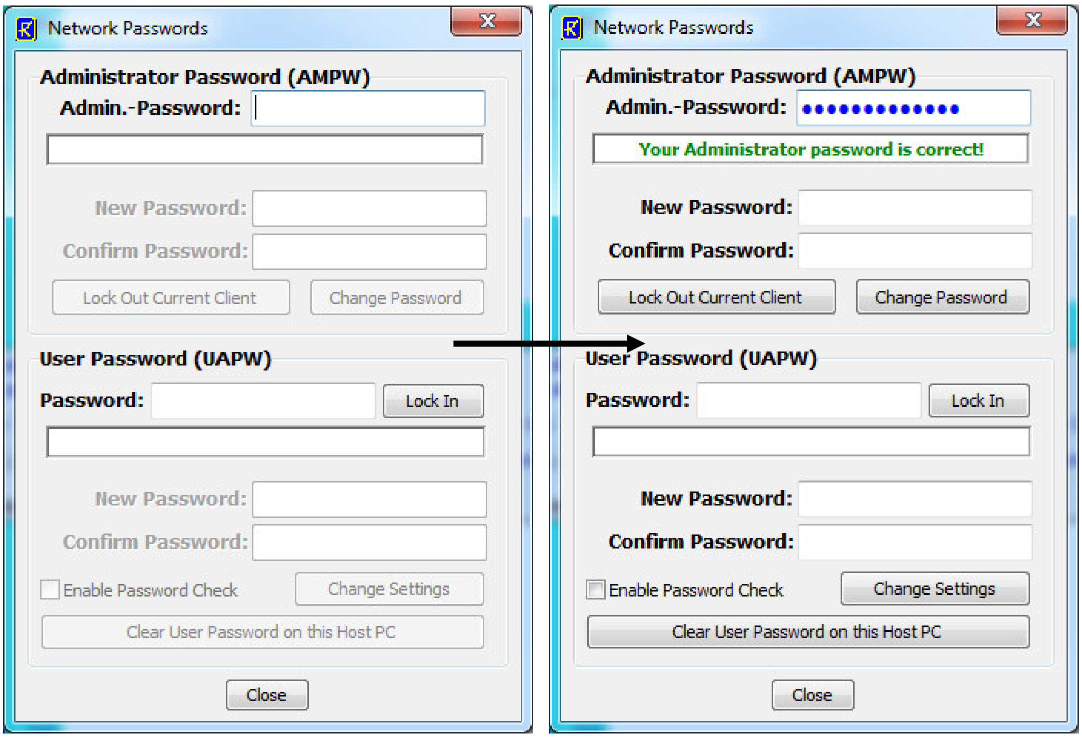

A user who tries to connect to the radiometer with a valid UAPW (***Lock In*** button) will be accepted if no other client is currently present. Otherwise he will be rejected and informed about the radiometer connection being occupied. Only the Administrator has the right to interfere in an established communication between the radiometer and a H-PC by clicking the ***Lock Out Current Client*** button. The Administrator client then becomes the new H-PC.

.

When an administrator has entered a valid AMPW, he can define a new UAPW or enable / disable password checking by the radiometer. Once a UAPW check is enabled and the UAPW has been defined by the Administrator, a client must enter the UAPW when he connects to the radiometer. Otherwise the access will be denied. If a client has entered the correct UAPW, the connection to the radiometer can be established (assuming the client is the first client) and the UAPW is stored on the client's disk so that a new entry of the UAPW is not required if the client tries to connect to the radiometer multiple times. The UAPW can be deleted from disk by ***Clear User Password on this Host PC*** to enforce the entry of the UAPW next time a user wants to access the radiometer again.

The UAPW entry cannot be over-ruled by an entry of the AMPW. When the UAPW entry is requested, only the correct UAPW is accepted. An Administrator, who has forgotten the UAPW, can enter the correct AMPW and define a new UAPW or disable the password checking to get access to the R-PC.

If ***Auto Connect*** is checked, the host software automatically tries to connect to the radiometer when it is started. This feature enables an auto-start up function after a power failure of the host PC. The radiometer embedded PC will automatically continue a measurement when the power returns after a power failure. To start the host software automatically after reboot of the operating system, a link to the ***XCHDP.EXE*** should be copied into the operating system's Auto Start directory or an appropriate task should be defined in the operating system scheduler.

The interface parameters are stored in the configuration file (***XCHDP.CFG***) that is loaded each time ***XCHDP.EXE*** is started. This file is backed up on exiting ***XCHDP.EXE***. A redefinition of the serial interface parameters is only necessary at the first start of ***XCHDP.EXE***.
New radiometer models (delivered after 2010) are equipped with 2 –line fibre optics data cables. The fibre optics cable eliminates the risk of damaging the radiometer's and host PC's serial interfaces during thunderstorms when lightning strokes may hit the ground close to the radiometer location. Also long cable lengths up to 2000 m can be realized.

After the TCP-IP settings have been defined and the connection is in STANDBY mode, the user can connect to the radiometer by clicking 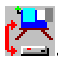. The radiometer's IP number is then visible in the host application's main window caption while the host IP is stated in the status line on the bottom of the screen.

5.3 Radiometer Status Information

The various status displays in the ***Radiometer Status*** group box are:

- Software Version: Indicates the version number of the radiometer PC software ***XCHDP_R.EXE*** for reference (the host software version is printed in the main window caption).

- Instrument ID: The radiometer identifies itself by sending the instrument ID to the host when a connection is established (e.g. *RPG-8CH-DP*, *RPG-6CH-DP*, *RPG-4CH-DP, RPG-XCH-DP*).
- ***Controllers***: Lists the status of the two instrument controllers:
    - The main controller handles all communication activities between the radiometer PC and the radiometer hardware.
    - The elevation / azimuth controller generates the driving signals for the positioner. In old positioner versions, an external controller was used to run the scanner (**Ext Elev/Azi**), which had to be controlled by the host PC via serial interface. New radiometers are controlling this interface directly and no external contoller unit is needed (**Int Elev/Azi**).

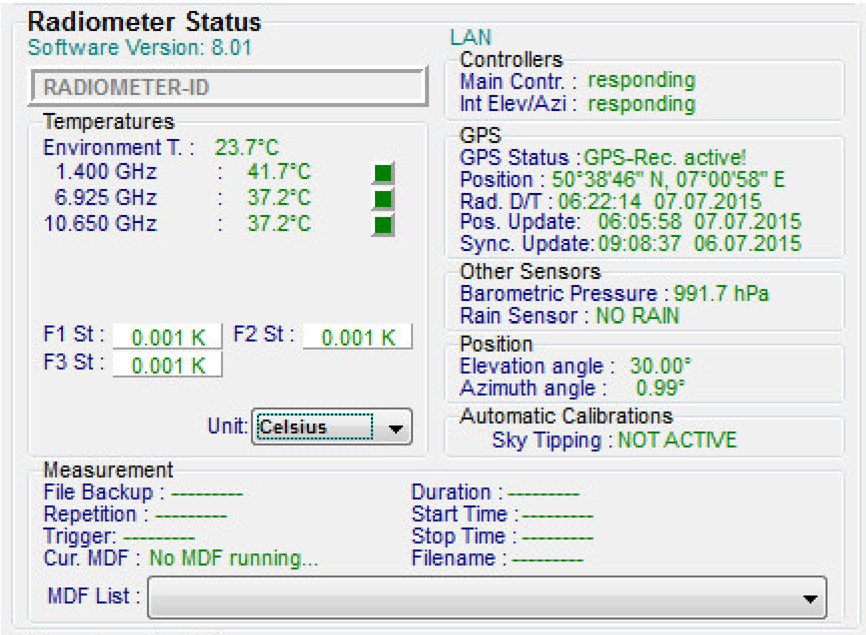

- ***Temperatures***: X+1 temperature sensors are implemented:
    - The environmental temperature sensor is located outside of the radiometer box. The sensor data is an important parameter for the absolute calibration hot target temperature measurement, for corrections of L-band antenna temperature and is also used to derive T_{mr} (needed for tip curve calibrations, see section 4.3).
    - Receiver1 / Receiver 2 / …: These temperature sensors reflect the physical temperatures of the receiver modules which are stabilized to an accuracy of < 0.05 K. Typical sensor readings are around 40°C. The thermal receiver stabilisation is continuously monitored. If the receiver temperature is kept constant to within +/- 0.05 K the status indicator on the right of the temperature display is green. If it turns to red the stability is worse than this threshold. In addition the actual stabilisation values are listed. The colour of the stability status indicator turns to yellow if not enough temperature samples have been acquired to determine the stability.
- ***Other Sensors***:

- Barometric Pressure: The pressure sensor measures the barometric pressure in mbar (accuracy ±1.0 mbar). The data is used in the determination of the precise boiling temperature of the liquid nitrogen coolant used in the external calibration target during absolute calibration.
- Rain sensor: Rain flag for controlling rain mitigation and for additional measurement parameter.

- ***Automatic Calibrations***: Here the status of automatic calibrations (sky tipping, see section 4) is monitored during measurements. All calibration data is automatically logged in the ***CAL.LOG*** file located in ***MY_DIRECTORY\RPG-XCH-DP\LOG***. The contents of that file can be inspected with the command (described later).
- ***Position***: The data displayed here is the current elevation and azimuth position of the elevation and azimuth scanner.
- ***Measurement***: During measurements this group box displays details like the file name of the current measurement, when the measurement was started and when it will end, if file backup is enabled on the radiometer PC and the batch repetition factor.

5.4 Data Storage Host Configuration

The ***Host Configuration*** group box on the main screen displays the data storage details. It is possible to change the settings by clicking (***Define Directories***). The automatic host data storage during measurements can be enabled or disabled and the data storage directory is selected from the directory tree shown in ***Data Directory***. In the same menu one can specify if an ASCII version of the data files (which are in binary format by default) shall be generated. ASCII files will then (if this option is selected) be stored to the same data directory as the binary files.

Data archiving is a useful feature to prevent the data directory to be filled with ten thousands of files which may overload the operating system. MS operating systems cannot handle many (in the order of ten thousands) files in a single directory. If ***Enable*** is checked, the software automatically creates sub-directories in the data directory and stores the data files according to the year, month and day they are generated. E.g. a file ***08111623.BRT*** would be stored in a directory ***…\RPG-XCH-DP\Data\Y2008\M11\D16***\ if ***daily*** is checked or in ***…\RPG-XCH-DP\Data\Y2008\M11*** if monthly is checked. Archiving, if enabled, is performed for data files immediately, after midnight or after 2 days, depending on the radio button selection. If the user wants to immediately archive data files, he may click the ***Start Archiving*** button.

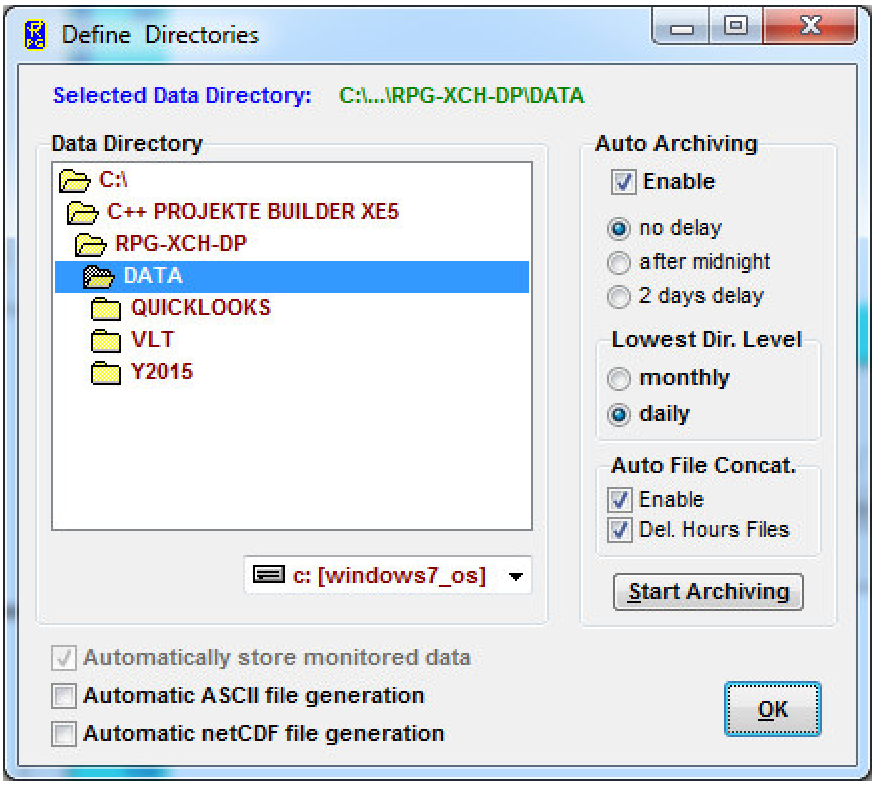

Define Directories Menu including data file directory and file archiving selection.

5.5 Exchanging Data Files

The radiometer PC is running a Windows®7 operating system. The radiometer software is stored in the directory ***C:\RPG-XCHDP-R\.*** Write processes to this directory or its sub-directories is password protected. When upgrading the radiometer software, the new executable *XCHDP_R.EXE* needs to be transferred to this root directory. This task should only be performed by the system administrator. **Overwriting *XCHDP_R.EXE* with a non-operating software or deleting this executable file will disable all radiometer functions and requires to restore the executable directly to the radiometer PC!**

To get access to the radiometer directories click 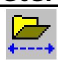 (***File Transfer***). The menu in Fig.5.2 will be displayed.

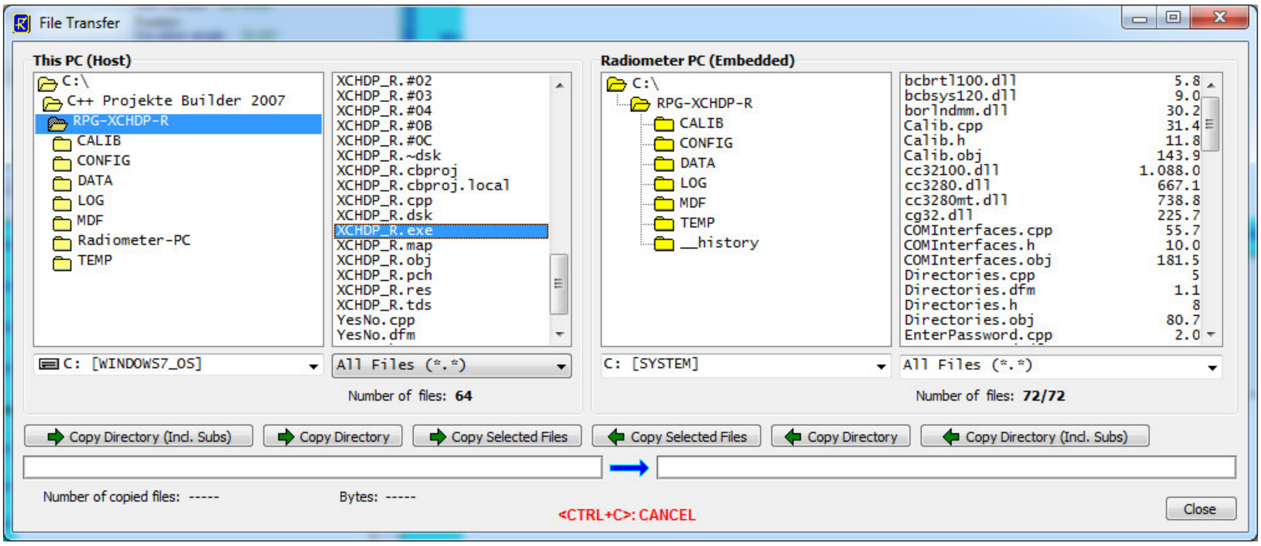

Fig.5.2: File transfer menu.

File transfer is necessary when backup data files need to be copied from the radiometer hard disk to the host computer. If file backup is enabled for a measurement, the instrument stores all data files in its data directory ***C:\RPG-XCHDP-R\DATA***. This data can then be downloaded after or during a measurement.

Files can be copied from one PC to the other by selecting them on the source directory, marking a directory on the destination PC and click ***Copy Selected File***. Alternatively, a complete directory, with or without its sub-directories may be copied (***Copy Directory***, ***Copy Directory (Incl. Subs)***).

Files or directories can be deleted by marking them and clicking the right mouse button:

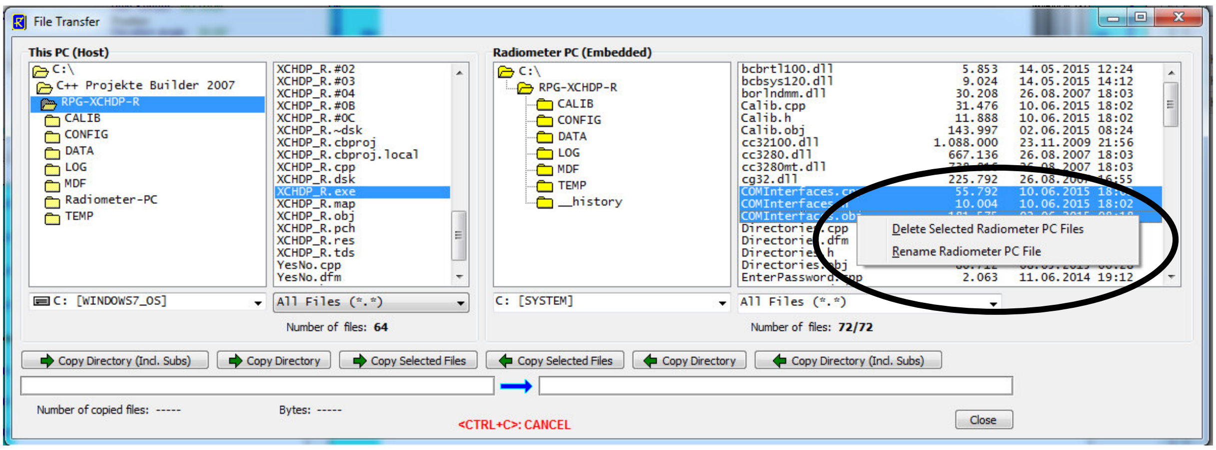

From the displayed drop-down list the user may select '***Delete Selected Radiometer PC Files***' or '***Rename Radiometer PC File***'. These functions are also available for directories.

If the user tries to send files to the ***C:\RPG-XCHDP-R*** directory (the root directory), a password check is initiated:

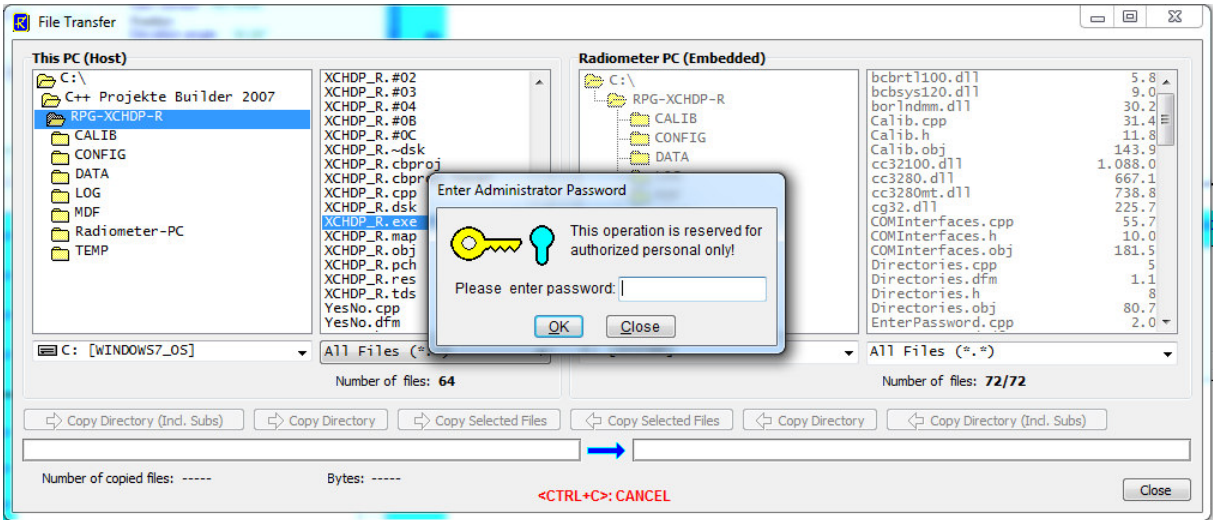

The H-PC is asking for the entry of the Administrator password (AMPW) to complete the desired action. This mechanism prevents unauthorized users to overwrite important R-PC system files.

5.6 Inspecting Absolute Calibration History

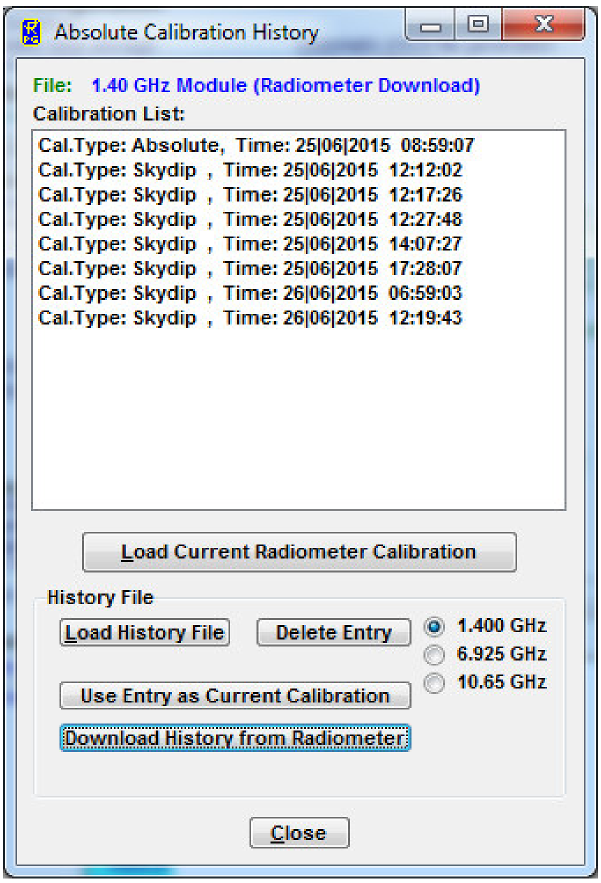

Fig.5.3: Loading calibration data to the calibration history list.

As mentioned in section 5.4 the ***ABSCAL.HIS*** file, located in the directory ***C:\RPG-XCHDP-R\CALIB*** on the radiometer PC, stores all absolute calibration results. This also includes the successful tip curve calibration results. In order to inspect this calibration history, click (***Open Data Files***) and select to invoke the ***Absolute Calibration History*** menu.

Load the calibration history data of a frequency module by selecting it from the radio-button list and click ***Download History from Radiometer*** and the list of calibrations is displayed (see Fig.5.3).

The list entries show the date and time of the calibration and the type of calibration for each receiver module in the sequence from lowest to highest frequency like e.g. 6.925 GHz / 10.75 GHz / 18.70 (21.0) GHz / 36.50 GHz.
Double clicking on one of the entries opens the ***Calibration Results*** menu in Fig.5.4. For each receiver channel the three parameters *G*, T_{sys} and T_n (see section 4.1.3) are listed. In addition the calibration type, calibration time and physical temperature of calibration targets are stated.
Depending on the receiver module, the parameter 'Leak. / A. Loss' has different meanings. For all modules except for the L-band module, this parameter indicates the Dicke Switch leakage. An ideal switch would have zero leakage, meaning it would perfectly isolate from the antenna port. But in reality Dicke Switches always leak a small fraction of the antenna signal into the receiver, even when switched to the internal calibration target. This fraction is measured during absolute calibrations. For L-band modules the parameter indicates the antenna loss, which has to be taken into account to determine the accurate scene temperature under changing environmental temperatures.

Fig.5.4: Display of absolute calibration parameters.

5.7 Inspecting Automatic Calibration Results

Automatic calibrations are those described in section 4.3 (Tip Curve). These calibrations are performed automatically by the radiometer following the calibration settings in the measurement definition file (see section 5.9.1). Monitoring of automatic calibrations is carried out by the (enabled) ***Radiometer Status*** window on the main screen. The corresponding log file ***CAL.LOG*** is located in ***MY_DIRECTORY\RPG-XCH-DP\LOG*** (or ***MY_DIRECTORY\RPG-Solar Patrollers\LOG***).

For inspecting this log file, click (***Display Automatic Calibration History***). The menu in Fig.5.5a appears. In the ***Sky Tipping Calibrations*** gain parameters (***Gain***), T_{sys} (***Tsys***) and T_n (***Tnoise***) are selectable. The user may zoom into the data by clicking on the graphics display (holding the left mouse button pressed) and dragging the mouse cursor to a second position. When the mouse button is released the new data window appears. ***Zoom Out*** reverts to the previous zoom. The precise moment of each calibration is indicated by a dot (and toggle this feature).

Below the ***Sky Tipping Calibrations*** data display the successful calibrations are marked by a green bar while failed calibrations are marked in red. By clicking on one of these bars, the tip curve calibration details are listed and a graphical display of the sky dip is shown (Fig.5.5.b).

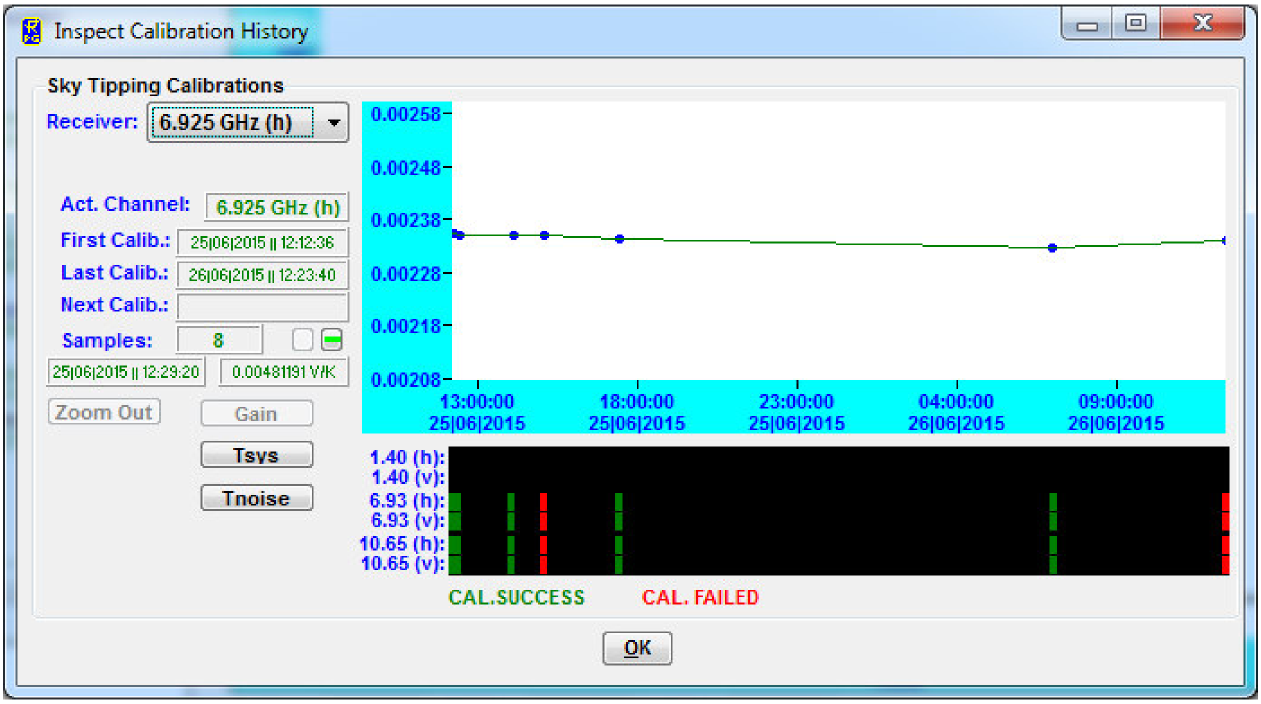

Fig.5.5a: Display of automatic calibration parameters.

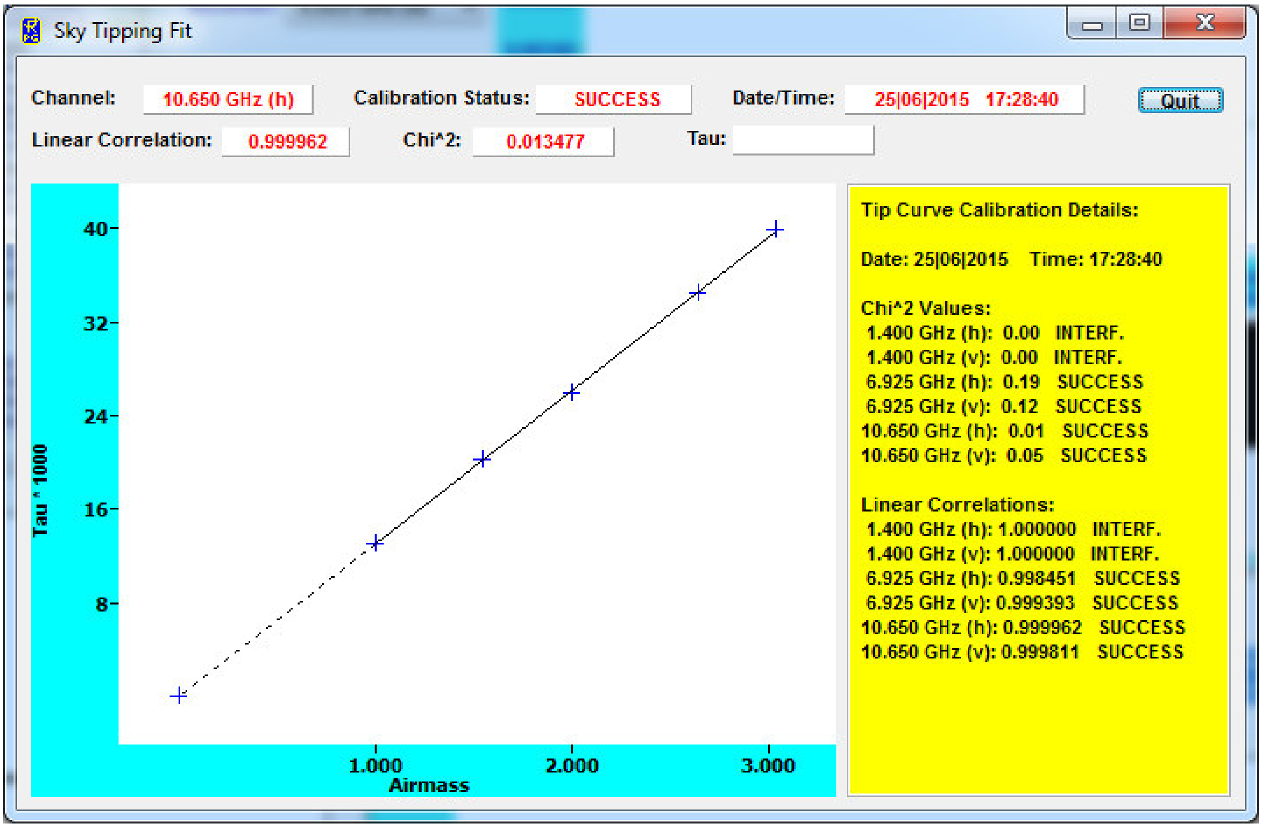

Fig.5.5b: Example of sky tipping results.

5.8 Absolute Calibration

As mentioned before, RPG performs absolute calibrations based on LN2 (liquid nitrogen) standards in the lab. These do NOT need to be repeated by the user because all modules can be more easily and accurately calibrated by sky tipping or sky pointing (L-band).

For the reason of completeness, the menu for manual absolute calibrations is described here:

After setting up the external cold target as described in chapter 4.1.2, an absolute calibration is initiated by pressing  (***Perform Absolute Calibration***). The menu in Fig.5.6 is shown.

The integration time T_i is selectable between ***5 Seconds*** and ***60 Seconds*** (***Integration Time*** group box) and defines the integration time period for each calibrated channel.
The four receivers are calibrated independently because the cold target has to be pushed underneath the antenna of each receiver package. The receiver to be calibrated is specified in the ***Receiver Selection*** group box.
Start Calibration starts the absolute calibration procedure. During calibration the current activity is displayed in the message line. When the integration cycles have completed, the message ***Calibration successful! Save?*** is displayed and the user has to confirm to save the

calibration with ***Continue***. The absolute calibration parameters are then stored on the radiometer PC. Leave the calibration menu by clicking ***Finished***.

If the error message ***No response to cold load. Calibration terminated!*** appears, the cold target was probably not filled with liquid nitrogen or was not installed at all.

No noise diode response. Calibration terminated! indicates a malfunction of one of the noise sources.

Fig.5.6: Absolute calibration menu.

5.9 Defining Measurements

Before a measurement can be started, it has to be defined. The various measurement parameters are then stored in a MDF (Measurement Definition File, extension *.MDF*). The radiometer is capable of processing multiple MDFs automatically which are combined in a MBF (Measurement Batch File, extension *.MBF*). The MBF is a batch file similar to DOS batch files but only intended to group MDFs. Both, single MDFs or MBFs can be sent to the radiometer.

To enter the ***Definition of Measurement and Calibration Parameters*** menu click 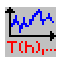 (***Define Measurement Parameter Files (MDF and MBF)***).

The measurement definition menu has several tab sheets (***Sky Tipping***, ***Standard Calibrations***, ***Products + Integration***, ***Elevation Scanning***, ***Timing + …***, ***MDF + MBF Storage***) which should be processed from left to right (see Fig.5.7).

5.9.1 Sky Tipping

The sky tipping (or tip curve) calibration is described in detail in section 4.4. Fig.5.7 shows the corresponding definition tab sheet.
The scanning angles listed in the ***Elev. Scan Angles [DEG]*** group box are predefined to give equidistant air mass samples in the sky tipping scan (the air mass is proportional to 1 / sin(α), see section 4.4). They can be modified by ***Add*** and ***Delete*** but it is recommended to only define angles >20°. If the radiometer's horizontal view is blocked by obstacles the lowest elevation angle should be adjusted appropriately but should not be >30° to maintain the calibration accuracy.

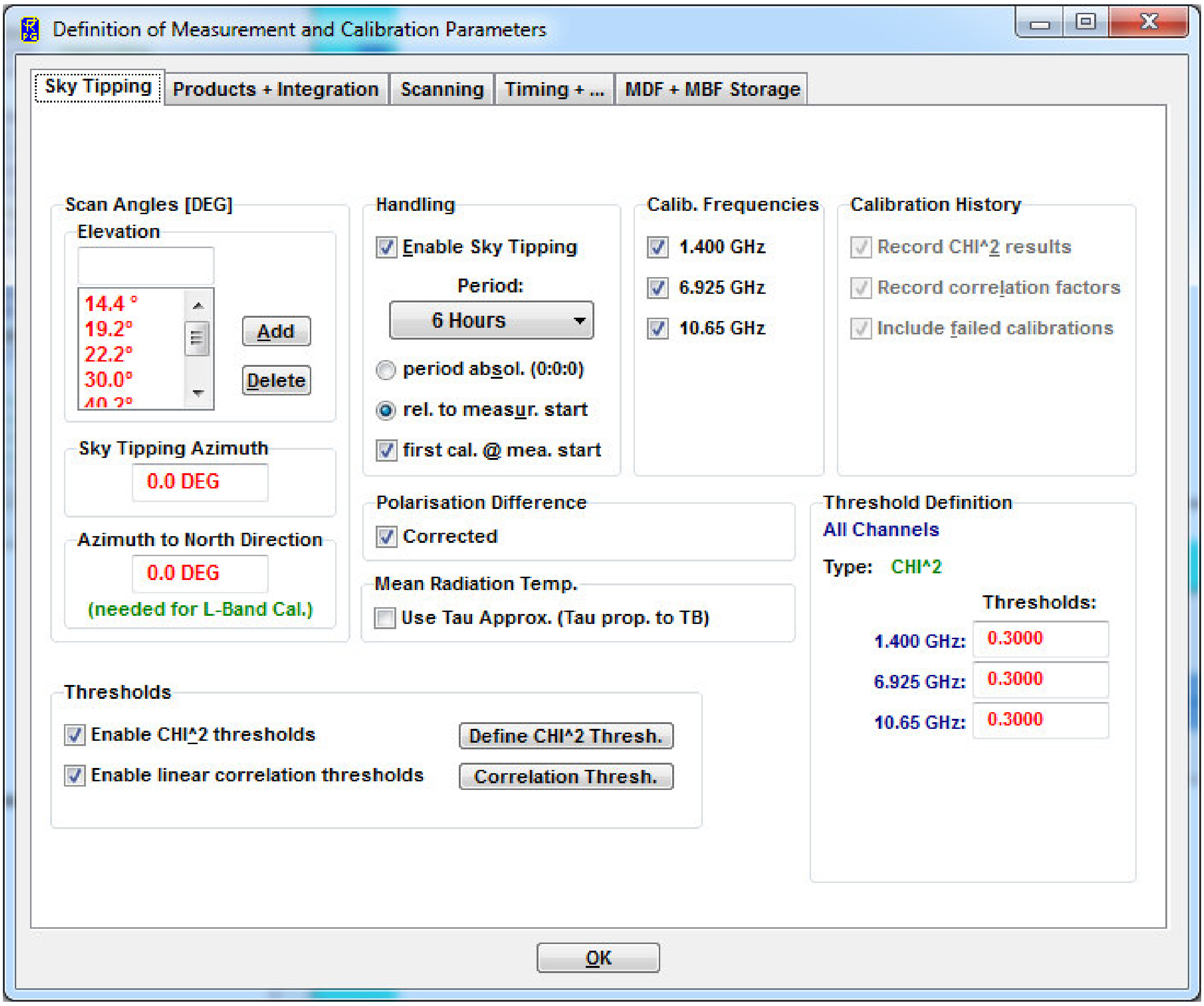

Fig.5.7: Measurement definition file menu, sky tipping tab sheet.

Sky Tipping is enabled by checking ***Enable Sky Tipping***. The user can specify how often a calibration shall be performed by selecting a period between ***10 Minutes*** and ***24 Hours***.

Practical periods are 2 to 24 hours because the radiometer gain is continuously calibrated by the noise standards and a noise diode recalibration is not required so frequently. In addition a tip curve interrupts the measurement for more than three minutes which should be kept to a minimum.
Furthermore it is possible to define the time of the first tip curve calibration in the measurement. By checking ***period absol. (0:0:0)*** the calibration will start relative to midnight time, e.g. with a period of 6 hours and a measurement start at 3:00 pm the first calibration will take place at 18:00 assuming that ***first cal. @ mea. start*** is not checked. If ***rel. to measure. start*** is checked the calibration timing is relative to measurement start time.
So far two quality checks (thresholds) are implemented which can be individually enabled or disabled:

- Linear correlation factor. This measures the correlation of the optical thickness samples (as a function of air mass) with a straight line. Typical linear correlation factor thresholds are >0.9995. The linear correlation factor is not very sensitive to the noise of the optical thickness samples caused by clouds etc.
- χ^2-test. This measures the variance of the optical thickness samples relative to the straight line. Typical threshold values are <=0.3 for a good quality calibration.

With ***Define CHI^2 Thresh.*** and ***Correlation Thresh.*** the corresponding thresholds can be entered in the ***Threshold Definition*** group box.
The calibration sky position for L-band modules is towards north direction. The ***Azimuth to North Direction*** angle defines the azimuth angle pointing to north. For a north aligned radiometer this would be 0.00° but if the radiometer positioner is not north aligned, any other azimuth angle may be entered here.

5.9.2 Products + Integration

On the ***Products + Integration*** sheet the user selects the products he wants to be acquired and calculated by the system.

For each enabled product a separate integration time is selectable (the LV0 integration time is the same as the integration time for brightness temperatures).

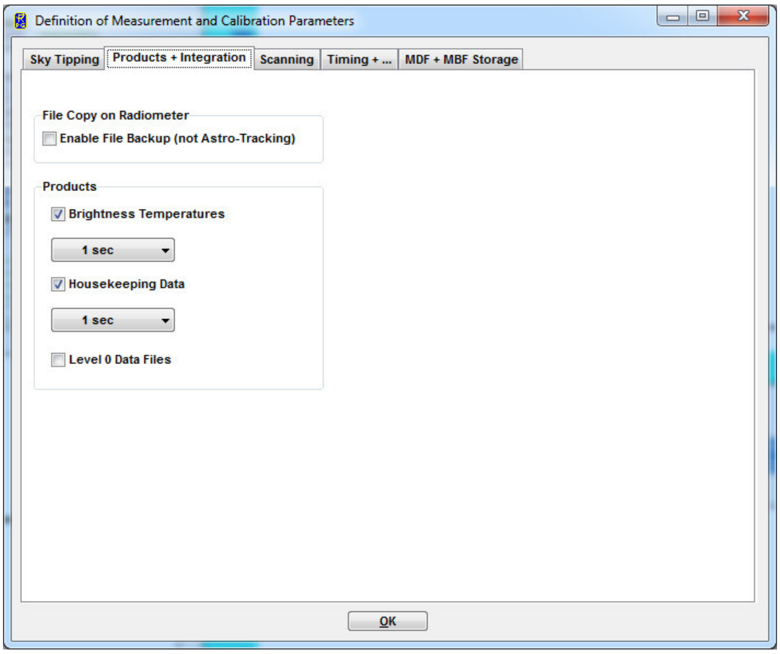

Fig.5.8: Specifying the products available for the radiometer configuration.

Another feature of the ***Products + Integration*** tab sheet is the ability to enable a file backup on the radiometer PC. When backup is enabled, the checked products will be automatically stored in the radiometer’s data directory. This is usually done for safety reasons because the standard mode of measurements is to enable automatic data storage on the host (online monitored data). With this method the data transfer virtually does not require any time. Without monitoring the data on the host and only storing it on the radiometer as backup the user will sooner or later have to transfer the data from the embedded PC to the host using the ***Transfer Data and System Files*** menu.

5.9.3 Scanning

Sometimes it is desirable to scan the elevation / azimuth angle while taking measurement samples. The details for this scanning are defined in the ***Scanning*** tab sheet. When scanning is disabled a constant elevation / azimuth angle is used for observations.

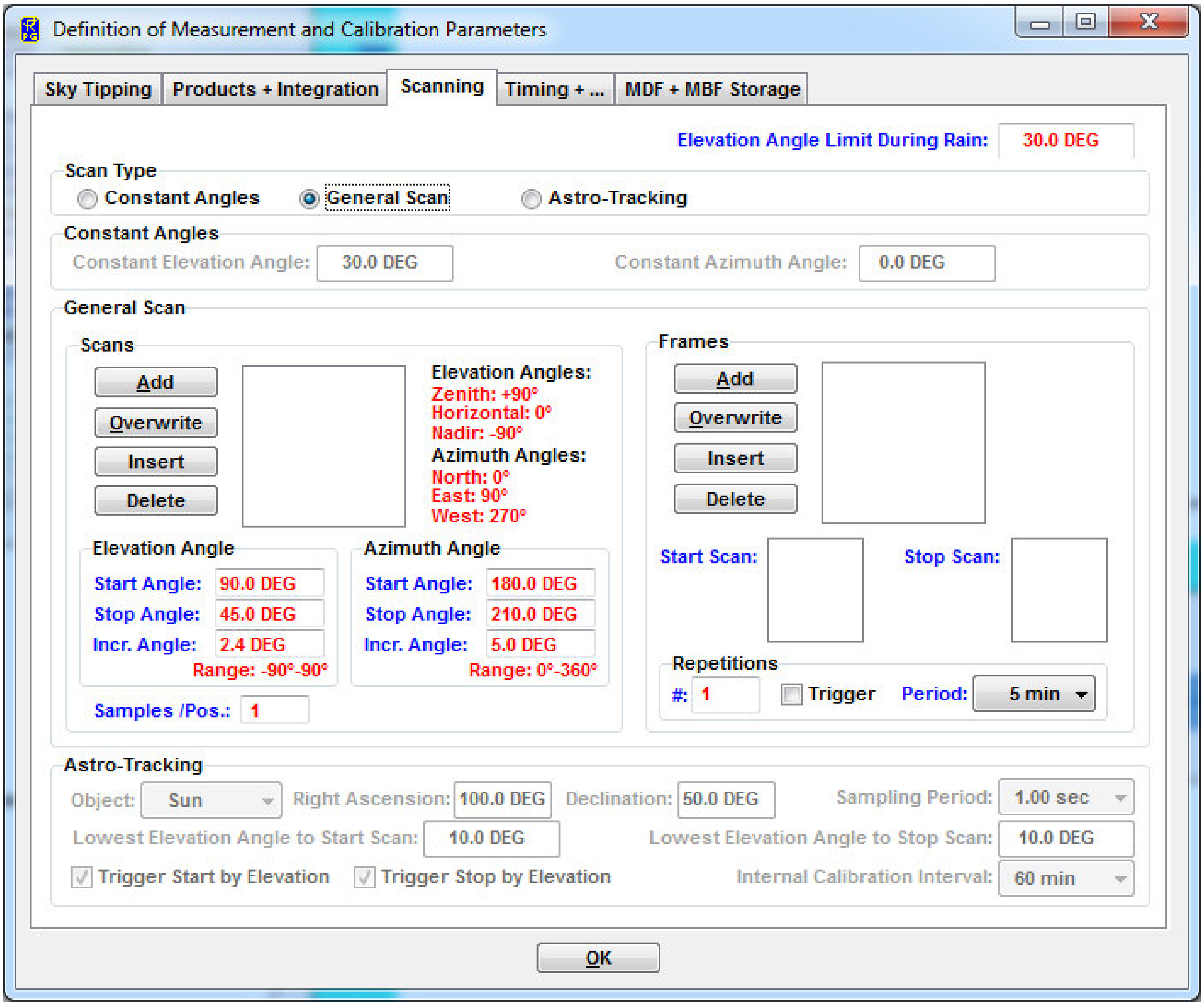

The radiometer is equipped with a rain sensor. If the sensor detects rain, the elevation positioner automatically limits the maximum elevation angle to the value entered in the 'Elevation Angle Limit During Rain' entry box. This way a whettening of the receiver module microwave windows can be avoided.
The positioner moves are subdivided into elementary scans from a start angle to a stop angle with a certain incremental angle and a given number of samples measured at each position. These scans are numbered as Scan#1, Scan#2.
The radiometer does not execute single scans but only frames of scans. Each frame has a start scan and a stop scan (can be identical) which form a 'loop' of scans that can be repeated arbitrarily. The concept of having two levels of movement definitions allows for designing complex scan procedures. The positioner speed is always constant.
A frame is simply defined by clicking on one of the scans in the start scan list and then clicking on one in the stop scan list. After entering the repetition number the frame is added (or inserted) to the frame list (***Add*** or ***Insert***). Three examples illustrate how a frame is executed:

1) Start: Scan#4, stop: Scan#6, repetitions: 3 ⇒
   Scan#4,Scan#5,Scan#6,Scan#4,Scan#5,Scan#6,Scan#4,Scan#5,Scan#6
2) Start: Scan#4, stop: Scan#2, repetitions: 2 ⇒

Scan#4,Scan#3,Scan#2,Scan#4,Scan#3,Scan#2

3) Start: Scan#2, stop: Scan#2, repetitions: 1 ⇒ Scan#2

Sun Tracking is another scan type for continuously tracking the sun. The radiometer is using its GPS antenna to determine the precise time and location information to calculate the sun position on the sky. The temporal sample resolution in this mode is 10 ms. The scan start can be triggered by a lowest elevation angle and terminated by another lowest elevation angle. The period for internal calibrations can be freely selected in this mode and should be kept to a minimum (e.g. every 10 minutes) to widely achieve an undisturbed time series.

5.9.4 Timing +...

Start time, end time and time reference are important parameters for a measurement setup. The time reference is set to UTC or local time which is UTC + time shift [h]. The radiometer determines UTC from a GPS clock reading which is synchronized to the radiometer's real time clock (RTC) every 10 minutes.
There are two ways of triggering a measurement: Immediately after launching the MDF or at a certain time and date. Using a start time before the current time is equivalent to an immediate start. If the measurement start is triggered to a certain time, the check boxes ***Ignore Date*** and ***Ignore Hour*** allow for a date or hour independent triggering. This is particularly useful in a repeated multiple MDF batch measurement, where MDFs are repeated multiple times. A triggering to a certain date / time would trigger the MDF only once but not repeatedly. E.g. if ***Ignore Hour*** is checked (assuming ***Triggered*** mode is activated) and the 'Start Time' entry is set to 22|36|15, the measurement is triggered to 00:15:00, 01:15:00, 02:15:00, …, ignoring the current date and hour. If a more frequent trigger is required, one can use the ***Raster*** feature combined with a raster period. E.g. if a start time of 22|36|15 is defined in combination with raster mode and a raster period of 10 minutes, the trigger sequence is: 22|36|15, 22|46|15, 22|56|15, 23|06|15 etc.
Two options are available for measurement termination. In LIMITED mode the user can set a duration or termination time. If the stop time is before the start time, the measurement duration is adjusted to 100 seconds.
In the case that the measurement has a well-defined end time (automatic measurement termination, LIMITED mode) the radiometer needs a filename for storing backups. The user may enter any filename not longer than 8 characters. The host also uses this filename when it is operated in automatic storage mode. If measurement timing is set to UNLIMITED mode the radiometer automatically generates filenames deduced from the actual time and date and ignores the measurement filename entry.

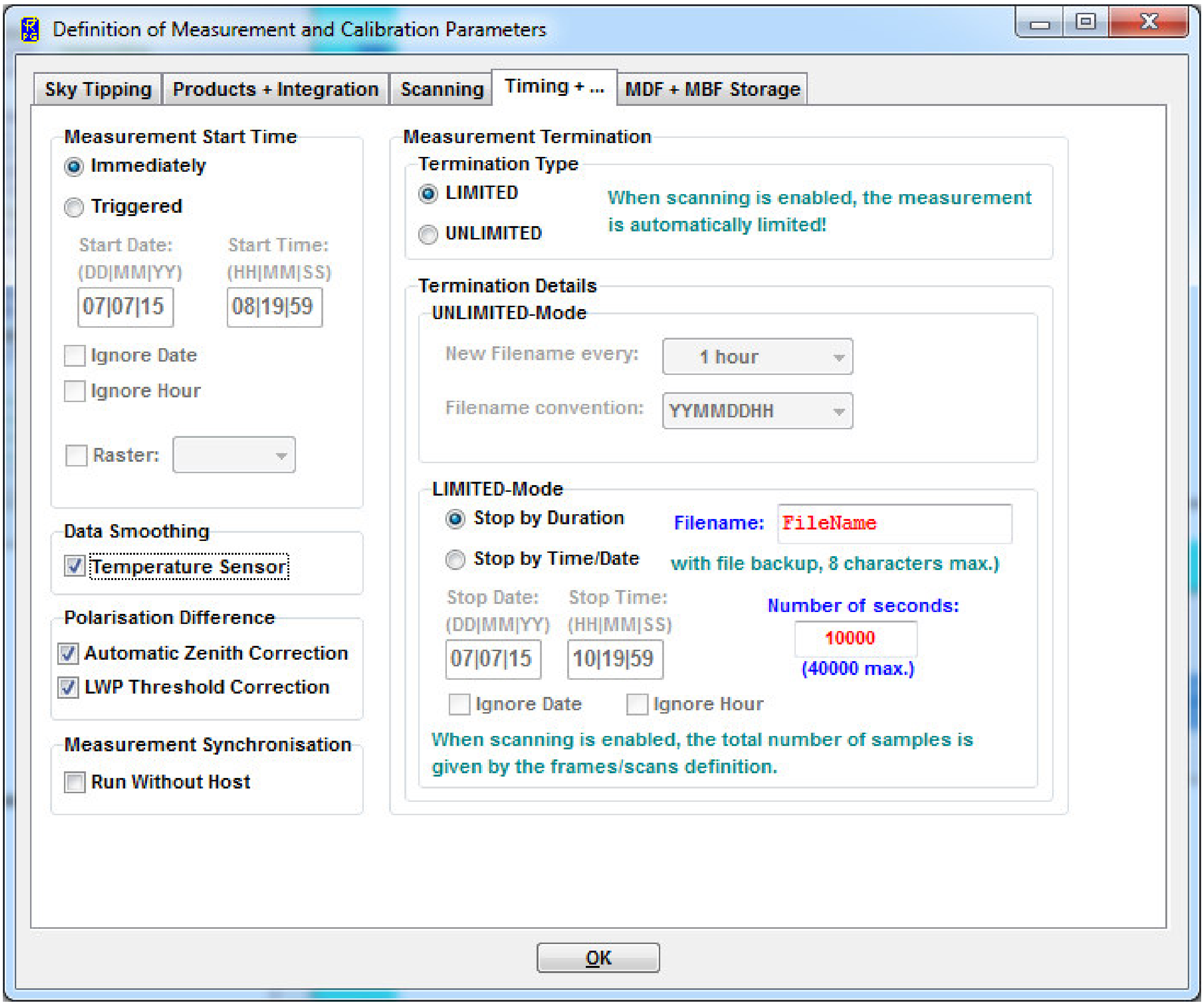

Fig.5.9: Timing definition menu.

In UNLIMITED mode the measurement is terminated manually. A new filename is generated every X hours where X is selected from the ***Filename Interval*** list box. The file format is one of 14 possible versions given in the ***Name Convention*** list box. In the format string HH=hours, DD=days, MM=month and YY=year are taken from the actual time and date. During measurement, this filename is also transmitted to the host, which uses it for file storage of monitored data (assuming the host is operated in ***Enable File Backup*** mode).
Since the temperature environmental sensor responds quickly to changes of the corresponding parameter (caused by turbulence in the vicinity of the radiometer) it is sometimes desirable to smooth the data samples of temperature. The detailed surface turbulence at the radiometer location is not of interest. In ***Data Smoothing*** one can activate a 10 minutes LIFO filter to smooth the environmental temperature readings.
It is useful to activate the ***Polarisation Difference*** corrections in order to maintain zero polarisation difference under conditions when no polarisation difference can occur.
When the radiometer shall be run as a stand-alone unit without the host PC permanently connected to it, the measurement synchronisation must be set to ***Run Without Host*** checked.

5.9.5 MDF + MBF Storage

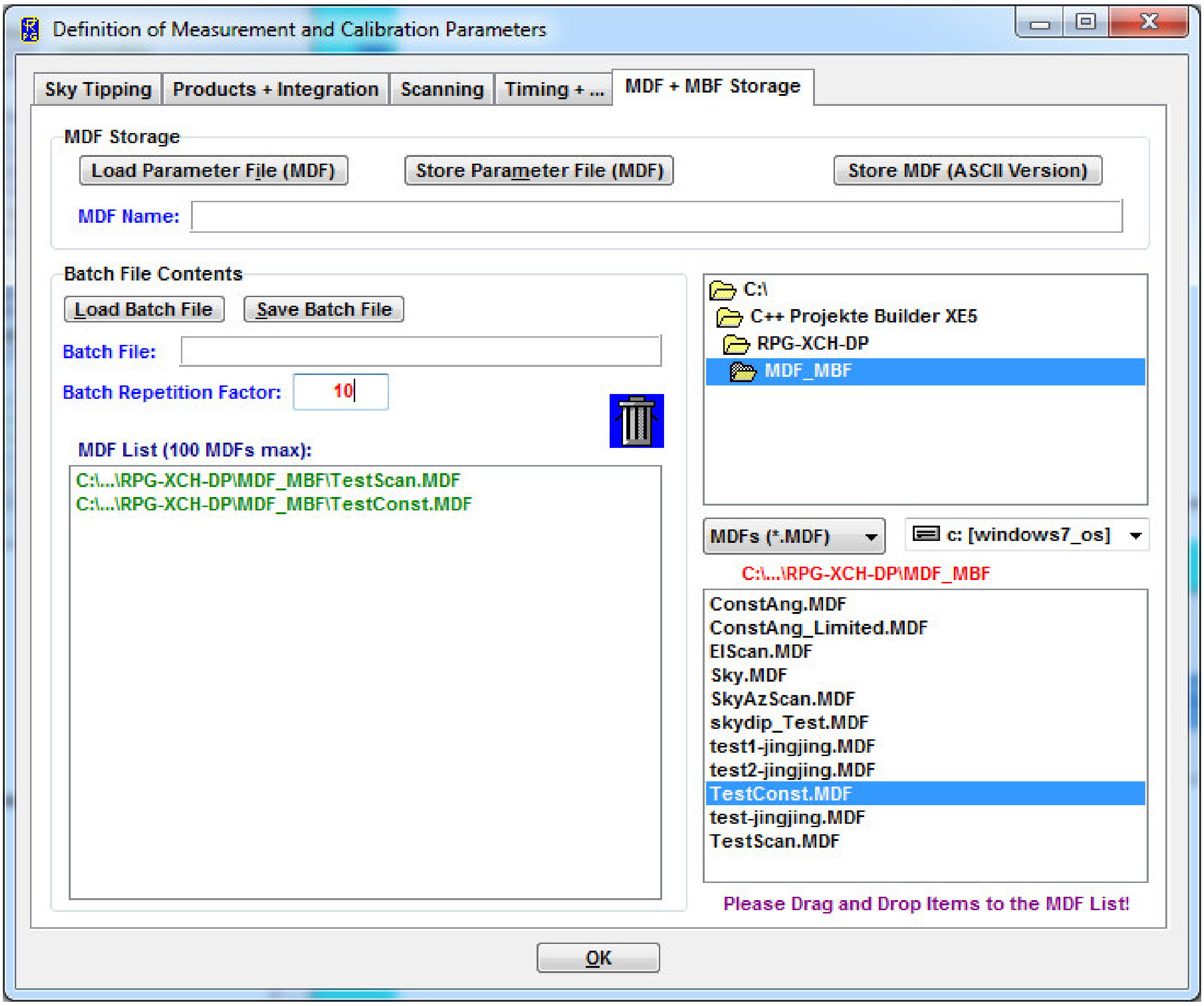

Fig.5.10: Batch file configuration menu.

The MDFs in a batch file are executed sequentially in the order they are listed in the MDF list (see Fig.5.10). The batch repetition number has the same meaning as the frame repetition factor for scanning: The MDF list forms a loop, which is repeated an arbitrary number of times. This offers the user a flexibility of combining different measurement tasks, which would otherwise not be compatible in a single MDF. For instance, if one wants to do a scanning measurement followed by a constant angle measurement and repeat this 10 times the solution is to define two different MDFs, one for scanning and one for constant angle observation and combine them in a batch file with a repetition factor of 10. The only restriction for MDFs in multi-MDF batches is that the UNLIMITED mode must be avoided.

It is a good practice to store all MDFs in one directory (e.g. ***...\RPG-8CH-DP\MDF_MBF***). All MDFs in the selected directory are listed in the box in the lower right corner. From this list the user may select each MDF he wants to add or insert to the MDF batch list (by drag and

drop). MDFs may also be deleted from the MDF batch list. Store your measurement batch files (MBFs) in a single directory (like "…***\RPG-8CH-DP \MDF_MBF***").
If file backup is enabled in the MDFs and the batch repetition factor is >1 there will be only one filename for each MDF. The data of successive executions of a certain MDF in the batch loop is stored to multiple files. Each time the MDF is repeated in the loop, its measurement data is archived to the data directory tree.

5.10 Sending a MDF / MBF to the Radiometer

MDFs and MBFs can be sent to the radiometer (assuming the host is connected to it) from the ***Send Measurement Configuration*** menu by clicking  .
When an MDF or MBF is loaded (***Load MDF/MBF File***), its contents and repetition factor are displayed. In addition some pre-checks are performed, e.g. correct radiometer configuration, frequency list consistency, etc. A variety of other checks ensure that no erroneous command data is sent.
When the consistency check of a MDF is finished, the test result is displayed in the ***Check List***. The batch can only be sent to the radiometer if all consistency checks have finished with the status OK. Then the MBF is automatically transmitted.
The host PC 'remembers' the directory where MDFs and MBFs are stored from a previous ***Load MDF/MBF File***. This directory is marked in red and its content is listed below the directory label. In the list, MDFs are separated from MBFs by a dashed line. Dragging a file (or double-clicking it) from the list and dropping it on the radiometer image on the right sends the MDF / MBF to the radiometer and starts its execution.

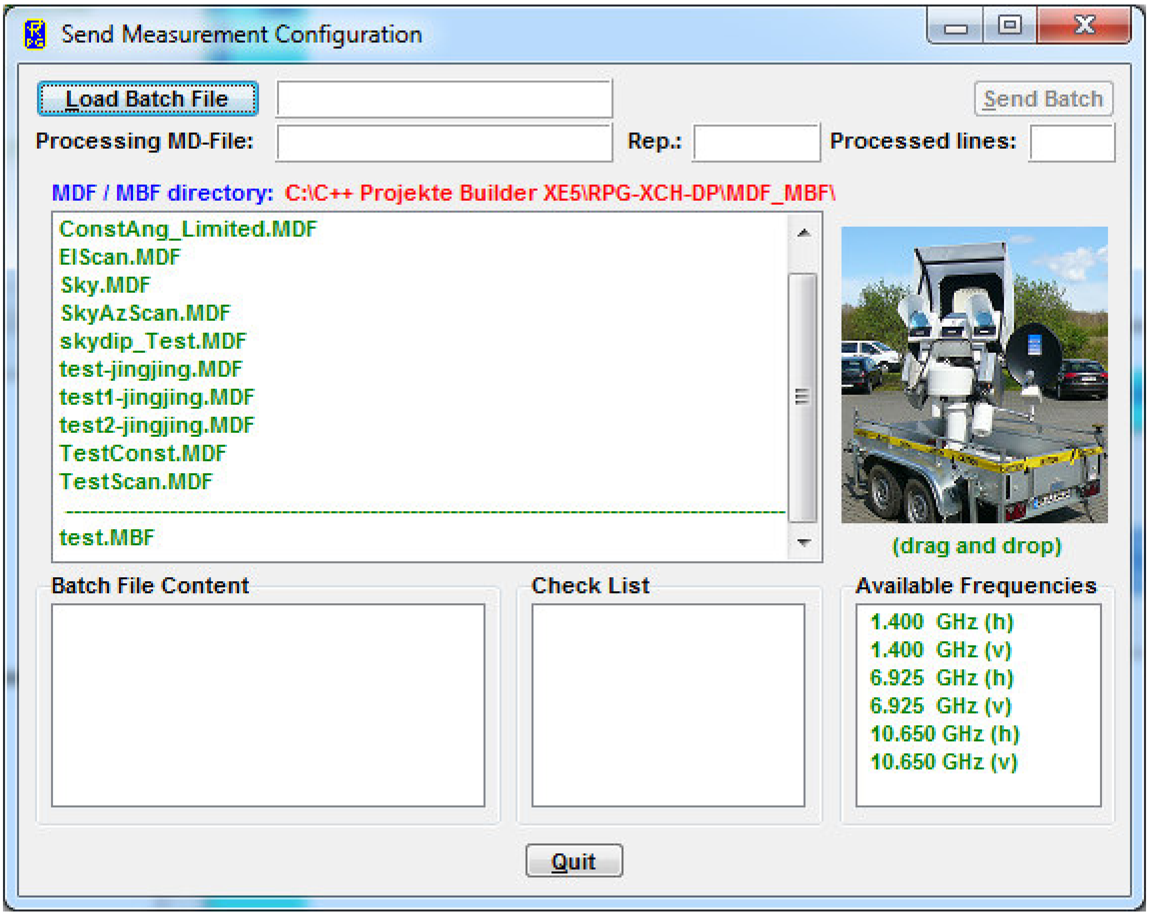

5.11 Commanding the Radiometer Processes

When a valid non-empty MDF / MBF has been transmitted to the instrument the following functions are enabled:

 (***Halt Running MDF/MBF***)
A running measurement can be halted any time except during a calibration. This might be useful when e.g. the user wants to manually change the elevation angle. The status bar display switches to “MEASUREMENT HALTED” and the manual control button (, discussed later) is enabled (among other commands) which offers manual control over elevation stepper and other radiometer features.

 (***Continue Interrupted MDF/MBF***)
Used to continue a halted measurement. The status bar display changes back to “MEASUREMENT RUNNING” and the manual control button is disabled.

 (***Terminate Running MDF/MBF***)
This command terminates the execution of the currently running measurement. The radiometer switches to STANDBY mode and is ready to receive the next MDF / MBF.

5.12 Monitoring Data

The usual way of starting measurements is:

- Define a MDF with (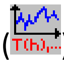).
- Send the batch file to the radiometer (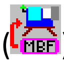).

The monitoring windows of the products that were selected in the MDF are automatically opened and the measured data is displayed (see Fig.5.11). Since the data is transmitted online from the radiometer to the host no additional file transfer is required afterwards. The file backup on the radiometer is activated for safety reasons to prevent data loss in the case of a host PC malfunction (e.g. hard disk crash, etc.).

The time axis scale is modified by selecting the time axis width in the drop-down list of the window. The monitor window displays the current time, date, sample number, sample value and cursor position (if the mouse cursor is moved into the display area).

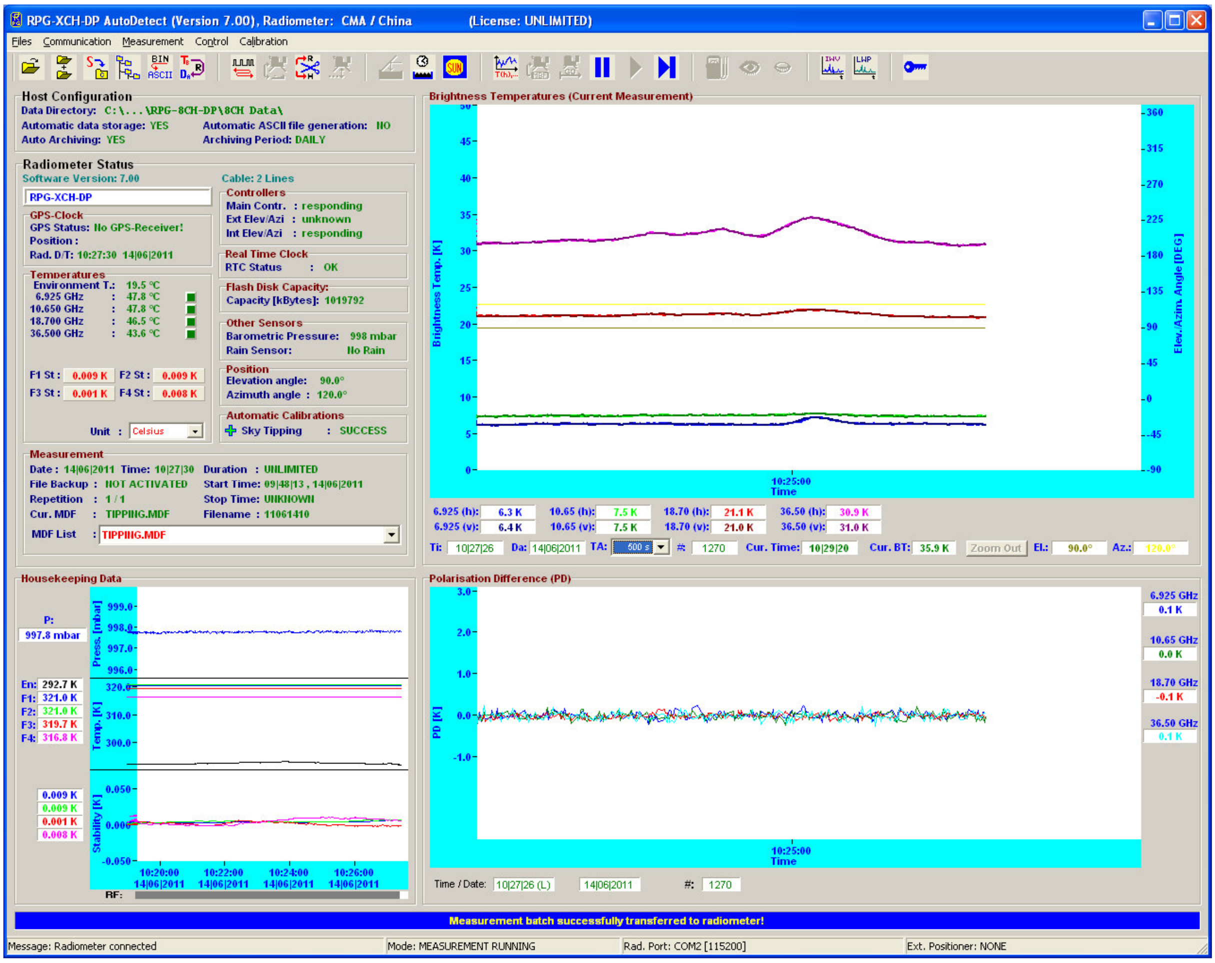

Fig.5.11: Active monitoring window.

5.13 Concatenate Data Files

In UNLIMITED mode the radiometer periodically generates new data filenames (e.g. every hour). It is often desirable to concatenate data files of the same type (*.BRT, *.HKD etc.) to form bigger files (e.g. 24 hour files). This is possible by clicking (***Concatenate Data Files***) which opens the menu in Fig.5.12. A set of filenames is selected from the list and then concatenated to a single file with ***Generate Concatenated File***.
By using the ***Concatenate Daily Files*** command, the file concatenation of complete directories, with or without its sub-directories, may be concatenated to 24 hour files.

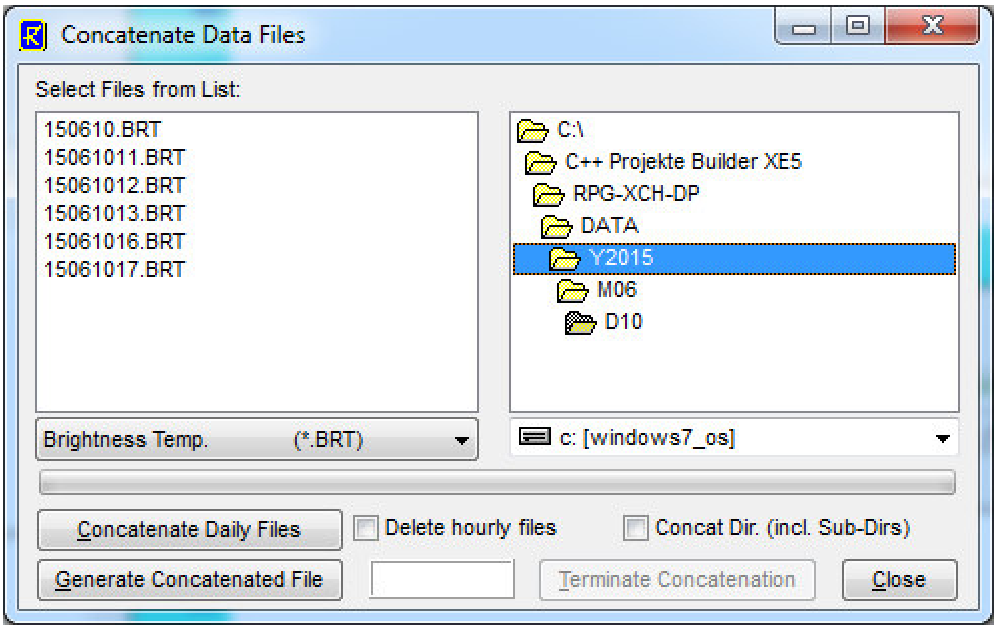

Fig.5.12: File concatenation menu. The user may concatenate multiple files from a file list or perform the concatenation process in complete directories (all types in a row), with or without sub-directories. This way the post processing can be realized in a few mouse clicks for a complete data set, e.g. by selecting a 'year' directory (for instance Y2015).

.

5.14 Cutting Connection

(***Cut Connection to Radiometer***)
If the user wants to disconnect the host from the interface cable or turn off the radiometer after having been connected this command should be used first. It ensures that all communication activities between host and radiometer are disabled.

5.15 Data Display Menus

For each measurement data product a display window is available. Click on the open button and select a product from the pull down list. Then load a product data file. Fig.5.14a is an example of a BT chart.
All data display menus indicate start time, end time, time reference, duration, and number of samples.

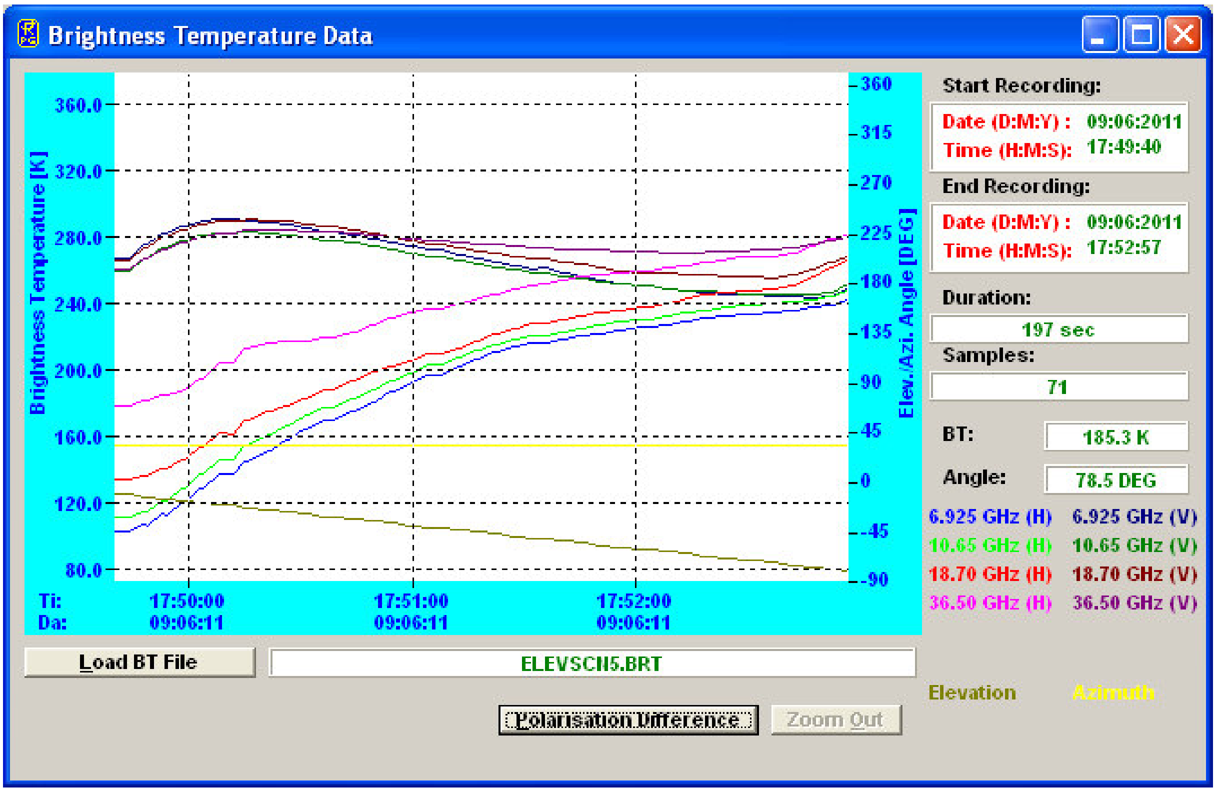

Fig.5.14: BRT chart window.

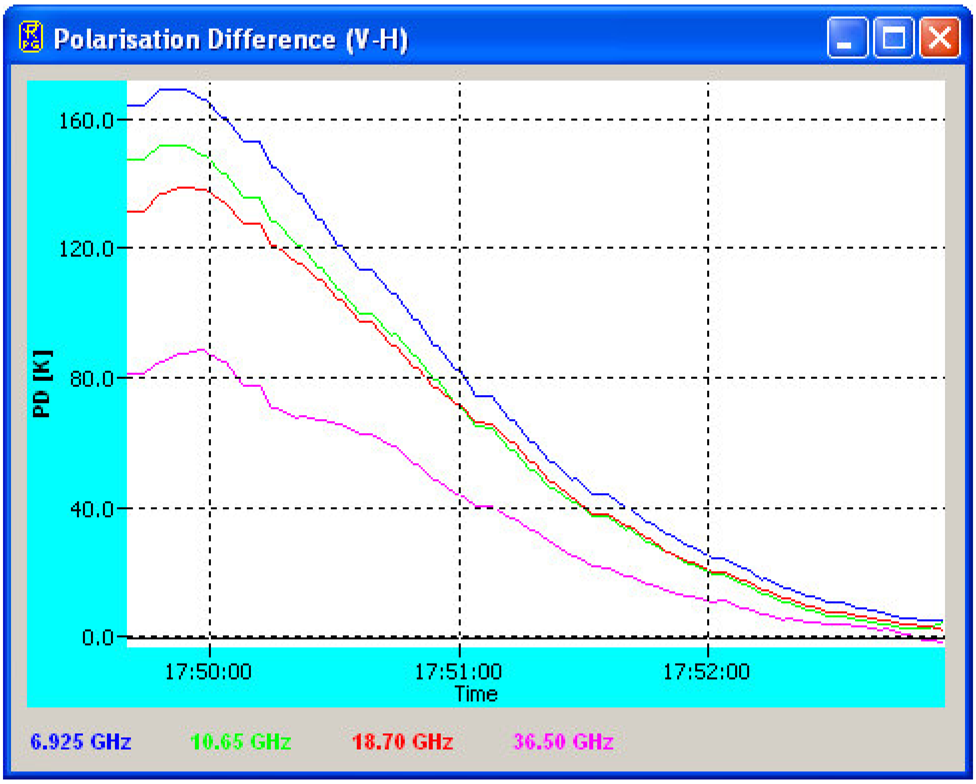

One may zoom into the data by pressing the left mouse button in the display area and drag the mouse to a different position (mouse button still pressed) to define a rectangle (indicated by a black frame). For zooming back click ***Zoom Out***.
Brightness temperature data files contain the elevation / azimuth angle information for each sample. The elevation / azimuth angles are also displayed.
Most display menus can be stretched in size (resized) by positioning the mouse on the menu window edge and drag it to the desired size. The display is then adjusted in size. The Brightness Temperature Data Display menu offers an additional display feature ***Polarisation Difference*** which opens another window showing the difference in the TBs (V-H polarisation).

5.16 Manual Radiometer Control

When the host is connected to the instrument and the radiometer is in STANDBY- or HALTED-mode, the manual control functions are enabled. Click  (***Manual Radiometer Control***) to enter the ***Diagnostics and manual control*** menu in Fig.5.16.
The reason of implementing these functions is mainly for diagnostic purposes. When a radiometer is assembled every single electronic component must be tested. The receivers' long term stability is checked for several weeks by monitoring the detector voltages. However, some of the diagnostic functions are also useful for other tasks.

5.16.1 Positioner Control

The ***Positioner*** tab sheet is used (for instance) to change the observation angle during a measurement in HALTED mode. If ***Reset Position*** is checked the stepper is reset to its original position after leaving the diagnostics menu. If the user wishes to keep the new position he must uncheck ***Reset Position***.
Stepping positions can be set relative or absolute in DEG. The absolute elevation stepper positions in elevation are as follows:

- Zenith: +90°
- Horizontal: 0°
- To ground: -90°

The angular stepper resolution is 0.01°. The azimuth value range is set to 0° to 360°
With the **<<**, **<**, **||**, **>**, and **>>** keys the positioner can be moved. Slow and fast motions can be selected and stopped by clicking the **||** button.
The user should not manipulate the driver parameters in order to maintain a smooth positioner motion.

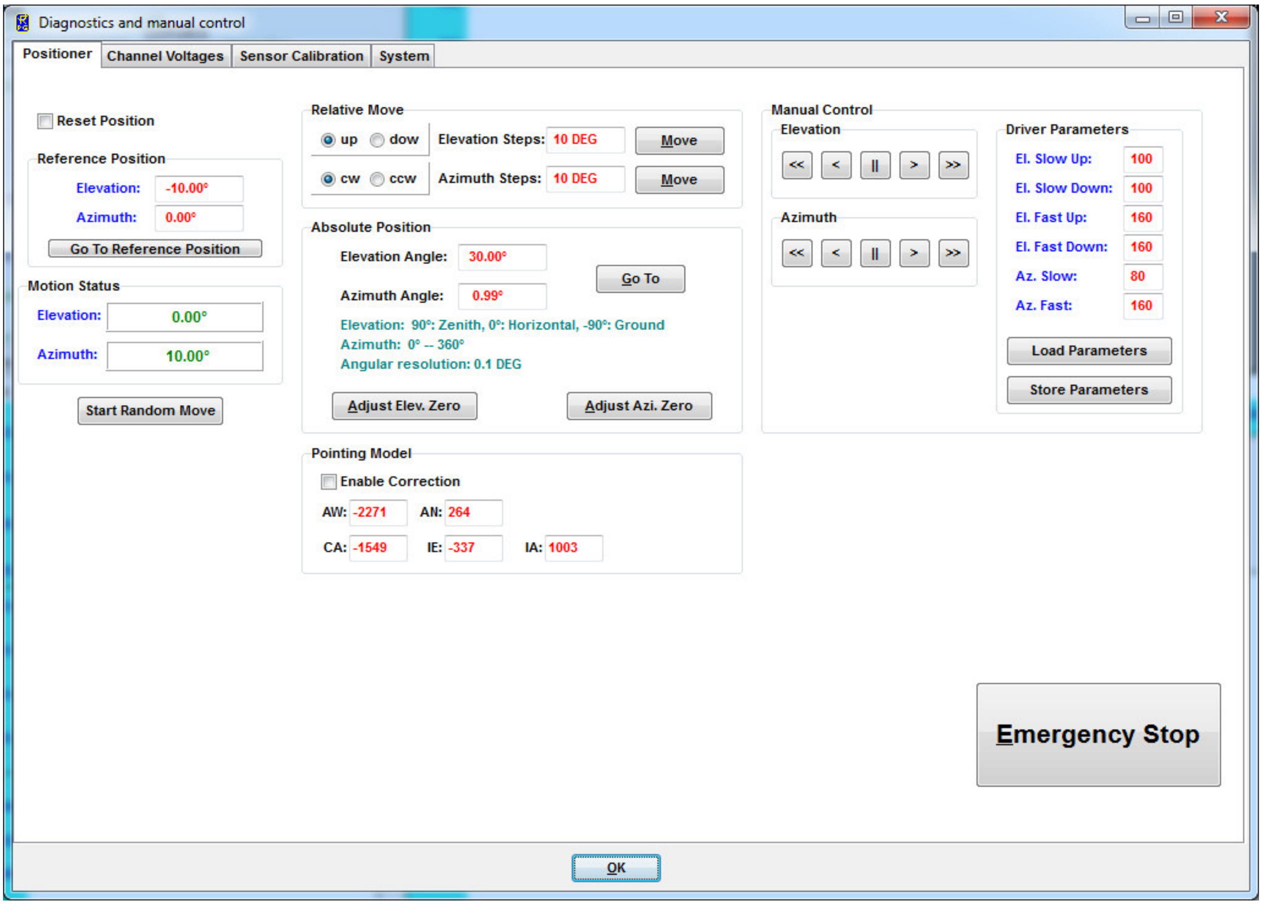

Fig.5.16: The positioner control tab sheet.

5.16.2 Channel Voltages

The ***Channel Voltages*** tab sheet is the main diagnostics tool (Fig.5.17).
The following data is displayed:

- Receiver 1-4 detector voltages (1:1)
- Receiver 1-4 board temperatures (T=voltage*100 [K])
- Environmental temperature (T=voltage*100 [K])
- Barometric pressure (P=voltage*1000 [mbar])

The sample rate and maximum number of samples are set in ***General Parameters***.
While sampling detector voltages, one can manually turn the noise diodes on and off to check for a correct operation (***Noise Diode***). The channel readings are displayed graphically and also in the ***Receivers*** frame. Data zooming is possible. After stopping the sampling one can use a ruler to measure the precise voltage at a certain time (↕).
Reset clears the acquisition display and sets the Y-axis to +5 V (maximum).

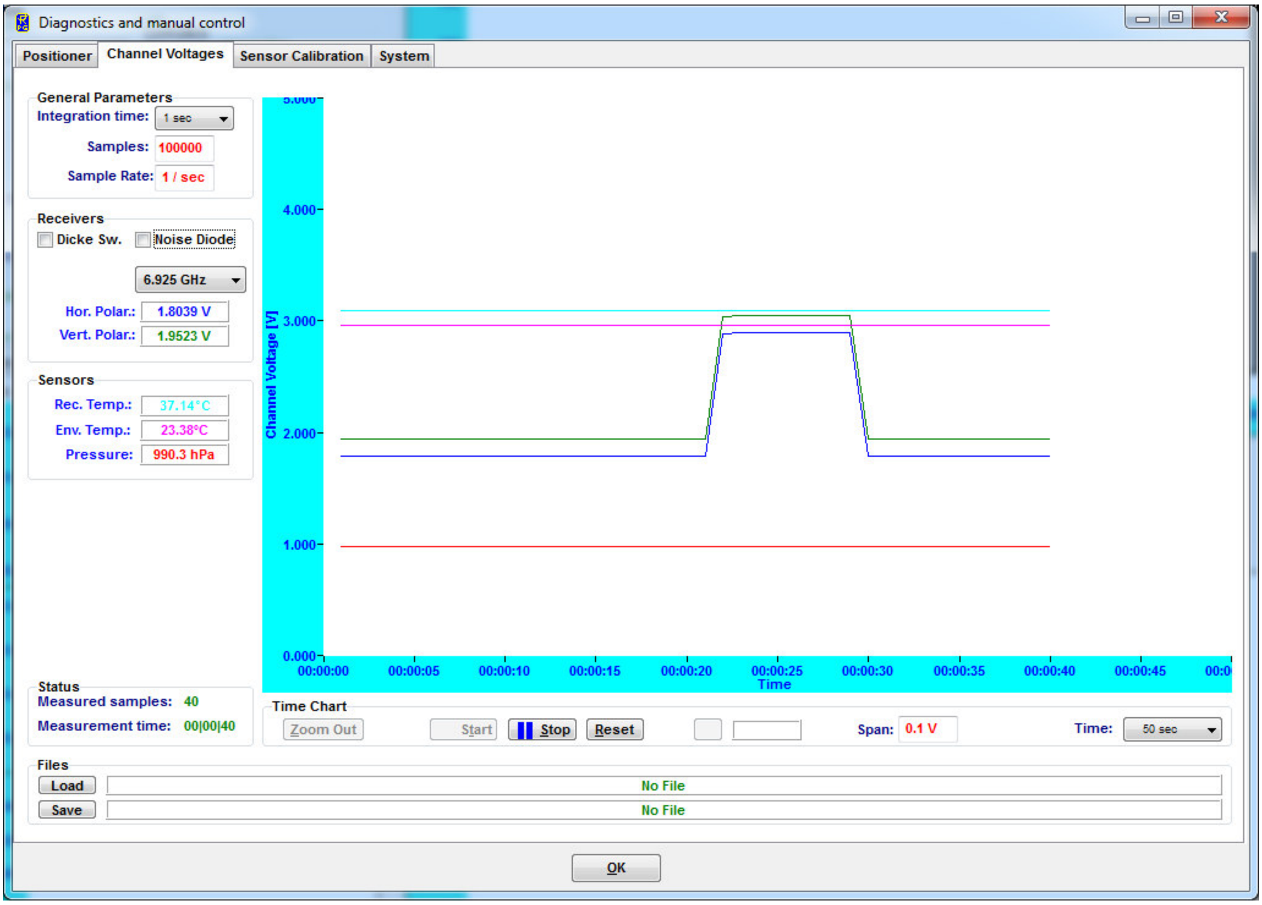

Fig.5.17: Channel voltages tab sheet.

5.16.3 Sensor Calibration

This tab sheet is used to calibrate the thermal sensors and pressure sensor. It is not intended for user purposes. The sensor calibration must be performed by qualified personal only and is done before the radiometer delivery.

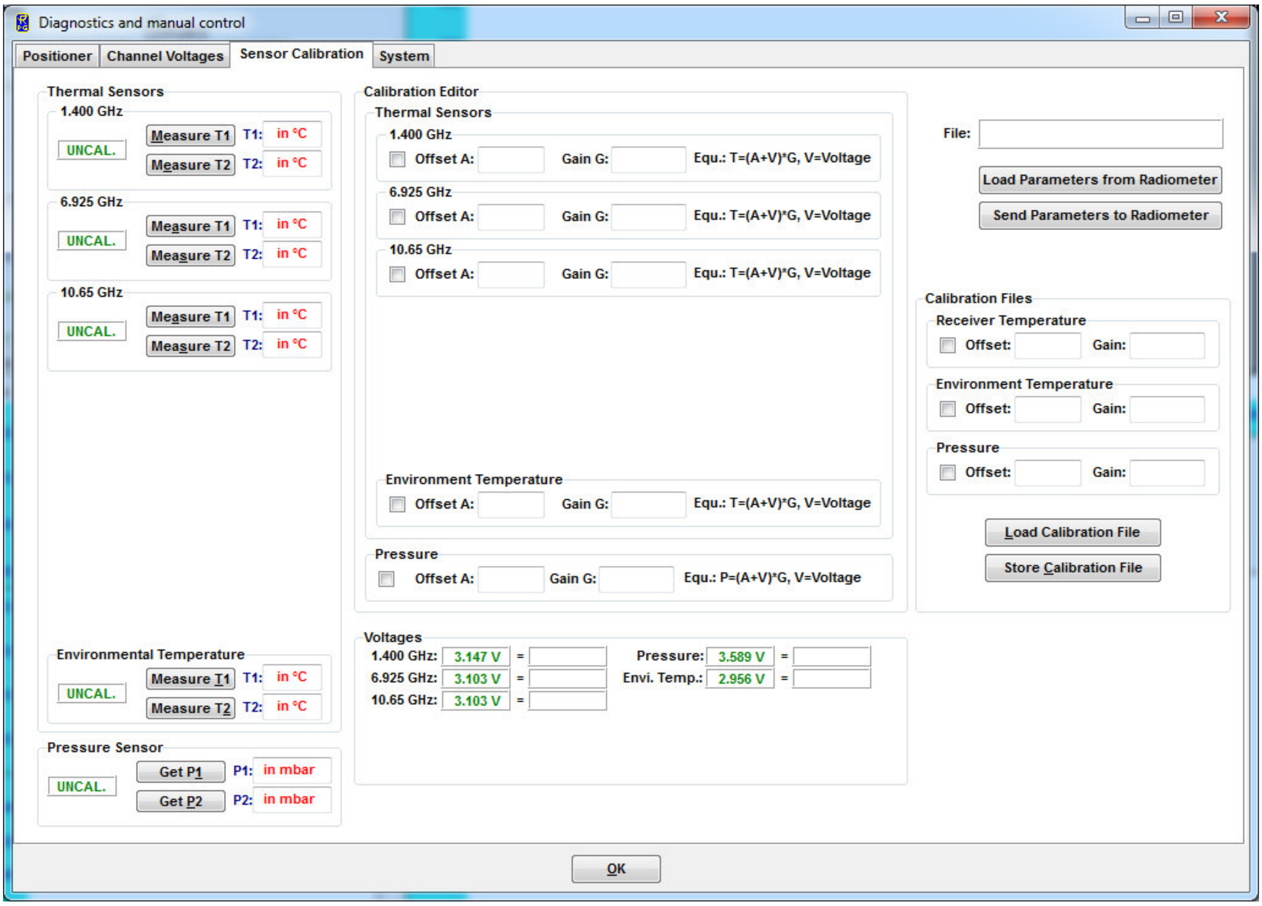

Fig.5.18: Sensor calibration tab sheet.

5.16.4 System

The tab sheet in Fig.5.19 is related to system issues.
A very useful feature is the ***Reload Radiometer SW*** function. When a radiometer software update has been performed by transferring a new ***XCHDP_R.EXE*** file to the radiometer's root directory, a software reload is required to run the new software version. When clicking on the ***Reset Radiometer PC*** button a warning message is displayed to inform the user that if he confirms to continue this command this will result in a radiometer reset and requires a re-connection to the radiometer afterwards.
The radiometer is capable of an automatic recovery from power failures. When a MDF is sent to the radiometer, the measurement parameters are stored on the radiometer's internal SATA DOM. This information is deleted when a measurement is terminated. In the case of a power failure, the parameter file(s) are not deleted and after power return the software checks for undeleted parameter files. If recovery mode is activated, the radiometer

PC automatically restores the measurement that had been interrupted by the power failure. The commands ***Set Recovery Mode***, ***Clear Recovery Mode*** and ***Read Recovery Mode*** allow the user to activate / deactivate this mode.
The other features of the 'System' tag are reserved for system engineers and should not be touched by operators.

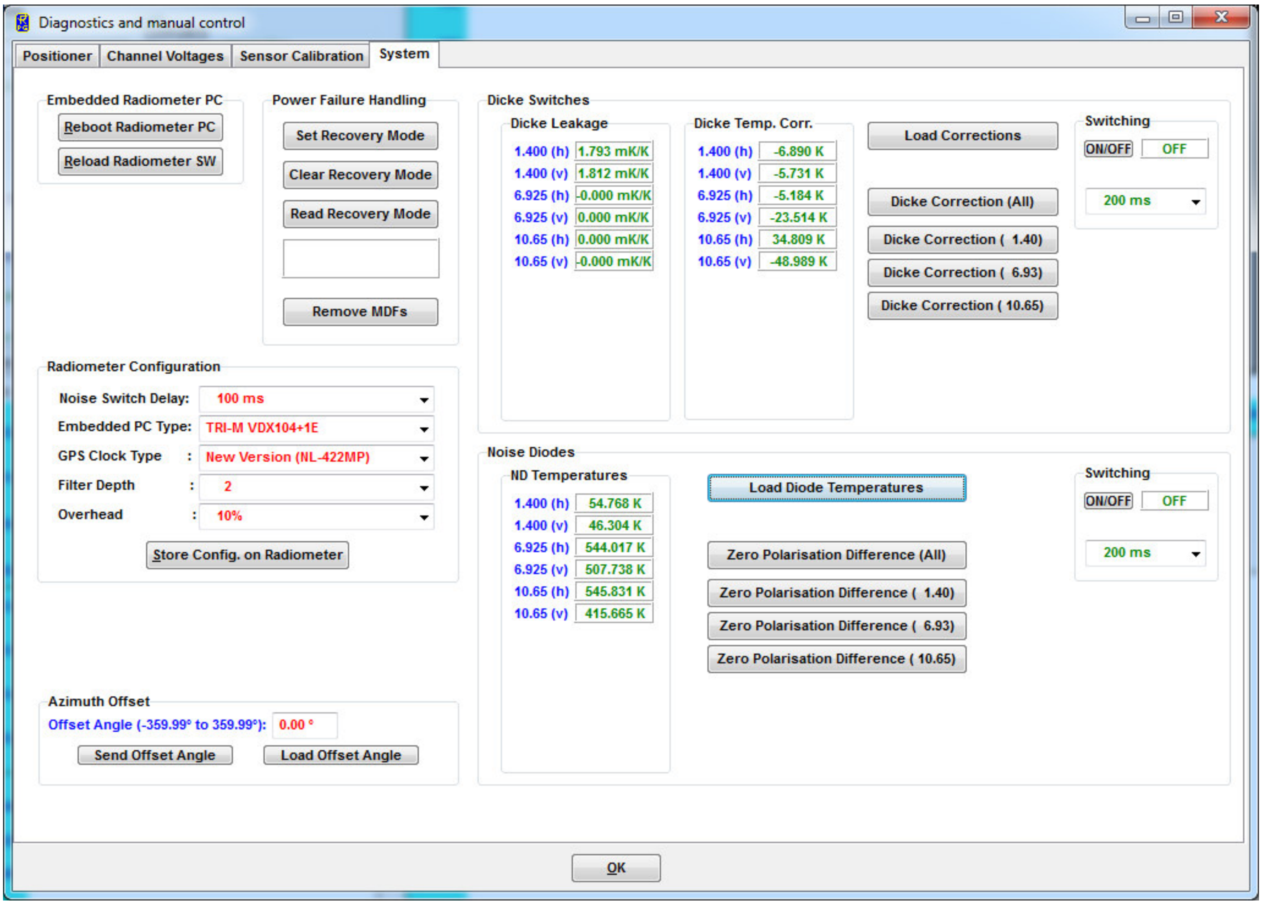

Fig.5.19: System settings.

5.17 Transform Data Files to ASCII Format

The standard data file format is binary (file structures listed in Appendix A) because it is more compact than other formats. In the case that a readable format is required the binary files can be transformed to ASCII. By using the  command (***Transform Data Files to ASCII Format***) a binary data file is converted to an ASCII file. The file name of the new file is the binary file name with appended '.ASC', for instance the BT binary format file ***MyFileName.BRT*** is converted to ***MyFileName.BRT.ASC***.
Beside this manual ASCII file generation it is possible to automatically store data in ASCII format during the monitoring process (active measurement). See section 5.4 for details.
Examples of ASCII files are described in Appendix B.

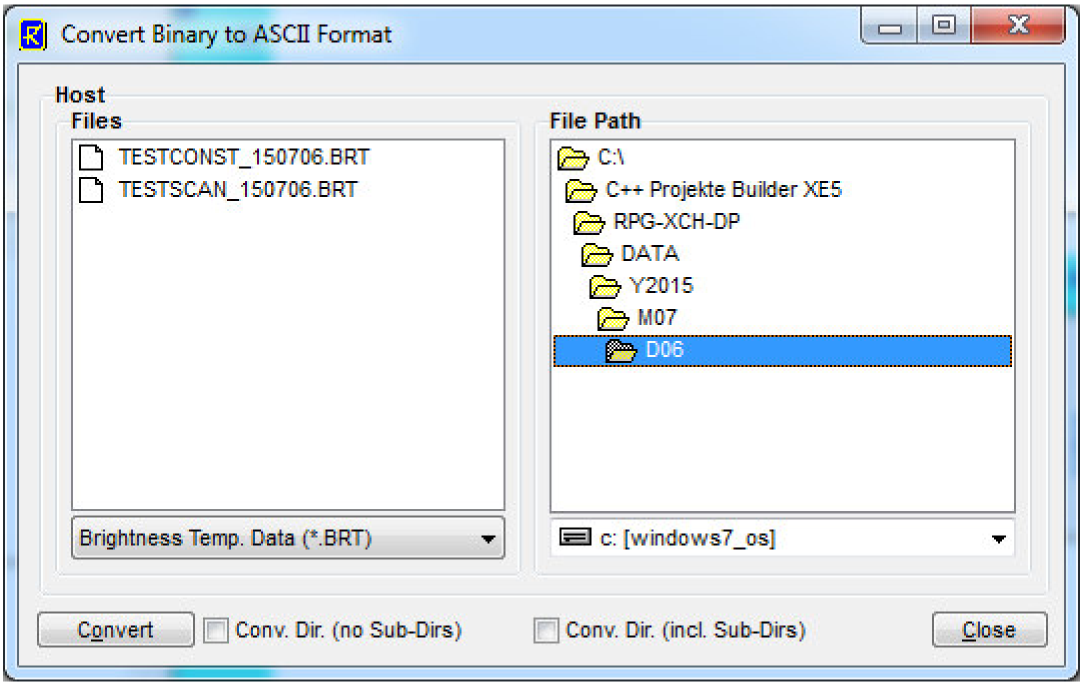

5.18 License Manager

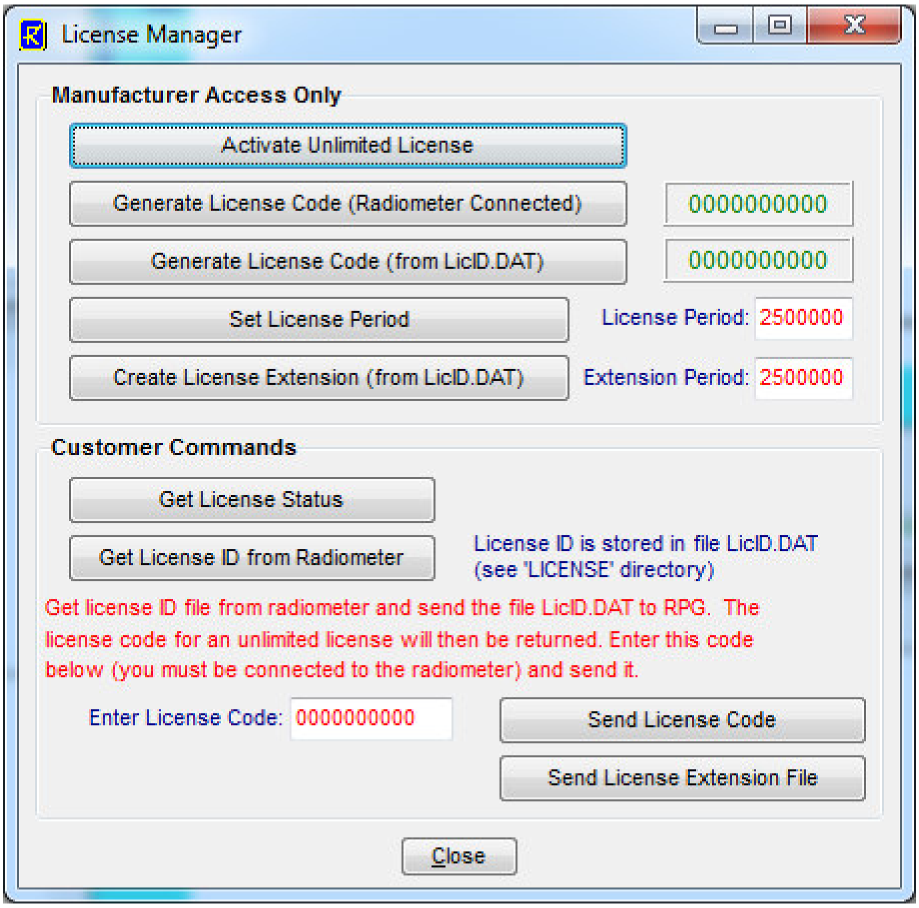

License manager menu.

RPG's radiometers are delivered with a preliminary limited license of 30 days. Without activating an unlimited license, the radiometer will stop measurement execution when the limited license is expired. The common procedure to avoid this is the following:

Invoke the **License Manager** by clicking the button. The menu below pops up.

The user retrieves license status information with the ***Get License Status*** command. The license type (limited or unlimited) as well as the expiration date and time will be displayed. In order to obtain an unlimited license, the following steps have to be performed:

1. Connect to the scintillometer and click the ***Get License ID from Scintillometer*** button. The license ID code is then written to the file 'LicID.DAT' stored in the license directory …***LICENSE*** (see section 4.1.2).
2. Send the 'LicID.DAT' file to RPG (by e-mail to info@radiometer-physics.de). Then the 10 digit license code will be returned (also by e-mail).
3. Enter the 10 digit license code into the edit box in the license manager and click ***Send License Code***. The license manager will inform the user if the unlimited license installation was successful or not. If not successful, please contact RPG again.

5.19 Software Updates

Sometimes it is desirable to update the radiometer and host software version, in order to add advanced features to the data processing or to correct software bugs.

The radiometer SW is running on an embedded PC and is named ***XCHDP_R.EXE***. This file is located in the radiometer's root directory ***C:\RPG-XCHDP-R***.

The host SW name is ***XCHDP.EXE*** and it is located in the application's root directory (…***RPG-XCHDP***) on the host PC.

For a SW update the following steps should be followed:

1. Step: Save the old software versions

a) Create a directory to save the old software versions (e.g. ***C:\MyPath\Save***).

b) Connect the H-PC to the radiometer and enter the File Transfer Menu ( ). On the left side (H-PC, 'This PC (Host)') browse to the directory for saving the files (e.g. C:\MyPath\SAVE) and on the right side (Radiometer) in the …***RPG-XCHDP-R*** directory mark the ***XCHDP_R.EXE*** file. Then click ***←Copy Selected Files***.

c) Locate the ***XCHDP.EXE*** file in the …***RPG-XCH-DP*** directory on the H-PC and copy this file to the ***C:\MyPath\Save*** directory (by using the Operating System File Explorer).

2. Step: Overwrite the old versions by the new ones

a) Copy the new version of ***XCHDP_R.EXE*** (the R-PC software) to an arbitrary directory on your host PC (e.g. …***RPG-XCH-DP\Radiometer PC***). In the file transfer menu, browse to that directory. Mark the ***XCHDP_R.EXE*** file in the file list within the ***This PC***

(Host) box and mark the …***RPG-XCHDP-R*** directory in the ***Radiometer PC (Embedded)*** box. Click the ***Copy Selected Files→*** button. Because you are now going to overwrite a file in the radiometer's root directory, you must enter the Administrator password to proceed.

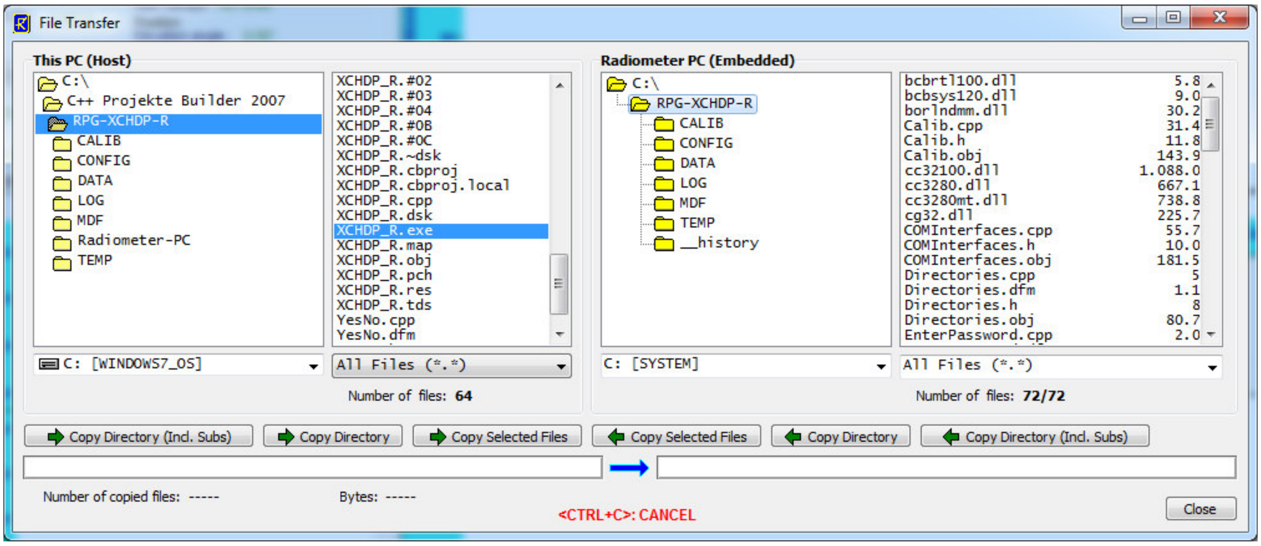

File Transfer Menu during software update procedure.

b) Reload the R-PC software as described in section 6.16.4 to run the new ***XCHDP_R.EXE*** version. Wait for approximately 30 seconds until the R-PC has finished its booting process.

c) Terminate ***XCHDP.EXE*** on the host and overwrite it by the new version.

d) Execute ***XCHDP.EXE*** and reconnect to the radiometer.

The software upgrade is finished. You can confirm the successful upgrade by reading the software version numbers of both, the embedded R-PC (see main window, ***Receiver Status*** box on the right side) and the H-PC (see main window caption).

5.20 Application Size on Screen

The host SW can scale the application to almost any common screen size. This may be useful if you want to use a beamer to display the host application in the beamer's screen resolution and size.

Click 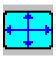 to enter the **Application Size** menu:

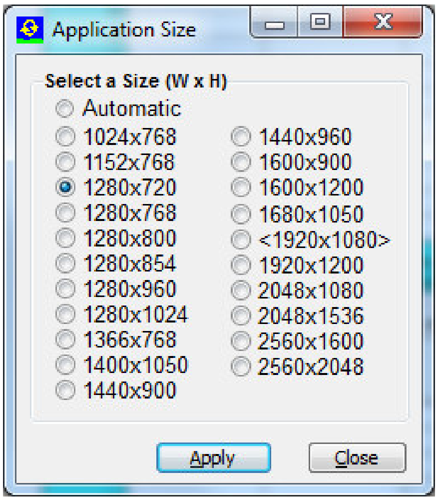

The screen size in brackets <…> is the host's maximum screen size but you can select any (smaller) sizes to fit the application on other screens (like a beamer). The application sizing can be done any time, even during a running measurement.

6. Instrument Maintenance and Recommendations

This chapter summarizes recommended maintenance activities to ensure a reliable radiometer operation.

6.1 Cleaning

Due to environmental conditions the radiometer can be covered with dust, spider webs, etc. The following should be considered:

- Cleaning the microwave windows: Clean the microwave windows once per month with pure water or soap and a soft cloth. Never use any aggressive chemicals like acetone, alcohol, benzene or others. These substances might damage the window coating.
- It is recommended to cover the radiometer with a tarpaulin when not in use. This is in particular advisable if the instrument is exposed to a lot of dust, humidity and rain.
- Cleaning of radiometer housing: Clean the housing of the radiometer every few month. Use a soft cloth and soap and water.

Fig.6.1: Location of the microwave windows for cleaning.

6.3 Maintenance Schedule

In the table below the given maintenance intervals are average periods. Depending on the deployment site these intervals should be optimized. For instance required cleaning intervals strongly depend on climate zones (arctic, sub-tropic, etc.), the vicinity to polluted areas (cities, sand deserts, airports etc.) or the abundance of insects or other animals (e.g. spider webs).

Activity	Recommended Service Interval
Cleaning of radiometer housing	3 month
Cleaning of microwave window	2 month
Cleaning of cooler slits	12 month
Absolute calibration with liquid nitrogen or sky tipping	6 month
Inspection of cables	12 month

6.4 Resetting of Radiometer Embedded PC

Sometimes it is necessary to reset the internal embedded PC. This may be the case after disconnecting the radiometer from the host computer during a measurement or after transfer of a new software version. Fig.6.2 shows the location of the embedded PC interface which is protected from humidity and dust by a black plastic cover. When this cover is removed the PC's interface connectors (monitor socket, 2 USBs for keyboard and mouse and reset button) become visible. By pressing the reset button the embedded PC is rebooted. After 2 minutes this initialization is finished and the user can connect the host to the radiometer PC by clicking on  (***Connect to Radiometer***). **Do not forget to re-install the black plastic protection cover.**

The radiometer can also be reset by turning off the power and turn it on again. This will require a re-balancing of the thermal stabilisation system which requires about 5 minutes. It is therefore recommended to reset the PC by using the reset button.

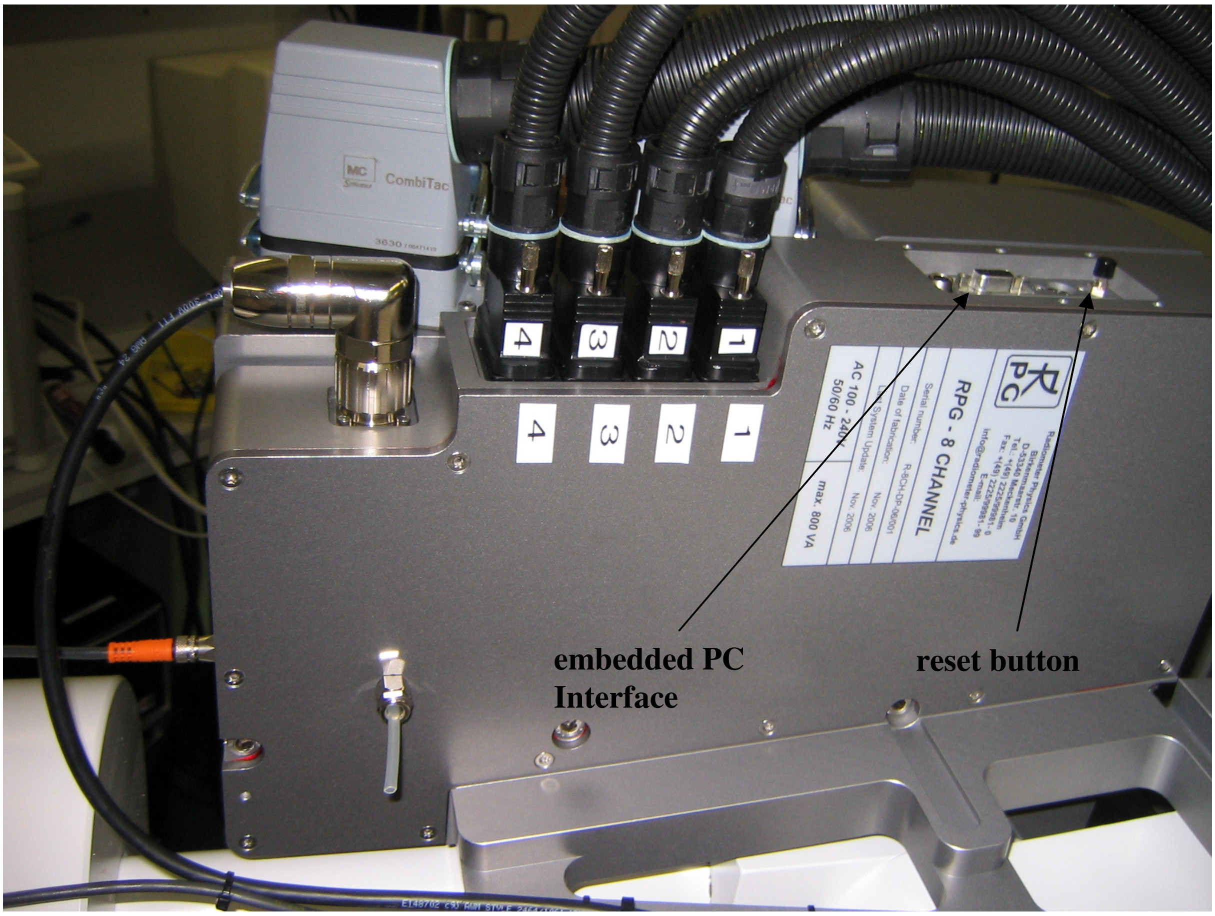

Fig.6.2: Position of radiometer PC interface and reset button.

6.6 Instrument Viewing Range

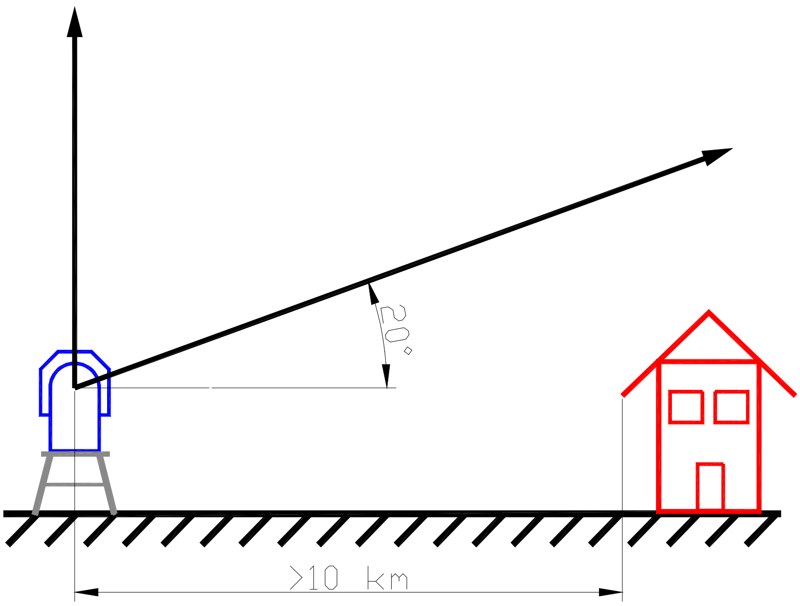

Fig.6.3: Tip curve calibration viewing range.

Fig.6.3 shows the requirement for the free viewing range when sky-dip (tip curve) calibration is enabled. The radiometer performs an elevation scan from zenith to close to 20° elevation. No obstacles should be in that viewing range to ensure a good calibration.

6.7 Adjusting Azimuth Positioner Direction

The host software includes the possibility of precisely adjusting the azimuth scanner's zero index position to North direction. This is useful for volume scans or when different instruments shall be aligned to the same scanning directions. The described method assumes that the instrument stand is horizontally aligned (see Installation Manual).

The azimuth adjustment menu is entered with the 

command, as shown in Fig.4.33.

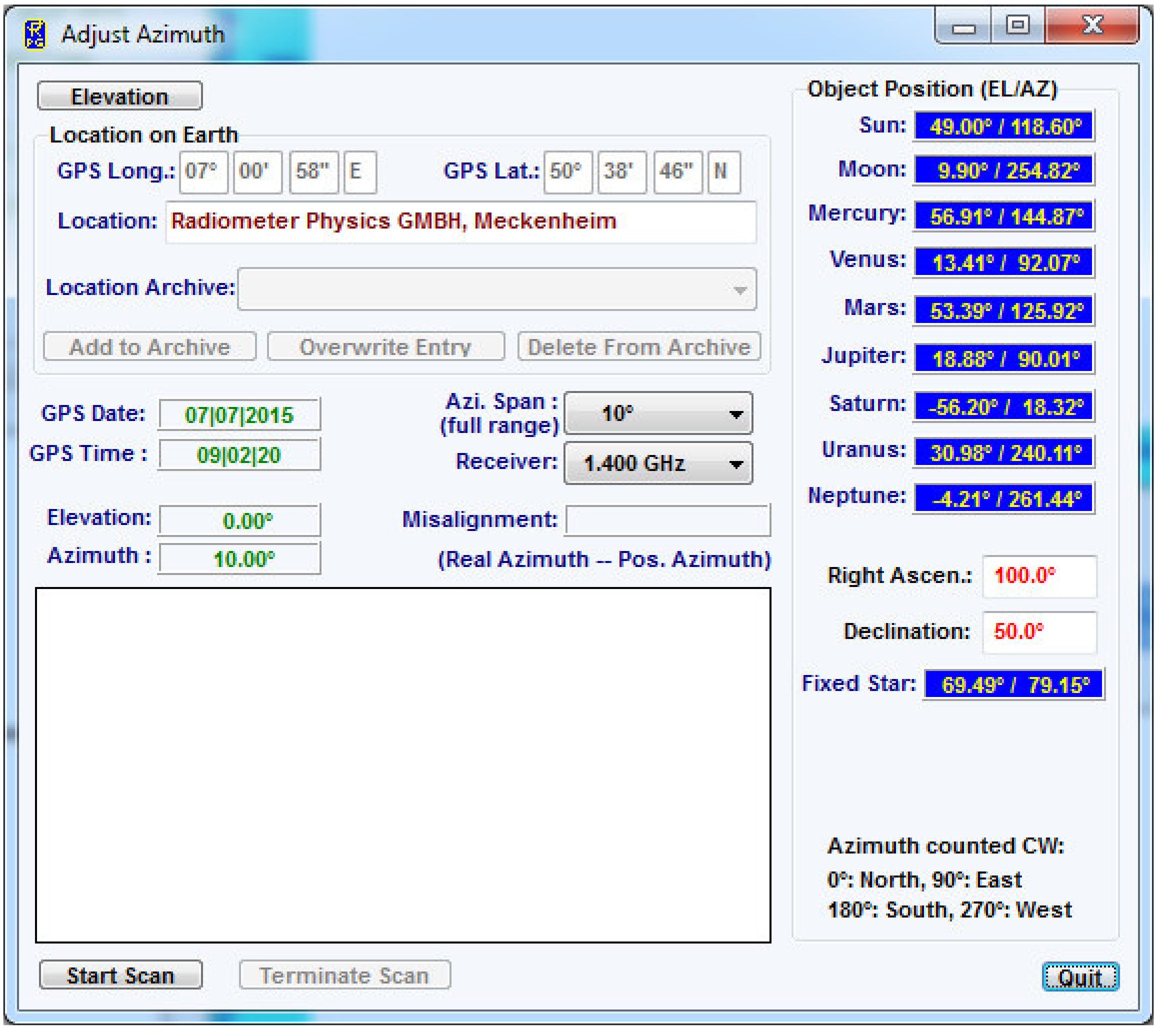

Fig.4.33: Azimuth angle adjustment using the sun position.

The host software calculates the sun position in elevation and azimuth from the GPS position and UTC time available from the GPS clock. The radiometer stand should be pre-adjusted so that the azimuth scanner's zero position is pointing to North with an accuracy of better than 30°. This can be easily achieved with a standard low cost compass.

The user should start the adjustment procedure with a relatively wide azimuth scanning span (e.g. >=50°) and start the scan (click ***Start Scan***) as shown in the upper left corner of Fig.4.33. After the scan is finished, the misalignment between the real north direction and the scanner's north direction is printed in the 'Misalignment' box. A positive misalignment indicates that the stand is directed towards the West and should be rotated eastwards. In an iterative process like indicated in Fig.4.33, the stand's orientation can be adjusted to the real North with an accuracy of better than 0.5°.

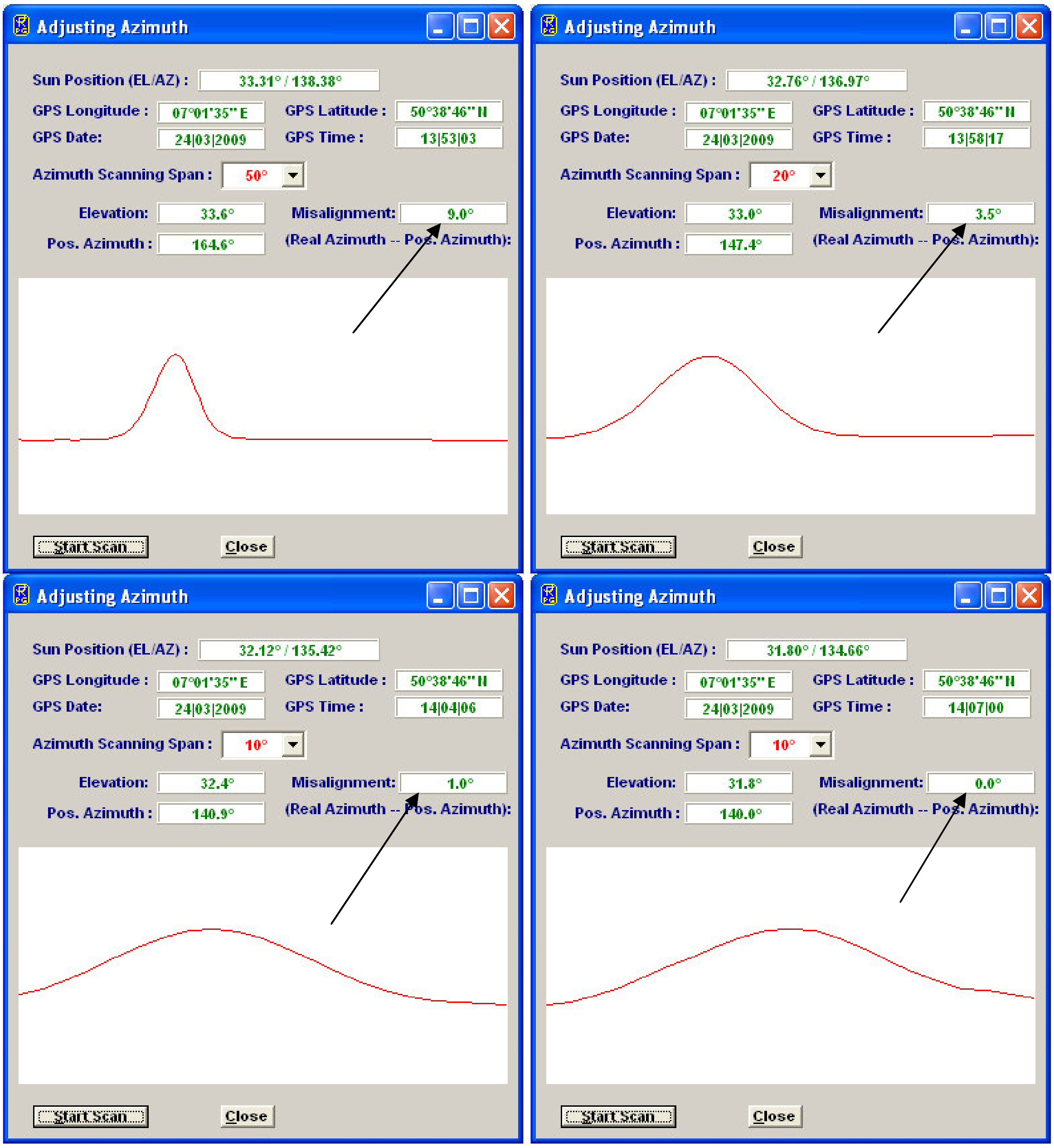

The radiometer uses the receiver's detector voltages as the display data. Therefore, the north alignment can be performed even with an un-calibrated radiometer.

The host software includes the possibility of precisely adjusting the azimuth scanner's zero index position to North direction. This is useful for volume scans or when different

6.8 Operation Safety Issues

The RPG dual polarization radiometers are huge and heavy instruments. The installation and operation of these systems requires the application of a few safety rules which are listed below together with their international signs:

1) The radiometer is made for outdoor use only. Operating the positioner inside a building requires the permanent attention of trained personal. A remote operation inside a building is forbidden!

2)  Turn off the radiometer power, while working on it.

3)  The radiometer rotates 360° about its azimuth axis and +/- 90° about its elevation axis. The positioner applies strong forces to lift the several hundred kg heavy equipment. During operation, keep a safety distance of at least 2 m from the radiometer.

4)  While the positioner is moving, keep away your hands from the instruments. Otherwise there is the risk of crushing hands, arms or legs. The strong forces of the positioner can easily brake bones!!

5)  For safety reasons, install a fence around the radiometer for warning people to enter the danger zone (a circle of 2 m radius circle around the centre of the radiometer).

6)  When installing the radiometer, make sure the

power cord is plugged into a power socket with proper grounding pin (PE = protection earth). Otherwise, the radiometer parts are electrically floating and the instrument may get more easily hit by lightning strokes. The user may also get accessed to high voltages when touching the instrument, if the PE pin is not connected.

7) 

Use at least 2 people to carry the module boxes and when installing them on the mounting table. The heaviest module (combination module 6.9 / 10.7 weights about 30 kg).

6.9 Dimensions

1. **Medium duty El/Az positioner:**

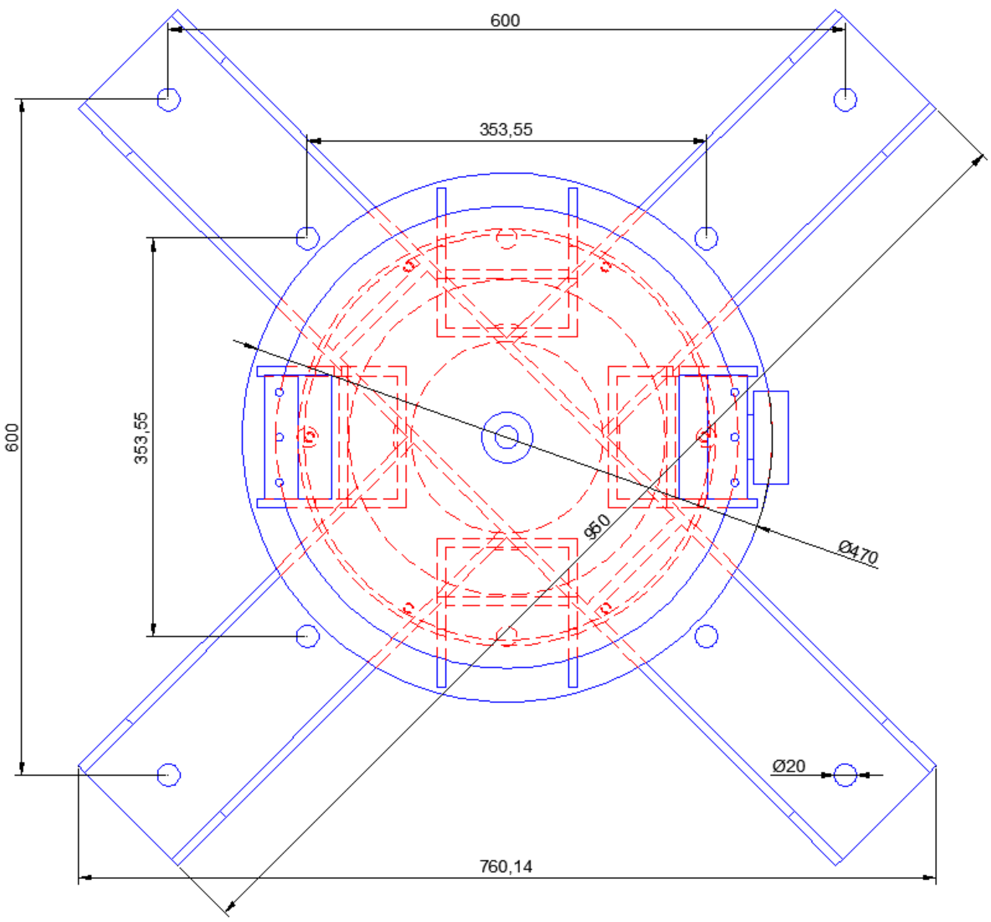

Positioner base, dimensions in mm.

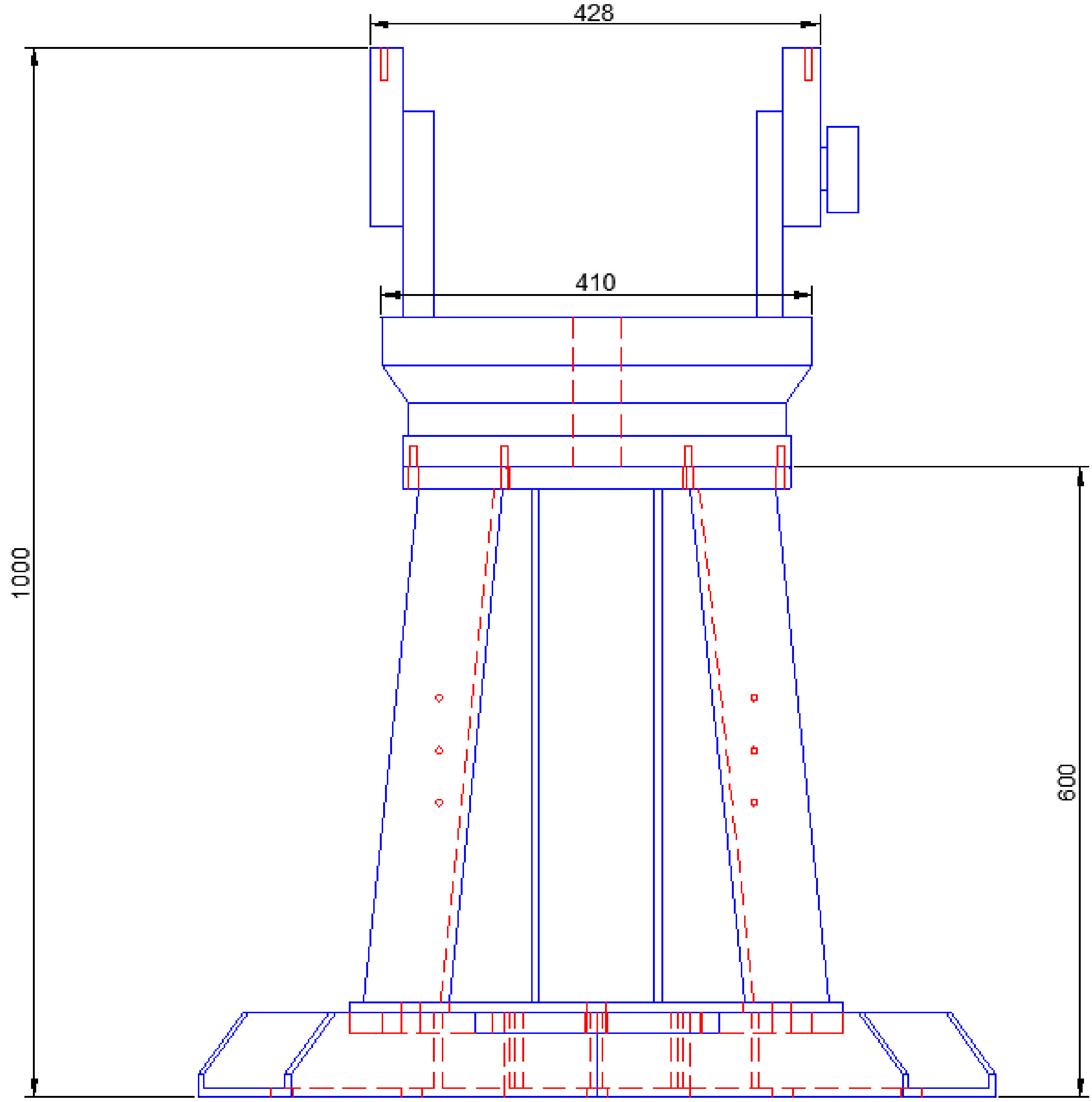

Positioner weight: 70 kg

Example:

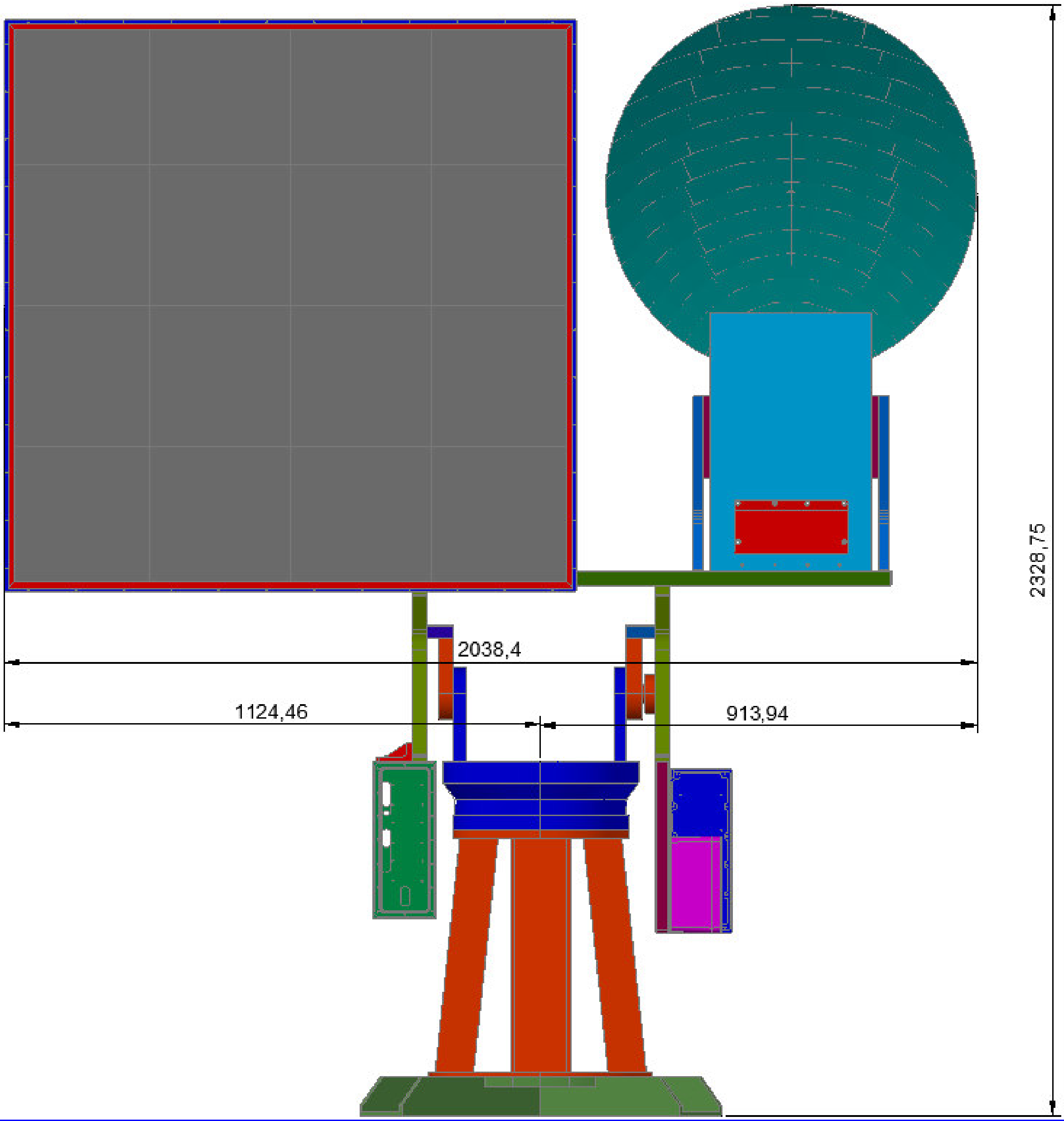

Medium duty positioner with L-band antenna plus 6.925 / 10.7 GHz combi-module.

2. Heavy duty El/Az positioner:

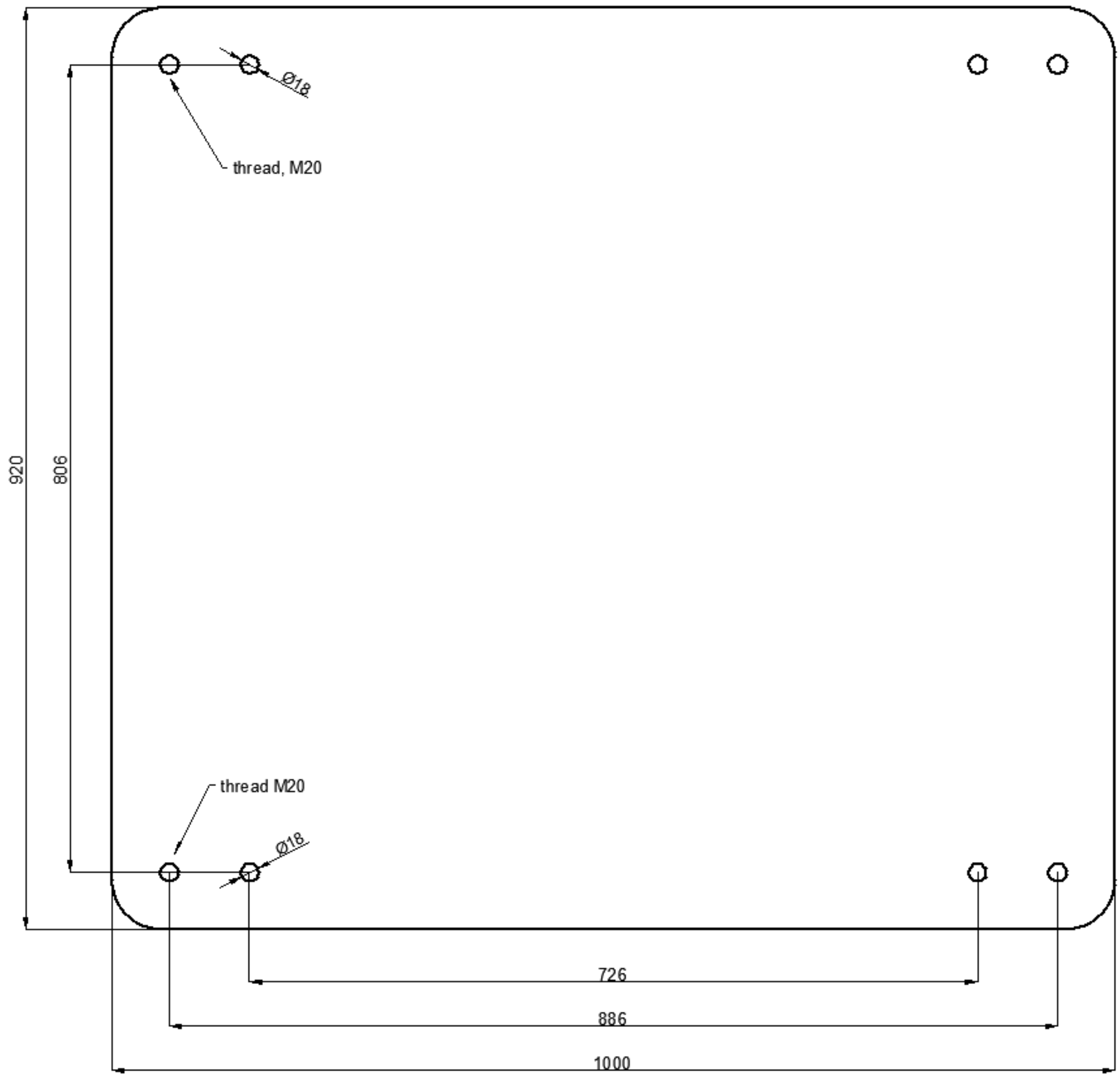

Base plate of heavy duty positioner, all dimensions in mm.

Example:

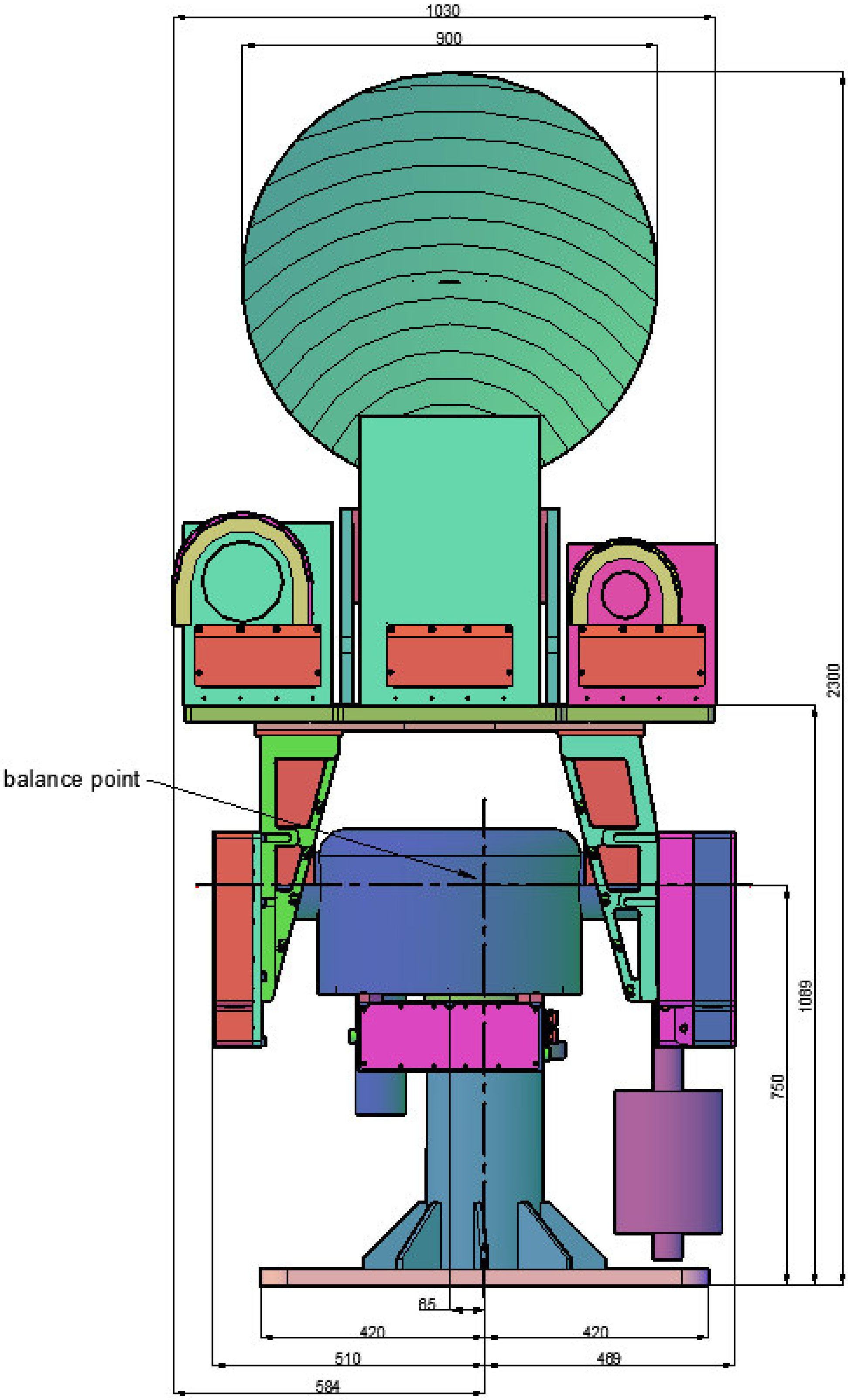

6.925 / 10.7 / 18.7 /36.5 GHz module combination.

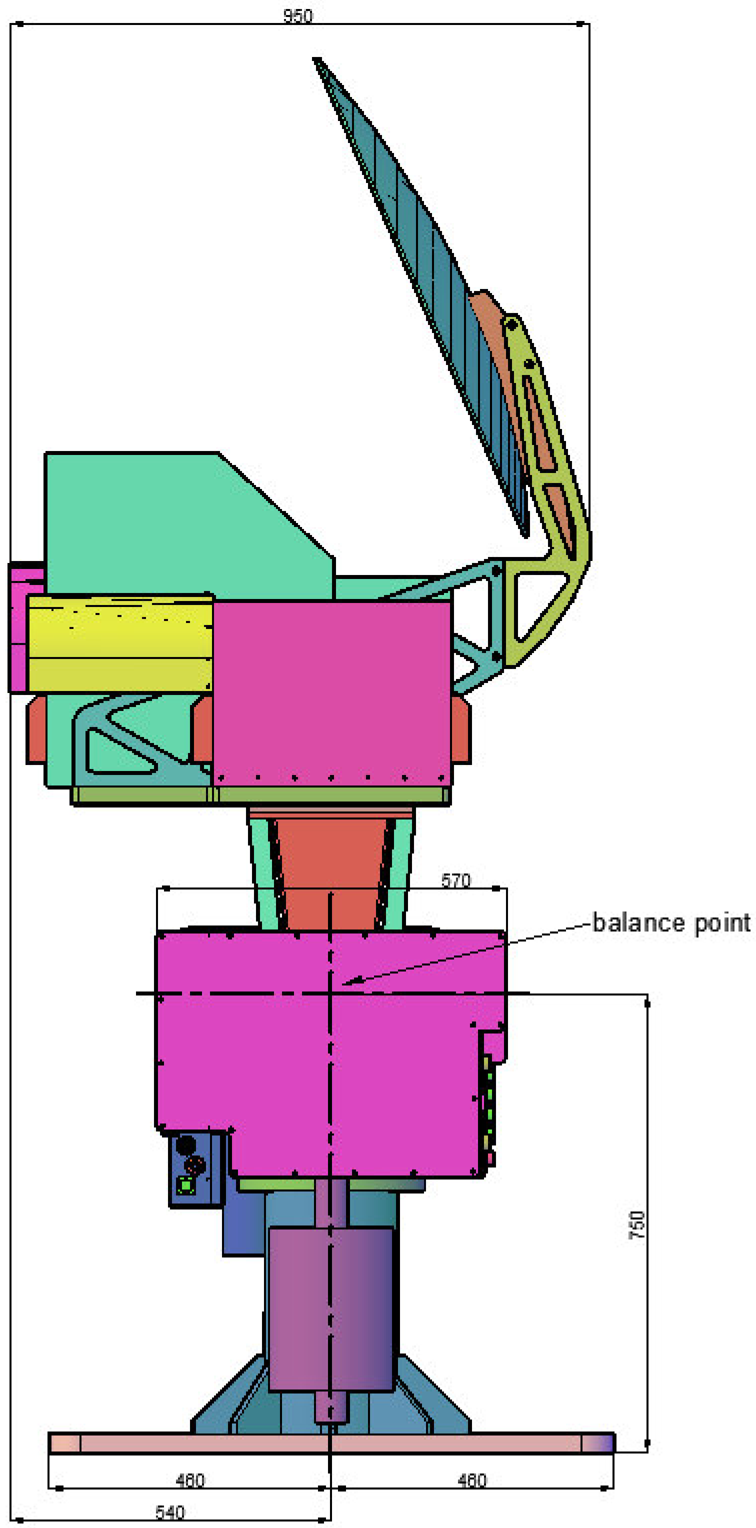
950
570
balance point
750
460
460
540

7. Theory of Operation (Atmospheric Applications)

7.1 Introduction

We present a new approach for ground based remote sensing of liquid water path (LWP) in the presence of precipitating clouds. Dual polarized ground based microwave radiometers are capable of detecting the unique scattering signature of non-spherical precipitation sized particles. This polarization signal is only produced by the precipitation particles for which the brightness temperature emission has a different sensitivity to LWP than the smaller cloud drops. By using the information that is contained in the polarization difference of the down-welling brightness temperature, the cloud and rain liquid water fractions can be estimated independently.

Future retrieval algorithms based on our proposed approach will enable the detection of small precipitation fractions in thick clouds and also allow for estimates of cloud and rain LWP in raining conditions.

The path-integrated liquid water content (liquid water path, LWP) is of considerable interest to the meteorological community for a number of applications, ranging from climate research to radio telecommunications. Measurements of LWP can be provided by different methods, such as satellite imagery, cloud radar, and ground based passive microwave radiometry.

The latter is the most precise method for LWP estimation over land surfaces. Thus, ground based microwave radiometers are used operationally for the remote sensing of integrated water vapour and LWP, offering the capability of performing measurements in nearly all types of weather conditions (Gueldner and Spaenkuch, 1999). The main limit on their capabilities is the occurrence of rain, which reduces the precision of LWP retrievals by current microwave methods. The retrieval techniques for LWP from brightness temperatures (TB) at microwave frequencies used so far are limited to cloud LWP (called LWC) in the absence of rain LWP (called LWR). The reason for this limitation is the varying sensitivity of emitted TB with drop size. Above a certain radius ***r*** the dependence of TB on radius slightly exceeds being proportional to r^3. The LWP (proportional to the third moment of the drop size distribution) is no longer unambiguously coupled to the TB signal if such large drops are mixed with smaller cloud droplets.

As a consequence, a LWP retrieval in raining clouds is highly ambiguous with current methods. This fact not only reduces the operational utility if raining conditions are masked out, but also adds a possible error source to LWP retrievals in many clouds.

Radar measurements do not offer an advantage when cloud and rain particles simultaneously occur because the sensitivity of the radar signal to drop size is even worse: The radar reflectivity factor is proportional to the sixth moment of drop radius. Thus the signal will always be dominated by the largest drops in the sampled volume (Fox and Illingworth, 1997}.

While a change of the drop size distribution (DSD) from a cloud drop spectra to a convective rain drop size distribution will increase the TB signal of a microwave radiometer by a factor of 2 to 3, the reflectivity factor will change by several orders of magnitude. Thus LWP values

derived from the radar reflectivity factor depend more critically on the assumption of the true drop size distribution than those derived from microwave radiometry.
Up to now passive ground based microwave measurements only used the brightness temperature information, which alone cannot deal with the ambiguity introduced by large raindrops within the cloud. New findings from radiative transfer models (Czekala and Simmer, 1998} suggest a possibility to resolve this size dependent ambiguity by measuring a second signal that is also related to raindrop size: The polarization difference (PD), which is defined as the amount of linear polarization PD=TB_V –TB_H. This scattering induced signal depends on drop deformation, and hence on drop size. The modeling of somewhat realistically shaped non-spherical rain drops has recently become possible due to advances in single scattering methodology and computer efficiency.
The aim of this chapter is to propose a new approach for LWP retrieval in the presence of raining clouds by adding polarization information to the current un-polarized measurement systems and retrieval methods. We will illustrate the physical processes which relate the TB and PD signal to the varying partitioning of total LWP between cloud and rain. We will show how the information content due to the unique scattering signature of non-spherical rain drops can be used to improve the accuracy of widely used LWP retrieval techniques.
However, we do not propose a complete retrieval algorithm for a specific instrument that properly incorporates all the uncertainties that may arise from imperfect instruments, uncertain temperature and humidity profiles, and uncertain cloud microphysics. At this stage we focus on explaining the general method and its possible advantage for obtaining a LWP retrieval without restriction to non-raining clouds.
Such improvements are expected to have significant impact on future operational services as well as cloud process studies which may be based on the new retrieval approach. Such studies offer the opportunity to gain knowledge about internal structures and cloud microphysical properties. The onset of precipitation, specifically the transition from small particle dominated cloud DSD to precipitation sized DSD (which is very important in cloud parameterizations in numerical weather prediction models), should be detectible. A systematic bias in LWP retrieval is expected if rain drops are not considered.

7.2 Polarisation Signal

The shape of raindrops is known to be non-spherical (Pruppacher and Pitter, 1971) due to wind stress, surface tension and internal hydrostatic pressure. Chuang and Beard (1990) describe the shape of raindrops falling at terminal velocity by a series of Chebyshev polynomials. The radiative transfer results of Czekala and Simmer (1998) revealed remarkable differences between the effects of (commonly assumed) spherical and oblate spheroid shapes on polarized microwave brightness temperatures. The latter shape is used as a close approximation to the Chebyshev shape. While the brightness temperature (TB, defined as the average brightness temperature calculated from the vertically and horizontally polarized brightness temperatures according to (TB_V +TB_H)/2) showed only a weak dependence on the hydrometeor shape, the polarization difference for down-welling radiation (as seen by a ground based sensor) was altered from small positive values (always well below 2 K) in the case of spherical raindrops to large negative values (down to -15 K) in the case of oblate spheroids. The polarization in both cases is only produced by drops that are large enough (compared to wavelength) to cause a significant amount of scattering. The precise amount of negative PD varied with the optical thickness within the observed volume. Specifically, the amount of precipitation, the chosen frequency, and the elevation angle of the hypothetical ground based observation, and the cloud top and cloud base height controlled the amount of PD predicted by the radiative transfer model. The theoretically predicted signal of negative PD arising from precipitation sized water drops has recently been validated with ground based measurements (Czekala et al, 2000).

7.3 Model Calculations

The above mentioned studies (Czekala and Simmer, 1998) imply that polarization measurements might be exploited to learn more about the amount of precipitation sized particles within clouds. In order to illustrate the radiometric sensitivities to the partitioning of water between cloud and rain in a clear and simple way, we carried out a sensitivity study. Within an atmospheric column with a fixed vertical profile of temperature and humidity we positioned a cloud between 1 and 2 km height with a specified fraction of cloud water and rain water. For reasons of simplicity we assume a constant vertical profile of cloud and rain water within the cloud. This model is meant to simulate situations like a viewing of an isolated rain event from outside the rain cell or a cloud with no observed surface rain rate. Precipitating clouds with no surface rain rate frequently occur when precipitation starts to evolve within the cloud, but evaporates below the cloud base before reaching the surface.
Cloud and rain fractions were varied independently so that the resulting LWC ranges from 0.0 kg/m^2 to 2.5 kg/m^2 and the LWR from 0.0 kg/m^2 to 2.5 kg/m^2. The total LWP simply is the sum LWP = LWC + LWR. All possible combinations of both kinds of LWP were calculated, resulting in total LWP ranging from 0.0 to 5.0 kg/m^2. Although the pure rain cases without any LWC make sense for observations where the rain shaft of isolated showers is observed against a clear sky background, some of the LWC/LWR combinations (especially those with large LWC) are certainly unrealistic for the given vertical cloud extension. Nevertheless, the complete coverage of all possible combinations is well suited for explaining the nature of the signal expected from raining clouds, even in the presence of severe rain events.
The cloud LWP was modeled with a DSD given by a modified gamma distribution with a modal radius of 5.5 micron and an integration interval from 0.1 to 100 µm. The rain LWP was produced by a Marshall-Palmer distribution and an integration interval from 100 µm to 5 mm. Oblate spheroids with a fixed orientation and a size dependent aspect ratio were used for rain, spheres for cloud particles. The T-Matrix code from Mishchenko (Mishchenko, 2000) was used to calculate the amplitude scattering function for these particles.The surface emission, which has hardly any effect on the down-welling radiation, was set to 0.9, a reasonable value for land surfaces.

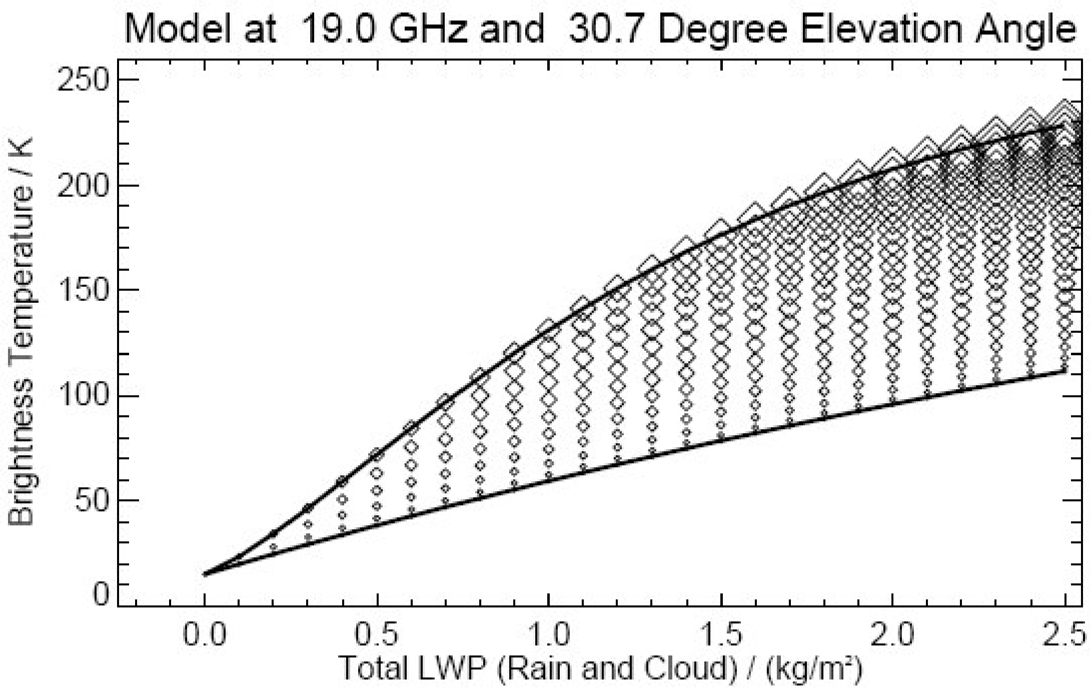

Fig.7.1

Fig.7.1 shows the brightness temperature obtained at 19 GHz with an elevation angle of 30.7 degrees for a hypothetical ground based observation. The amount of LWP due to rain is indicated by the size of the symbols. Smallest symbols are assigned to zero R-LWP, thus the lower line Fig.7.1 indicates the result for clouds without rain. The reverse situation (all LWP is made from LWR) is indicated by the upper line which shows a stronger increase with LWP and a saturation at large LWP values where the atmosphere (sum of gas and liquid constituents) becomes opaque. It is obvious from the different slopes of both extreme cases that a TB measurement can only be converted to a LWP if the mixture of rain and cloud fraction is known. Realistic cloud conditions are represented by a point somewhere between both limiting cases.

7.4 Proposed Retrieval Method

Combining the information of TB and PD that refer to a specific combination of cloud LWP (LWC) and rain LWP (LWR) into one diagram (Fig.7.2) shows that the information contained in the two signals is complementary. Fig.7.2 gives the response of all calculated mixtures of LWC and LWR in terms of their radiative response. Isolines of constant LWP are given for three different LWP variables: Dotted red lines indicate calculations with the same LWR but varying LWC, dash-dotted green lines show the results for same LWC, but with varying LWR. The solid blue lines are lines of constant total LWP, which may be formed by any mixture of LWC and LWR.

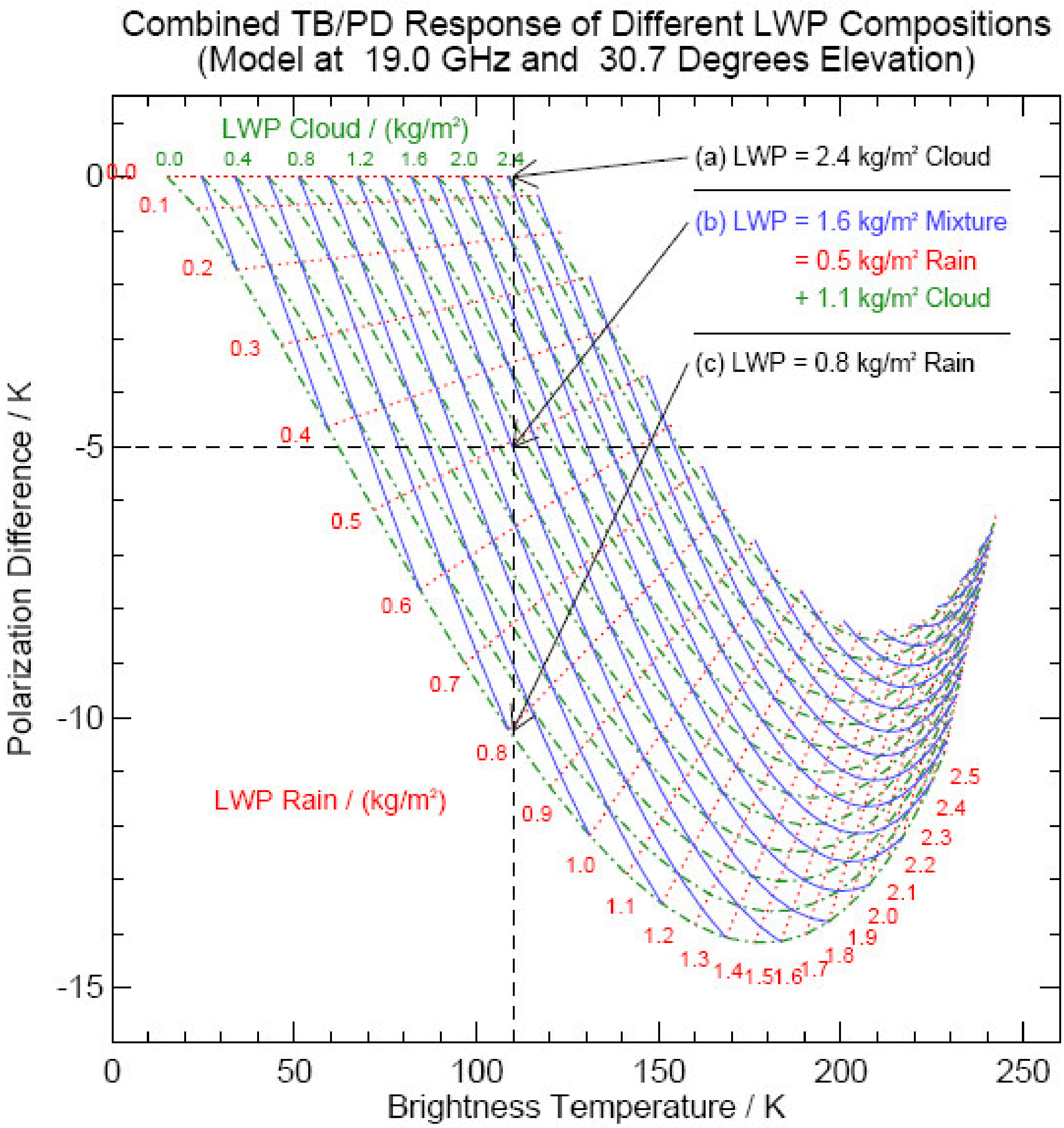

Pure cloud conditions are indicated by the uppermost horizontal dotted red line (no rain fraction). The increase in cloud liquid water path from 0.0 to 2.5 kg/m^2 leads to an increase in the corresponding TB, but no polarization is produced. Pure rain conditions (in the absence of cloud) produce the lower limit of the PD signal (indicated by the lowest dash-dotted green line). When mixing rain into the cloud, increasing amounts of LWR shift the horizontal line of pure cloud response towards negative PD. However, the lines of constant LWR do not remain horizontal. This means that a variation of LWC in the presence of considerable LWR (e.g. 0.7 kg/m^2) not only results in a change of TB, but also affects the PD signal: Increasing amounts of cloud water damp the PD. With further increase of LWR the PD signal ceases to increase in amplitude (beginning saturation due to increasing optical thickness) and then drops back towards zero. It is worth while to note that in the region of initial saturation (beginning of curvature in the dash-dotted green isolines of the LWC) the isolines of LWC and LWR remain roughly orthogonal. This means that LWC and LWR affect the TB/PD response in different ways, which is a prerequisite for a simultaneous retrieval of both properties. If the isolines of both quantities were parallel then a distinction of both quantities would be impossible. This would be the case when assuming spherical particles for all kinds of hydrometeors since spherical rain produces a TB signal with a different sensitivity than cloud drops and only very small positive PD (always below 2 K).

The advantage of the new approach of LWP retrieval by using the PD signal in addition to only the TB signal is obvious when looking at a hypothetical measurement of 110 K brightness temperature and -5 K polarization difference (indicated by the dotted black lines in Fig.7.2). The TB result of 110 K refers to 2.4 kg/m^2 liquid water path when assuming a pure cloud particle size distribution (retrieval (a), uppermost dotted red line) or 0.8 kg/m^2 liquid water path when assuming a composition of pure rain without clouds (retrieval (c), lowest dash dotted green line). These numbers give a good estimate about the uncertainty in LWP retrieval in the presence of raining clouds when only TB measurements are used.

In comparison, when the supplementary PD information is used (measurement (b) in Fig.7.2) the total LWP is reliably estimated to be 1.6 kg/m^2.

Furthermore, we are now able to separate the LWP between the fraction of cloud water (1.1 kg/m^2) and the fraction of rain water (0.5 kg/m^2).

7.5 Discussion

The above results are idealized model calculations that neglect the precise vertical distribution of the hydrometeors and use simplified cloud microphysical assumptions. For example the variability of drop size distribution functions and the effect of the melting layer need to be considered in more detail before a practical retrieval scheme can be based upon such radiative transfer calculations. Variations in water vapour and temperature profile will also affect the numerical results, mainly by an additional shift along the TB axis.

However, the results presented here clearly illustrate the profit of adding the polarization signal that is produced by non-spherical precipitation sized particles to the retrieval process. In addition, multi-frequency observations will help to overcome uncertainties that may arise from unknown drop size distributions. Since modern multi-channel microwave radiometers (solheimetal,1998, Crewell et al, 2000) can determine the temperature (RMS < 2 K) and humidity (RMS < 0.3 g/m^3) profile in the cloudy (non-raining) troposphere (below 5 km), they will also provide sufficient information about the atmospheric conditions that will improve the retrieval accuracy in case of raining clouds. For this purpose, a final retrieval scheme may also rely on secondary information, such as surface temperature, cloud base height, and humidity profile data from numerical weather prediction models.

For semi-transparent situations (less than 1.5 kg/m^2 LWR at 19 GHz) the vertical distribution of the hydrometeors is of minor importance and will not degrade the general dependence of TB and PD on the different LWP fractions.

Fig.7.3 shows the resulting TB/PD response at 30 GHz (instead of 19 GHz used in Fig.7.2). At higher frequencies the saturation of the PD signal begins at lower rain rates compared to the 19 GHz results. However, the sensitivity of PD to small amounts of LWR is significantly increased. This is partly due to the change in the size parameter (the ratio of particle size to the wavelength under consideration). Another reason is the increased optical thickness due to the frequency dependence of the refractive index. A lower total optical thickness (e.g. at 10 GHz) decreases the dynamic range of the TB signal, but prevents saturation of the PD and

TB signal. Since the accuracy of TB measurements is in the range of 1 K this reduction of the TB signal range is not a severe problem. The insensitivity of 10 GHz observations to smaller drops leads to a total signal that is dominated by the rain generated PD.

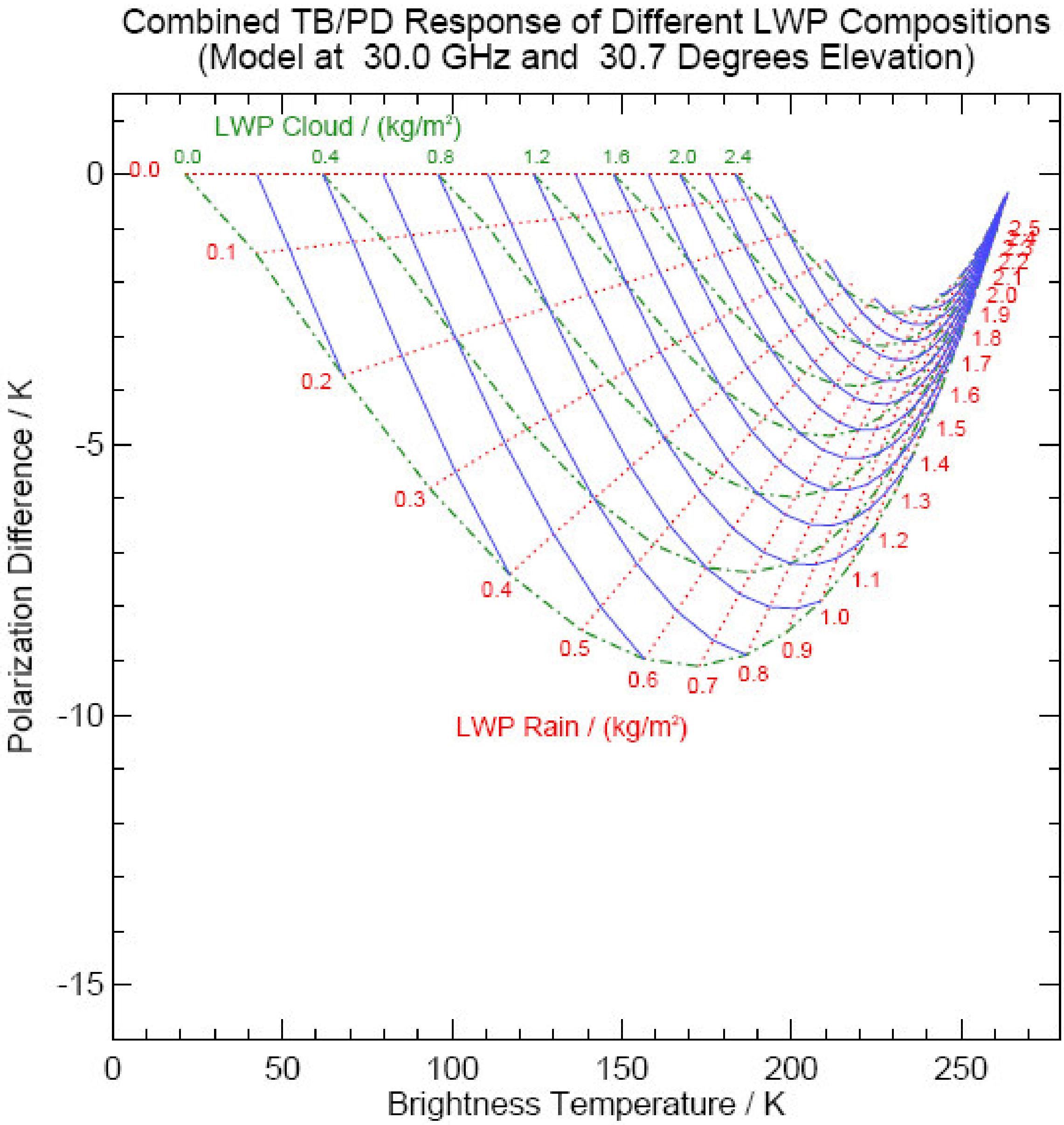

Fig.7.3

Similar changes in sensitivity to LWR can also be achieved by variation of the observation angle. Since the total optical thickness increases with increased geometrical path lengths through the atmosphere at lower elevation angles, the saturation of the PD is observed at different LWR fractions. This effect is not the same as a variation in frequency because elevation angle affects the radiation only by changing the optical thickness (due to varied path length). Changes in frequency induce a similar change in optical thickness, but additionally change the ratio of particle size to wavelength and thus lead to different single scattering parameters. Finally, the development of practical retrieval methods also needs to

incorporate instrument noise and antenna characteristics, thus leading to instrument specific algorithms.
Current research microwave radiometers have a sufficiently narrow beamwidth (less than 10 degree) to reveal cloud inhomogeneities in process studies (Crewell et al, 2000). With an absolute accuracy of 1 K and a relative calibration of the PD to 0.2 K with clear sky conditions it will be possible to detect the discussed signal.

7.6 Conclusions

The presence of precipitation sized rain drops within clouds inhibits a precise remote sensing of LWP by currently used ground based microwave methods. The brightness temperature is related to LWP, but if the drop size distribution is unknown it is not possible to partition the LWP between cloud droplets and rain drops using such measurements. We have presented a new approach to discriminate between the different contributions to total LWP by exploiting the additional information contained in the negative polarization difference caused by non-spherical rain drops. This signal depends on the drop size and therefore reduces the uncertainty that arises from the unknown partitioning of total LWP between the cloud and rain fractions of the drop size distribution. Future retrieval algorithms that use simultaneous measurements of brightness temperature and polarization difference will allow for a more accurate retrieval of total liquid water path. In addition, we expect that it will be possible to estimate independently the contributions by rain drops and cloud drops to the total LWP.
The uncertainties that may arise from insufficient knowledge of cloud microphysics and vertical distribution of the hydrometeors will be partly mitigated by the additional information that is gained by multi-frequency and making multi-angle measurements.

7.7 REFERENCES

Chuang and Beard, 1990
Chuang, C. and K.~V. Beard, A numerical model for the equilibrium shape of electrified raindrops, {\em J. Atmos. Sci.\/}, 47, 1374--1389, 1990.

Crewell et~al., 2000
Crewell, S., H.~Czekala, U.~Löhnert, and C.~Simmer, MICCY -- a 22 channel ground-based microwave radiometer for atmopsheric research, submitted to Radio Science, 2000.

Crewell et~al., 2000
Crewell, S., U. Löhnert, A. van Lammeren, and C. Simmer, Cloud remote sensing by combining synergetic sensor information, Phys. Chem. Earth (B), 25, No. 10-12, 1043-1048, 2000.

Czekala et al., 2000
Czekala, H., S. Crewell, A. Hornbostel, A. Schroth, C. Simmer, and A. Thiele, Validation of microwave radiative transfer calculations for non-spherical liquid hydrometeors with ground based measurements, J. Appl. Meteorol., 2000

Czekala and Simmer, 1998
Czekala, H. and C. Simmer, Microwave radiative transfer with non-spherical precipitating hydrometeors, J. Quant. Spectros. Radiat. Transfer, 60, 365--374, 1998.

Fox and Illingworth, 1997
Fox, N., and A.J. Illingworth, The potential of space borne cloud radar for the detection of stratocumulus clouds, J. Appl. Meteorol., 36, 676--687, 1997.

Güldner and Spänkuch, 1999
Güldner, J. and D. Spänkuch, Results of year-round remotely sensed integrated water vapour by ground-based microwave radiometry, J. Appl. Meteorol., 38, 981--988, 1999.

Mishchenko, 2000
Mishchenko, M.I., Calculation of the amplitude matrix for a non-spherical particle in a fixed orientation, Appl. Opt., 39, 1026--1031, 2000.

Pruppacher and Pitter, 1971
Pruppacher, H.R. and R.L. Pitter, A semi-empirical determination of the shape of cloud and rain drops, J. Atmos. Sci.}, 28, 86--94, 1971.

Solheim et al., 1998
Solheim, F., J. Godwin, E.R. Westwater, Y. Han, S. Keihm, K. Marsh, and R.Ware, Radiometric profiling of temperature, water vapor and cloud liquid water using various inversion methods, Radio Science, 33, 393--404, 1998.

8. Soil Moisture Applications

A polarised radiometer is also very useful for soil moisture and snow measurements. With the vertical polarisation it is straight forward to measure the refractive index of soil samples as shown in the following measurement where a ground scan is performed with a RPG-4CH-DP (18.7 GHz v/h, 36.5 GHz v/h). The elevation angle is scanned between -10° and -80°. The result of this scan is shown in Fig 8.1.
As can be seen from the diagram, the Brewster angle for the 18.7 (V) GHz channel is at 69° which corresponds to a refractive index of n=2.60 (tan(69°)). This is consistent with the observation at normal incidence where the reflection coefficient R is given by R=((n-1)/(n+1))^2 which leads to R=0.2 at 18.7 GHz for normal incidence. With a physical ground temperature Tg of 273K and a sky temperature of Ts=15K we get: Tb=(1-R)*Tg+R*Ts=220K which is really observed. For the 36.5 GHz channel we get: n=2.36 (Brewster angle: 67°), R=0.16, Tb=233 K which is totally consistent with the observations.
Horizontal and vertical polarizations precisely convert at normal incidence to the same brightness temperature (reflection angle 0° could not be directly measured).
In the horizontal polarization the Tb is dominated by the reflected sky brightness temperature. The higher the reflection angle, the higher the sky contribution and the lower

the total Tb. But with low elevation angle (El) the sky temperature Ts becomes larger, roughly the Ts measured at zenith angle multiplied by the airmass (am=1/sin(El)). At 10° elevation (reflection angle=80°) the sky temperature is close to 6 times higher compared to the zenith angle Ts. Therefore the Ts value at 80° reflection angle is approx. 90 K at 18.7 GHz (cloud free conditions). This is why the Tbs at high reflection angles tend to increase which is shown in the diagram (sky saturation).

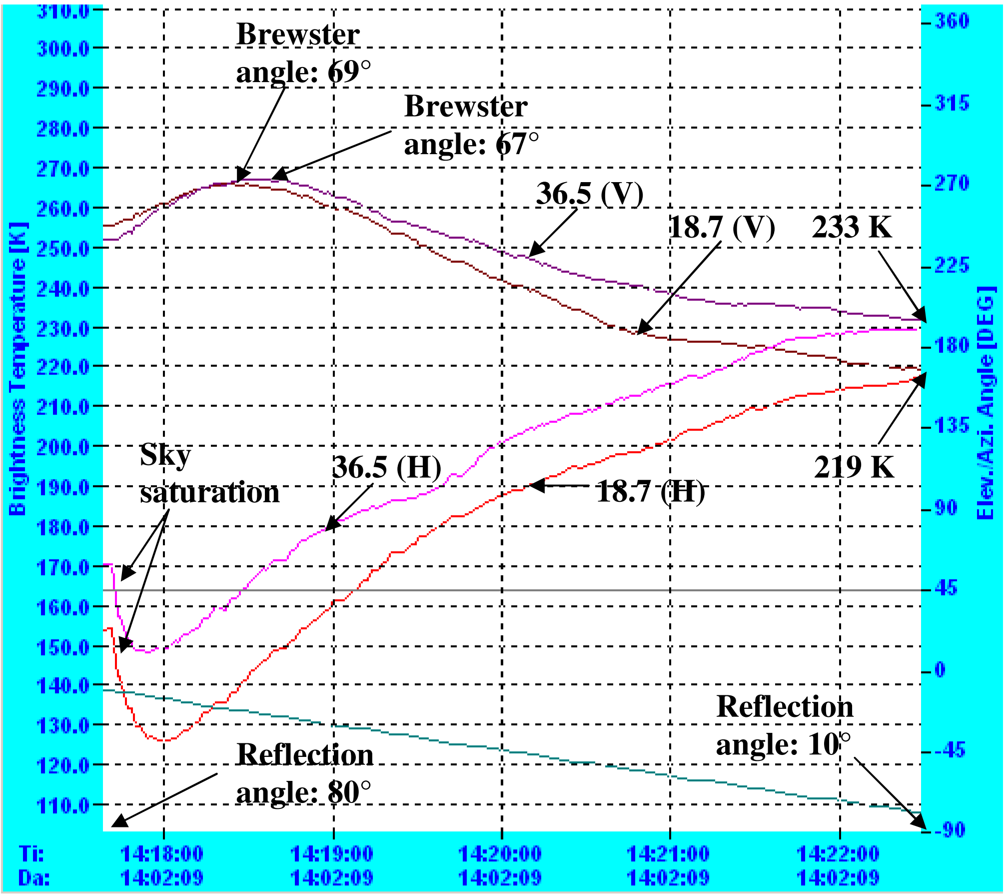

Fig.8.1: Soil measurement scan between -10° and -80° elevation.

The refractive index summarizes the soil properties like vegetation content, soil moisture, soil composition, etc. By comparing refractive indices of different frequencies, snow layers can be analyzed. A general rule is that the ground penetration depth increases with decreasing frequency. Therefore a radiometer dedicated for soil moisture measurements should be equipped with 6.925 GHz and 10.7 GHz channels.

Appendix A (File Formats)

A1: BRT-Files (.BRT), Brightness Temperature*

Variable Name	Type	# Bytes	Description
BRTCode	int	4	BRT-file code (=837854834)
N	int	4	number of recorded samples
FreqNo	int	4	number of frequencies
Freqs[]	float	4*FreqNo	recorded frequencies [GHz]
BRTMin	float	4	Minimum of recorded BRT values
BRTMax	float	4	Maximum of recorded BRT values
T_1	int	4	Time of sample 1 (# of sec. since 1.1.2001)
BRT_1[]	float	8*FreqNo	BRTs sample 1 [K], (h/v)
EL_ANG_1	float	4	elevation angle of sample 1 (DEG)
AZ_ANG_1	float	4	azimuth angle of sample 1 (DEG)
…	…	…	…
T_N	int	4	Time of sample N (# of sec. since 1.1.2001)
BRT_N[]	float	8*FreqNo	BRTs sample N [K], (h/v)
EL_ANG_N	float	4	elevation angle of sample N (DEG)
AZ_ANG_N	float	4	azimuth angle of sample N (DEG)

A2: TRK-Files (.TRK), Sun Tracking Brightness Temperatures*

Variable Name	Type	# Bytes	Description
TRK-Code	int	4	TRK-file code (=5566441)
N	int	4	number of recorded samples
FreqNo	int	4	number of frequencies
Freqs[]	float	4*FreqNo	recorded frequencies [GHz]
BRTMin	float	4	Minimum of recorded BRT values
BRTMax	float	4	Maximum of recorded BRT values
T_1	int	4	Time of sample 1 (# of sec. since 1.1.2001)
EL_ANG_1	float	4	elevation angle of sample 1 (DEG)
AZ_ANG_1	float	4	azimuth angle of sample 1 (DEG)
BRT_1[]	float	200* 4*FreqNo	200 x FreqNo 10 ms BRTs sample 1 [K]
…	…	…	…
T_N	int	4	Time of sample N (# of sec. since 1.1.2001)
EL_ANG_N	float	4	elevation angle of sample N (DEG)
AZ_ANG_N	float	4	azimuth angle of sample N (DEG)
BRT_N[]	float	200*	100 x x FreqNo 10 ms BRTs sample N [K]

		4*FreqNo	

A3: HKD-Files (.HKD), Housekeeping Data*

Variable Name	Type	# Bytes	Description
HKDCode	int	4	HKD-File Code (=86649439)
N	int	4	Number of recorded samples
FreqNo	int	4	number of frequencies
Freqs[]	float	4*FreqNo	recorded frequencies [GHz]
T_1	int	4	Time of sample 1 (# of sec. since 1.1.2001)
TEnv_1	float	4	Environmental Temperature [K], sample 1
TRec[]_1	float	4*FreqNo	Receiver temperatures [K], sample 1
StabRec[]_1	float	4*FreqNo	Receiver stabilities [K], sample 1
Press_1	float	4	Barometric Pressure[mbar], sample 1
RF_1	int	4	Rain Flag, sample 1
Res_1	float	4	Free, for later use, sample 1
…	…	…	…
T_N	int	4	Time of sample N (# of sec. since 1.1.2001)
TEnv_N	float	4	Environmental Temperature [K], sample N
TRec[]_N	float	4*FreqNo	Receiver temperatures [K], sample N
StabRec[]_N	float	4*FreqNo	Receiver stabilities [K], sample N
Press_N	float	4	Barometric Pressure[mbar], sample N
RF_N	int	4	Rain Flag, sample N
Res_N	float	4	Free, for later use, sample N

A4: LIW-Files (.LIW), Liquid Water Data*

Variable Name	Type	# Bytes	Description
LIWCode	int	4	LIW-File Code (=934501978)
N	int	4	Number of recorded samples
LIWMin	float	4	Minimum of recorded LIW values
LIWMax	float	4	Maximum of recorded LIW values
LIWTimeRef	int	4	Time Reference 0=Local, 1=UTC)
IWRetType	int	4	Retrieval type (0=linear, 1=quadr. regr.)
T_1	int	4	Time of sample 1 (# of sec. since 1.1.2001)
LIW_1(3)	float	3x4	LIW_1(0)=LWP, LIW_1(1)=LWC, LIW_1(2)=LWR of sample #1
EL_ANG_1	float	4	Elevation angle of sample 1 (DEG)
AZ_ANG_1	float	4	Azimuth angle of sample 1 (DEG)
…	…	…	…
T_N	int	4	Time of sample N (# of sec. since 1.1.2001)

LIW_N(3)	float	3x4	LIW_N(0)=LWP, LIW_N(1)=LWC, LIW_N(2)=LWR of sample #N
EL_ANG_N	float	4	Elevation angle of sample N (DEG)
AZ_ANG_N	float	4	Azimuth angle of sample N (DEG)

A5: IWV-Files (.IWV), Integrated Water Vapour Data*

Variable Name	Type	# Bytes	Description
IWVCode	int	4	IWV-File Code (=594811068)
N	int	4	Number of recorded samples
IWVMin	float	4	Minimum of recorded IWV values
IWVMax	float	4	Maximum of recorded IWV values
IWVTimeRef	int	4	Time Reference 0=Local, 1=UTC)
IWVRetType	int	4	Retrieval type (0=linear, 1=quadr. regr.)
T_1	int	4	Time of sample 1 (# of sec. since 1.1.2001)
IWV_1	float	4	IWV of sample #1
EL_ANG_1	float	4	Elevation angle of sample 1 (DEG)
AZ_ANG_1	float	4	Azimuth angle of sample 1 (DEG)
…	…	…	…
T_N	int	4	Time of sample N (# of sec. since 1.1.2001)
IWV_N	float	4	IWV of sample #N
EL_ANG_N	float	4	Elevation angle of sample N (DEG)
AZ_ANG_N	float	4	Azimuth angle of sample N (DEG)

A6: Structure of Calibration Log-File (CAL.LOG)

Variable Name	Type	# Bytes	Description
STACode	int	4	CAL.LOG -File Code (=657644)
FirstEntTime	int	4	time of first entry (# of sec. since 1.1.2001)
LastEntTime	int	4	time of last entry (# of sec. since 1.1.2001)
N	int	4	number of recorded tip curve samples
N_ FreqNo	int	4	number of frequencies
Freqs[]	int	4*FreqNo	recorded frequencies [GHz]
CalTime1	int	4	Time of sample 1 (# of sec. since 1.1.2001)
Gain[]_1	float	8*FreqNo	array of gains cal. sample #1, (h/v

			pol. channels)
Tsys[]_1	float	8*FreqNo	array of system noise temps. cal. sample #1, (h/v pol. channels)
LinCorr[]_1	float	8*FreqNo	array of linear correlations cal. sample #1, (h/v pol. channels)
ChiSqr []_1	float	8*FreqNo	Chi square factors for calibration sample 1 , (h/v pol. channels)
NoiseTemp[]_1	float	8*FreqNo	Noise source temp. array for calibration sample 1, (h/v pol. channels)
SkyTipAngAnz_1	int	4	Number of sky tip angles for calibration sample 1
Airmass[]_1	float	4* SkyTipAngAnz_1	Airmass array
SkyDipUs [i][j]_1 i=0, …, 2*FreqNo-1 j=0, … , SkyTipAngAnz_1-1	float	8* FreqNo * (SkyTipAngAnz_1+1)	Sky dip detector voltages. For each frequency the det. voltage is given at all angles. The last entry is the voltage on the hot target
TauSuccess[]_1	int	8*FreqNo	Flag that indicates if the Tau calculation during the skydip was successful (0=not evaluated, 1=no success, 2=success)
TauArr[0][]_1	float	4* SkyTipAngAnz_1	Tau array for channel 1 (only if TauSuccess[0]_1 >0), cal. sample 1
LinFit1A[0]_1	float	4	Linear Fit parameter A (offset) for channel 1 (only if TauSuccess[0]_1>0)
LinFit1B[0]_1	float	4	Linear Fit parameter B (slope) for channel 1 (only if TauSuccess[0]_1>0)
…	…	…	…
TauArr[2*FreqNo-1][]_1	float	4* SkyTipAngAnz1	Tau array for last channel (only if TauSuccess [2*FreqNo -1]>0)
LinFitA[2*FreqNo -1]_1	float	4	Linear Fit parameter A (offset) for channel 1 (only if TauSuccess[2*FreqNo -1]_1>0)
LinFitB[2*FreqNo -1]_1	float	4	Linear Fit parameter B (slope) for last channel (only if TauSuccess[2*FreqNo -1]_1>0)
…	…	…	…
CalTimeN	int	4	Time of sample N (# of sec. since 1.1.2001)
Gain[]_N	float	8*FreqNo	array of gains cal. sample #N,

			(h/v pol. channels)
Tsys[]_N	float	8*FreqNo	array of system noise temps. cal. sample #N, (h/v pol. channels)
LinCorr[]_N	float	8*FreqNo	array of linear correlations cal. sample #N, (h/v pol. channels)
ChiSqr []_N	float	8*FreqNo	Chi square factors for calibration sample N , (h/v pol. channels)
NoiseTemp[]_N	float	8*FreqNo	Noise source temp. array for calibration sample N, (h/v pol. channels)
SkyTipAngAnz_N	int	4	Number of sky tip angles for calibration sample N
Airmass[]_N	float	4* SkyTipAngAnz_N	Airmass array
SkyDipUs [i][j]_N i=0, …, 2*FreqNo-1 j=0, … , SkyTipAngAnz_N-1	float	8* FreqNo * (SkyTipAngAnz_N+1)	Sky dip detector voltages. For each frequency the det. voltage is given at all angles. The last entry is the voltage on the hot target
TauSuccess[]_N	int	8*FreqNo	Flag that indicates if the Tau calculation during the skydip was successful (0=not evaluated, 1=no success, 2=success), sample N
TauArr[0][]_N	float	4* SkyTipAngAnz_N	Tau array for channel 1 (only if TauSuccess[0]_N>0), cal. sample N
LinFitA[0]_N	float	4	Linear Fit parameter A (offset) for channel 1 (only if TauSuccess[0]_N>0), sample N
LinFitB[0]_N	float	4	Linear Fit parameter B (slope) for channel 1 (only if TauSuccess[0]_N>0) , sample N
…	…	…	…
TauArr[2*FreqNo-1][]_N	float	4* SkyTipAngAnz_N	Tau array for last channel (only if TauSuccess[2*FreqNo-1]_N>0) , sample N
LinFitA[2*FreqNo-1]_N	float	4	Linear Fit parameter A (offset) for last channel (only if TauSuccess[2*FreqNo-1]_N>0, sample N)
LinFitB[2*FreqNo-1]_N	float	4	Linear Fit parameter B (slope) for last channel (only if TauSuccess[2*FreqNo-1]_N >0) , sample N

A7: LV0-Files (.LV0), Level Zero (Detector Voltages) Files*

Variable Name	Type	# Bytes	Description
LV0Code	int	4	LV0-File Code (=111112)
N	int	4	Number of samples
FreqNo	int	4	number of frequencies
Freqs[]	float	4*FreqNo	recorded frequencies [GHz]
L[8]	float	8*FreqNo	Dicke Switch Leakage array
T_1	int	4	Time of sample 1 (# of sec. since 1.1.2001)
RF_1	int	4	Rain flag of sample 1
Elevation_1	float	4	Elevation Angle [°] of sample 1
Azimuth_1	float	4	Azimuth Angle [°] of sample 1
Press_1	float	4	Barometric pressure [mbar] of sample 1
Tenv_1	float	4	Environmental temperature [K], sample 1
Tn_1[]	float	8*FreqNo	Noise diode temperatures [K], sample 1
Tds_1[]	float	8*FreqNo	Dicke switch temperatures [K], sample 1
G_1[]	float	8*FreqNo	Gain calibration parameters [V/K], sample 1
Ts_1[]	float	8*FreqNo	System Noise Temperature calibration parameters Tsys [K], sample 1
Ud_1[]	float	8*FreqNo	Detector voltages [V], sample 1
…	…	…	…
T_N	int	4	Time of sample N (# of sec. since 1.1.2001)
RF_N	int	4	Rain flag of sample N
Elevation_N	float	4	Elevation Angle [°] of sample N
Azimuth_N	float	4	Azimuth Angle [°] of sample N
Press_N	float	4	Barometric pressure [mbar] of sample N
Tenv _N	float	4	Environmental temperature [K], sample N
Tn_N[]	float	8*FreqNo	Noise diode temperatures [K], sample N
Tds_N[]	float	8*FreqNo	Dicke switch temperatures [K], sample N
G_N[]	float	8*FreqNo	Gain calibration parameters [V/K], sample N
Ts_N[]	float	8*FreqNo	System Noise Temperature calibration parameters Tsys [K], sample N
Ud_N[]	float	8*FreqNo	Detector voltages [V], sample N

<u>Notes on Calibrations</u>

Relation between detector voltage U_d and scene brightness temperature T_{sc} :

$U_d = G\ (T_s + T_{sc})$

System Noise Temperature T_s , Noise Diode Temp. T_n and Gain G:

Absolute Calibrations (Hot / Cold): detector voltages on black body target (temperature $T_H = T_{env}$): U_H , cold target (LN or Skydip, temperature T_C): U_C :

$Y = (U_H / U_C)$, $T_s = (T_H - Y * T_C)/(Y - 1)$
$G = U_C / (T_s + T_C)$
On black body target (T_{env}), noise diode turned off: U_{-N} , noise diode turned on: U_{+N}
$T_n = (U_{+N} - U_{-N}) / G$
Dicke Switch ON, radiometer pointing to amb. temp. target (U_{dsh}):
$DelT = U_{dsh} / G - T_s - T_{dsp}$, T_{dsp} = physical Dicke Switch temperature
$T_{ds} = T_{dsp} + DelT$, called Dicke switch temperature in the LV0 format description
Dicke Switch ON, radiometer pointing to cold target: U_{dsc}
Dicke Switch leakage L:
$L = (U_{dsh} - U_{dsc})/ (G * (T_{env} - T_C))$

If a liquid nitrogen cooled target is used, the following correction has to be applied:

T_C [K] = 77.36 -8.2507e-3*(1013.25- P) + 1.9 , P in mbar, 1.9 K is correction for surface reflection on LN (n = 1.2)

Continuous full calibration on scene: Noise Diode turned off: U_{-N} , noise diode turned on: U_{+N} , radiometers looking on scene temperature T_{sc}, Dicke switch turned ON (blocking scene):

$G = (U_{+N} - U_{-N}) / T_n$, $T_s = U_{-N} / G - (T_{ds} - L * (T_{ds} - T_{sc}))$, L= DS leakage (determined in absolute calibration)

Appendix B (ASCII File Formats)

Fig.B1 shows an example of an ASCII data file structure (BRT). All ASCII files start with a header giving information about the number of samples in the file, Minimum and Maximum values of the measured quantities for scaling purposes.Comments are preceded by '#'.
Each sample line starts with the date and time (Ye = Year, Mo = Month, Da = Day, Ho = Hour, Mi = Minute, Se = Second) this sample was. All data columns are separated by ',' from each other. Each line ends with CR/LF.

beams1.BRT.ASC - Editor

Datei Bearbeiten Format Ansicht ?

```
# BRT File
81    # Number of Samples
4   # Number of Frequencies
 6.925 , 10.650 , 18.700 , 36.500    # Frequencies
  3.8   # Minimum Brightness Temp. in File
 98.9   # Maximum Brightness Temp. in File
# Ye , Mo , Da , Ho , Mi , Se , BT(F1 (h)) [K] , BT(F1 (v)) [K] , ... , BT(Fn (v)) [K] , Elev. Ang [DEG],  Azi. Ang [DEG]
11 , 06 , 11 , 14 , 09 , 58 ,   6.36 ,   8.60 ,   5.16 ,   7.80 ,   6.63 ,   7.10 ,  19.03 ,  18.68 ,  49.99 , 199.01
11 , 06 , 11 , 14 , 10 , 02 ,   6.44 ,   8.57 ,   5.22 ,   7.78 ,   6.62 ,   7.08 ,  18.92 ,  18.79 ,  49.99 , 199.01
11 , 06 , 11 , 14 , 10 , 05 ,   6.32 ,   8.67 ,   5.13 ,   7.87 ,   6.52 ,   6.98 ,  18.73 ,  18.67 ,  50.49 , 199.01
11 , 06 , 11 , 14 , 10 , 06 ,   6.28 ,   8.67 ,   5.21 ,   7.90 ,   6.50 ,   6.89 ,  18.62 ,  18.61 ,  50.49 , 199.01
11 , 06 , 11 , 14 , 10 , 09 ,   6.34 ,   8.74 ,   4.99 ,   8.01 ,   6.48 ,   6.80 ,  18.42 ,  18.45 ,  51.00 , 199.01
11 , 06 , 11 , 14 , 10 , 10 ,   6.29 ,   8.83 ,   4.92 ,   7.95 ,   6.46 ,   6.85 ,  18.48 ,  18.39 ,  51.00 , 199.01
11 , 06 , 11 , 14 , 10 , 13 ,   6.34 ,   8.98 ,   4.91 ,   8.10 ,   6.27 ,   6.70 ,  18.43 ,  18.16 ,  51.50 , 199.01
11 , 06 , 11 , 14 , 10 , 14 ,   6.26 ,   8.91 ,   4.95 ,   8.05 ,   6.26 ,   6.66 ,  18.41 ,  18.20 ,  51.50 , 199.01
11 , 06 , 11 , 14 , 10 , 17 ,   6.51 ,   8.96 ,   5.13 ,   8.11 ,   6.20 ,   6.62 ,  18.31 ,  18.10 ,  52.00 , 199.01
11 , 06 , 11 , 14 , 10 , 18 ,   6.56 ,   8.99 ,   5.10 ,   8.16 ,   6.17 ,   6.57 ,  18.22 ,  18.15 ,  52.00 , 199.01
11 , 06 , 11 , 14 , 10 , 22 ,   6.76 ,   8.71 ,   5.67 ,   8.00 ,   6.27 ,   6.53 ,  18.05 ,  18.00 ,  52.50 , 199.01
11 , 06 , 11 , 14 , 10 , 26 ,   6.81 ,   8.71 ,   5.59 ,   7.99 ,   6.22 ,   6.51 ,  18.24 ,  18.07 ,  52.50 , 199.01
11 , 06 , 11 , 14 , 10 , 29 ,   7.24 ,   8.86 ,   6.42 ,   8.13 ,   6.32 ,   6.54 ,  17.91 ,  17.96 ,  53.00 , 199.01
11 , 06 , 11 , 14 , 10 , 30 ,   7.25 ,   8.81 ,   6.34 ,   8.21 ,   6.25 ,   6.53 ,  17.98 ,  17.96 ,  53.00 , 199.01
11 , 06 , 11 , 14 , 10 , 33 ,   7.96 ,   8.93 ,   7.04 ,   8.42 ,   6.52 ,   6.70 ,  17.84 ,  17.80 ,  53.50 , 199.01
11 , 06 , 11 , 14 , 10 , 34 ,   7.89 ,   8.90 ,   7.13 ,   8.42 ,   6.54 ,   6.74 ,  17.78 ,  17.76 ,  53.50 , 199.01
11 , 06 , 11 , 14 , 10 , 37 ,   8.77 ,   9.32 ,   7.53 ,   8.81 ,   6.96 ,   7.24 ,  17.59 ,  17.64 ,  53.99 , 199.01
11 , 06 , 11 , 14 , 10 , 38 ,   8.78 ,   9.22 ,   7.63 ,   8.74 ,   6.97 ,   7.19 ,  17.46 ,  17.65 ,  53.99 , 199.01
11 , 06 , 11 , 14 , 10 , 42 ,  10.15 ,  10.06 ,   7.95 ,   9.87 ,   7.85 ,   8.00 ,  17.29 ,  17.49 ,  54.48 , 199.01
11 , 06 , 11 , 14 , 10 , 43 ,  10.13 ,  10.16 ,   7.91 ,   9.88 ,   7.84 ,   8.03 ,  17.31 ,  17.55 ,  54.48 , 199.01
11 , 06 , 11 , 14 , 10 , 45 ,  12.33 ,  11.70 ,   8.65 ,  12.01 ,   9.32 ,   9.21 ,  17.39 ,  17.90 ,  55.00 , 199.01
11 , 06 , 11 , 14 , 10 , 50 ,  12.35 ,  11.75 ,   8.61 ,  12.02 ,   9.28 ,   9.21 ,  17.34 ,  17.92 ,  55.00 , 199.01
11 , 06 , 11 , 14 , 10 , 53 ,  15.18 ,  14.10 ,   9.50 ,  15.38 ,  11.31 ,  11.24 ,  17.79 ,  18.63 ,  55.50 , 199.01
11 , 06 , 11 , 14 , 10 , 54 ,  15.28 ,  14.13 ,   9.52 ,  15.36 ,  11.30 ,  11.24 ,  17.69 ,  18.58 ,  55.50 , 199.01
11 , 06 , 11 , 14 , 10 , 57 ,  19.23 ,  17.82 ,  10.90 ,  20.61 ,  14.05 ,  13.90 ,  18.96 ,  20.34 ,  56.01 , 199.01
11 , 06 , 11 , 14 , 10 , 58 ,  19.27 ,  17.85 ,  10.99 ,  20.63 ,  14.04 ,  13.96 ,  19.06 ,  20.40 ,  56.01 , 199.01
11 , 06 , 11 , 14 , 11 , 02 ,  24.13 ,  22.46 ,  12.89 ,  26.39 ,  17.18 ,  17.20 ,  21.02 ,  22.87 ,  56.48 , 199.01
```

Fig.B1: BRT ASCII data file structure.

Fig.B2 is an example for a housekeeping data file (HKD).

11061413.HKD.ASC - Editor

Datei Bearbeiten Format Ansicht ?

```
# HKD File
2564    # Number of Samples
4   # Number of Frequencies
 6.925 , 10.650 , 18.700 , 36.500    # Frequencies
# Ye , Mo , Da , Ho , Mi , Se , Tenv [K] , TR1 [K] , ..... , SR1 [K] , ..... , P [mbar], RF
11 , 06 , 14 , 13 , 04 , 22 , 297.4  , 321.1  , 321.1  , 319.9  , 316.9  , 0.001  , 0.002  , 0.017  , 0.004    997.8 , 0
11 , 06 , 14 , 13 , 04 , 23 , 297.4  , 321.1  , 321.1  , 319.9  , 316.9  , 0.001  , 0.002  , 0.017  , 0.004    997.9 , 0
11 , 06 , 14 , 13 , 04 , 24 , 297.4  , 321.1  , 321.1  , 319.9  , 316.9  , 0.001  , 0.002  , 0.016  , 0.004    997.9 , 0
11 , 06 , 14 , 13 , 04 , 25 , 297.4  , 321.1  , 321.1  , 319.9  , 316.9  , 0.001  , 0.002  , 0.016  , 0.005    997.9 , 0
11 , 06 , 14 , 13 , 04 , 26 , 297.4  , 321.1  , 321.1  , 319.9  , 316.9  , 0.001  , 0.002  , 0.016  , 0.005    997.8 , 0
11 , 06 , 14 , 13 , 04 , 27 , 297.4  , 321.1  , 321.1  , 319.9  , 317.0  , 0.001  , 0.002  , 0.016  , 0.005    997.8 , 0
11 , 06 , 14 , 13 , 04 , 28 , 297.4  , 321.0  , 321.1  , 319.9  , 316.9  , 0.001  , 0.002  , 0.016  , 0.005    997.9 , 0
11 , 06 , 14 , 13 , 04 , 29 , 297.4  , 321.0  , 321.1  , 319.9  , 316.9  , 0.001  , 0.002  , 0.015  , 0.006    997.8 , 0
11 , 06 , 14 , 13 , 04 , 33 , 297.4  , 321.1  , 321.1  , 319.9  , 316.9  , 0.001  , 0.002  , 0.015  , 0.006    997.9 , 0
11 , 06 , 14 , 13 , 04 , 34 , 297.4  , 321.0  , 321.1  , 319.8  , 316.9  , 0.001  , 0.002  , 0.014  , 0.006    997.9 , 0
11 , 06 , 14 , 13 , 04 , 35 , 297.4  , 321.0  , 321.1  , 319.8  , 316.9  , 0.001  , 0.002  , 0.014  , 0.006    997.9 , 0
11 , 06 , 14 , 13 , 04 , 36 , 297.4  , 321.1  , 321.1  , 319.9  , 316.9  , 0.001  , 0.002  , 0.014  , 0.006    997.9 , 0
11 , 06 , 14 , 13 , 04 , 37 , 297.4  , 321.1  , 321.1  , 319.9  , 316.9  , 0.001  , 0.002  , 0.014  , 0.006    997.9 , 0
11 , 06 , 14 , 13 , 04 , 38 , 297.4  , 321.1  , 321.1  , 319.9  , 316.9  , 0.001  , 0.002  , 0.014  , 0.006    997.9 , 0
11 , 06 , 14 , 13 , 04 , 39 , 297.4  , 321.1  , 321.1  , 319.9  , 316.9  , 0.001  , 0.002  , 0.014  , 0.006    997.8 , 0
11 , 06 , 14 , 13 , 04 , 40 , 297.4  , 321.1  , 321.1  , 319.9  , 316.9  , 0.001  , 0.002  , 0.014  , 0.006    997.9 , 0
11 , 06 , 14 , 13 , 04 , 41 , 297.4  , 321.1  , 321.1  , 319.9  , 316.9  , 0.001  , 0.002  , 0.013  , 0.006    997.9 , 0
11 , 06 , 14 , 13 , 04 , 42 , 297.4  , 321.1  , 321.1  , 319.9  , 316.9  , 0.001  , 0.001  , 0.013  , 0.006    997.9 , 0
11 , 06 , 14 , 13 , 04 , 46 , 297.4  , 321.1  , 321.1  , 319.9  , 316.9  , 0.001  , 0.001  , 0.013  , 0.006    997.8 , 0
11 , 06 , 14 , 13 , 04 , 47 , 297.4  , 321.1  , 321.1  , 319.9  , 316.9  , 0.001  , 0.001  , 0.012  , 0.006    997.9 , 0
11 , 06 , 14 , 13 , 04 , 48 , 297.4  , 321.1  , 321.1  , 319.9  , 316.9  , 0.001  , 0.001  , 0.012  , 0.006    997.9 , 0
11 , 06 , 14 , 13 , 04 , 49 , 297.4  , 321.1  , 321.1  , 319.9  , 316.9  , 0.001  , 0.001  , 0.012  , 0.006    997.8 , 0
11 , 06 , 14 , 13 , 04 , 50 , 297.4  , 321.0  , 321.1  , 319.8  , 316.9  , 0.001  , 0.001  , 0.012  , 0.006    997.8 , 0
11 , 06 , 14 , 13 , 04 , 51 , 297.4  , 321.0  , 321.1  , 319.8  , 316.9  , 0.001  , 0.001  , 0.012  , 0.006    997.9 , 0
11 , 06 , 14 , 13 , 04 , 52 , 297.4  , 321.1  , 321.1  , 319.9  , 316.9  , 0.001  , 0.001  , 0.011  , 0.006    997.8 , 0
```

Fig.B2: housekeeping ASCII data file structure.

Fig.B3 is an example for a LIW data file (LIW).

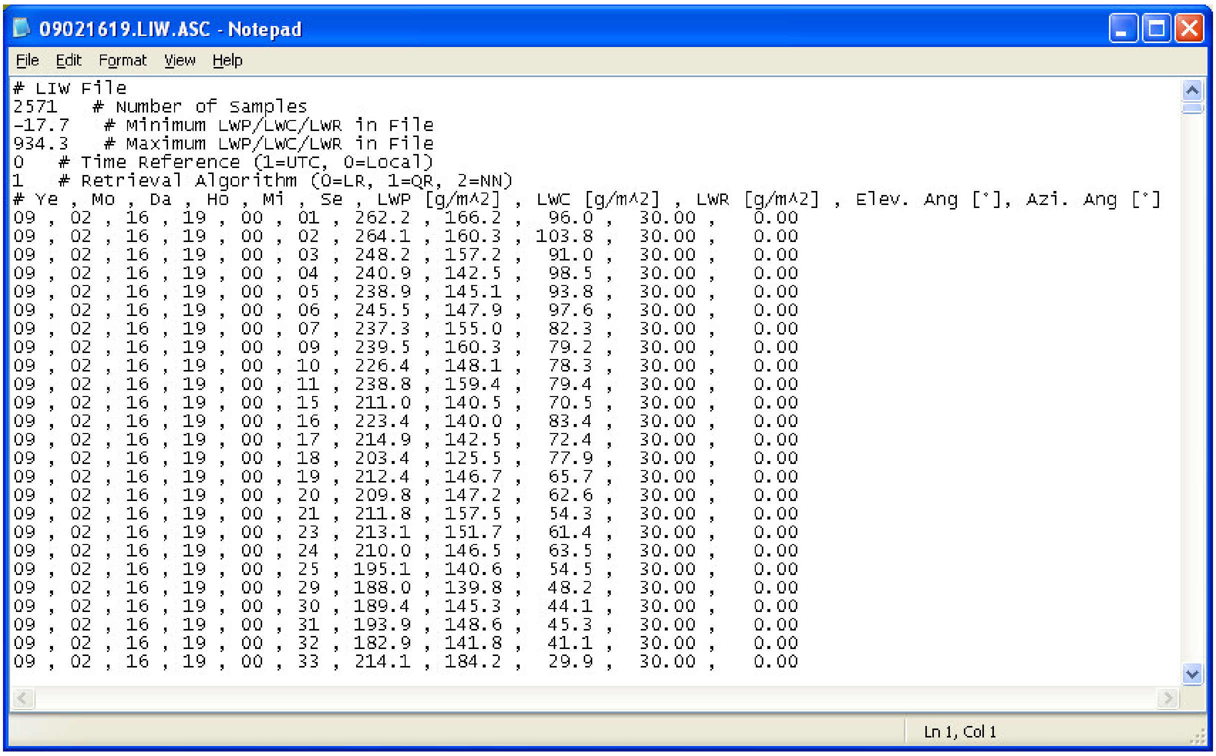

09021619.LIW.ASC - Notepad

File Edit Format View Help

```
# LIW File
2571   # Number of Samples
-17.7   # Minimum LWP/LWC/LWR in File
934.3   # Maximum LWP/LWC/LWR in File
0   # Time Reference (1=UTC, 0=Local)
1   # Retrieval Algorithm (0=LR, 1=QR, 2=NN)
# Ye , Mo , Da , Ho , Mi , Se , LWP [g/m^2] , LWC [g/m^2] , LWR [g/m^2] , Elev. Ang [°], Azi. Ang [°]
09 , 02 , 16 , 19 , 00 , 01 , 262.2 , 166.2 ,  96.0 ,  30.00 ,   0.00
09 , 02 , 16 , 19 , 00 , 02 , 264.1 , 160.3 , 103.8 ,  30.00 ,   0.00
09 , 02 , 16 , 19 , 00 , 03 , 248.2 , 157.2 ,  91.0 ,  30.00 ,   0.00
09 , 02 , 16 , 19 , 00 , 04 , 240.9 , 142.5 ,  98.5 ,  30.00 ,   0.00
09 , 02 , 16 , 19 , 00 , 05 , 238.9 , 145.1 ,  93.8 ,  30.00 ,   0.00
09 , 02 , 16 , 19 , 00 , 06 , 245.5 , 147.9 ,  97.6 ,  30.00 ,   0.00
09 , 02 , 16 , 19 , 00 , 07 , 237.3 , 155.0 ,  82.3 ,  30.00 ,   0.00
09 , 02 , 16 , 19 , 00 , 09 , 239.5 , 160.3 ,  79.2 ,  30.00 ,   0.00
09 , 02 , 16 , 19 , 00 , 10 , 226.4 , 148.1 ,  78.3 ,  30.00 ,   0.00
09 , 02 , 16 , 19 , 00 , 11 , 238.8 , 159.4 ,  79.4 ,  30.00 ,   0.00
09 , 02 , 16 , 19 , 00 , 15 , 211.0 , 140.5 ,  70.5 ,  30.00 ,   0.00
09 , 02 , 16 , 19 , 00 , 16 , 223.4 , 140.0 ,  83.4 ,  30.00 ,   0.00
09 , 02 , 16 , 19 , 00 , 17 , 214.9 , 142.5 ,  72.4 ,  30.00 ,   0.00
09 , 02 , 16 , 19 , 00 , 18 , 203.4 , 125.5 ,  77.9 ,  30.00 ,   0.00
09 , 02 , 16 , 19 , 00 , 19 , 212.4 , 146.7 ,  65.7 ,  30.00 ,   0.00
09 , 02 , 16 , 19 , 00 , 20 , 209.8 , 147.2 ,  62.6 ,  30.00 ,   0.00
09 , 02 , 16 , 19 , 00 , 21 , 211.8 , 157.5 ,  54.3 ,  30.00 ,   0.00
09 , 02 , 16 , 19 , 00 , 23 , 213.1 , 151.7 ,  61.4 ,  30.00 ,   0.00
09 , 02 , 16 , 19 , 00 , 24 , 210.0 , 146.5 ,  63.5 ,  30.00 ,   0.00
09 , 02 , 16 , 19 , 00 , 25 , 195.1 , 140.6 ,  54.5 ,  30.00 ,   0.00
09 , 02 , 16 , 19 , 00 , 29 , 188.0 , 139.8 ,  48.2 ,  30.00 ,   0.00
09 , 02 , 16 , 19 , 00 , 30 , 189.4 , 145.3 ,  44.1 ,  30.00 ,   0.00
09 , 02 , 16 , 19 , 00 , 31 , 193.9 , 148.6 ,  45.3 ,  30.00 ,   0.00
09 , 02 , 16 , 19 , 00 , 32 , 182.9 , 141.8 ,  41.1 ,  30.00 ,   0.00
09 , 02 , 16 , 19 , 00 , 33 , 214.1 , 184.2 ,  29.9 ,  30.00 ,   0.00
```

Ln 1, Col 1

Fig.B2: LIW data file structure.

Appendix C (Measurement Example)

C1. Zenith Sky Observations

When observing the sky in zenith direction, polarization splitting should be zero, even if clouds are passing the field of view. Falling rain droplets are vertically flattened, but this cannot be seen in zenith direction.

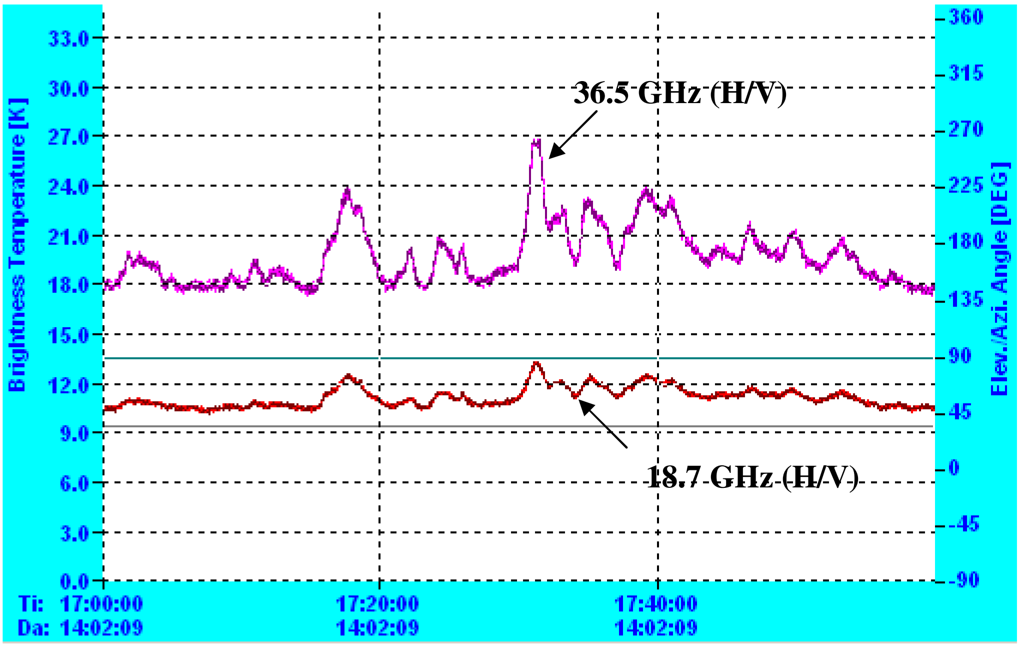

Fig.C.1.1

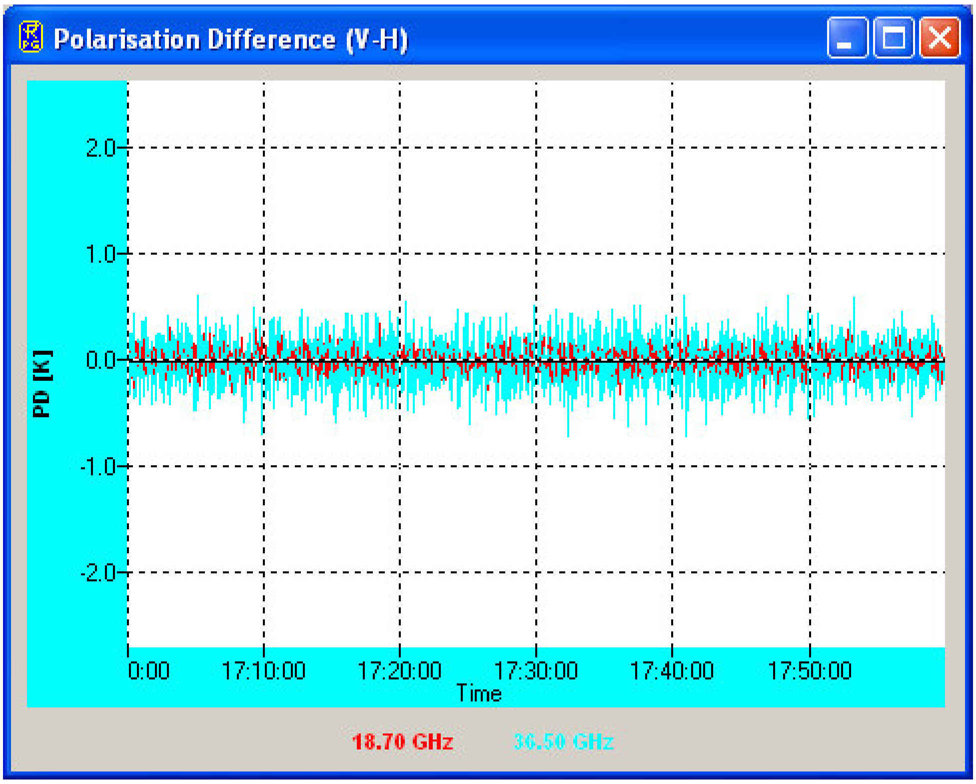

Fig.5.2

Polarisation effects due to falling rain droplets have to be observed under lower elevation angles (e.g. 30°). Therefore, by directing the radiometer to zenith, the polarization difference between V and H should vanish. Fig.C1.1 shows the TBs observed for a cloudy atmosphere and Fig.C1.2 is the polarization difference.

C2. Observations Under Low Elevation Angles

The following measurements were performed at 30° elevation angle, observing a raining atmosphere (rain rate 5 mm/h). The polarization splitting is very obvious but immediately drops down to zero, when the rain pauses.

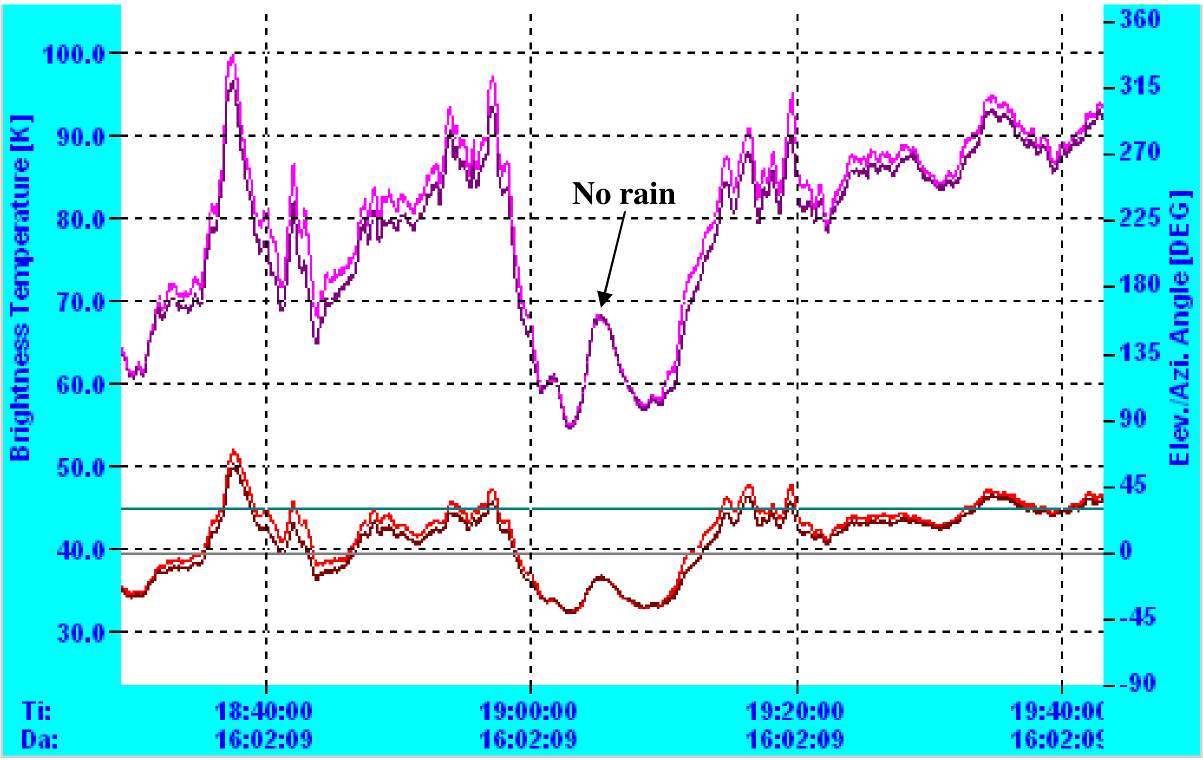

As expected, the 36.5 GHz channels respond much more sensitively to the liquid water and the polarization difference is more exaggerated. The 36.5 GHz channels are used for light rain detection while the 18.7 GHz channels cover the strong rain events with rain rates above 20-30 mm/h when the 36.5 GHz channels are starting to saturate.

Fig.C.1 shows the retrieval outputs for the Tb time series above. LWR is the liquid water content of the rain droplets, LWC denotes the cloud liquid and LWP is the total liquid water amount. The three time series are consistent even though the three quantities have been derived by three independent retrieval algorithms, one for each product.

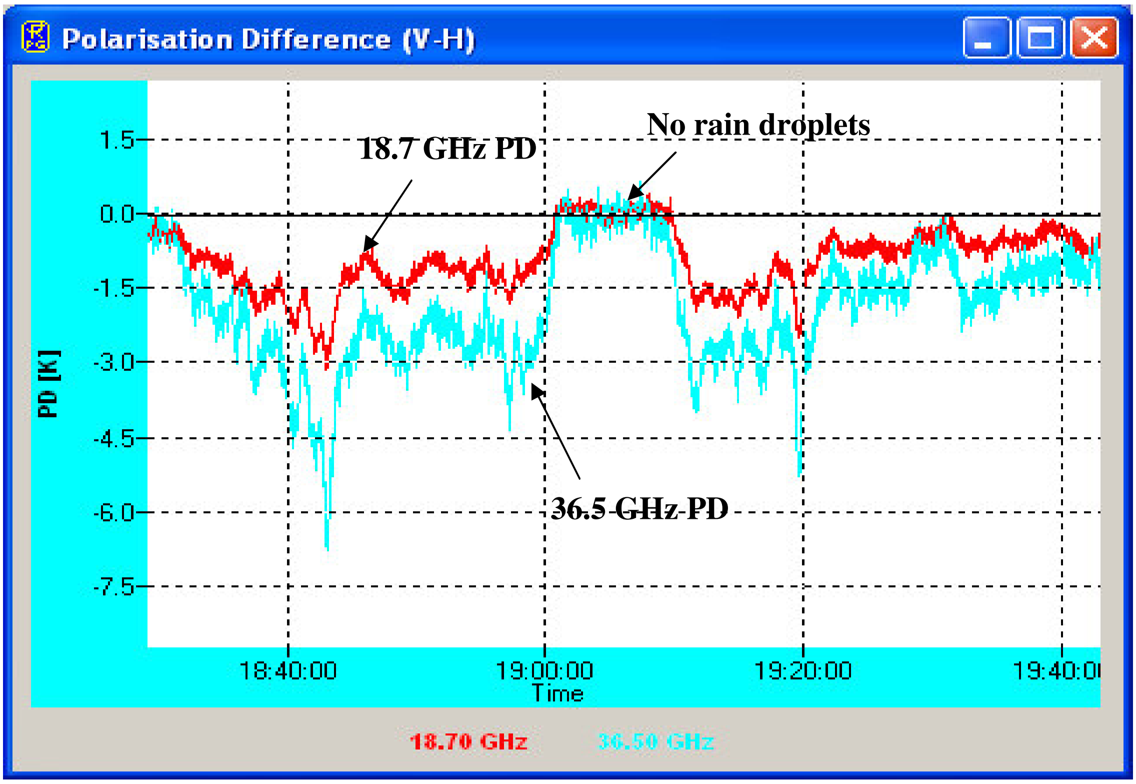

Polarisation Difference (V-H)
1.5
0.0
-1.5
-3.0
-4.5
-6.0
-7.5
PD [K]
18.7 GHz PD
No rain droplets
36.5 GHz PD
18:40:00
19:00:00
19:20:00
Time
18.70 GHz
36.50 GHz

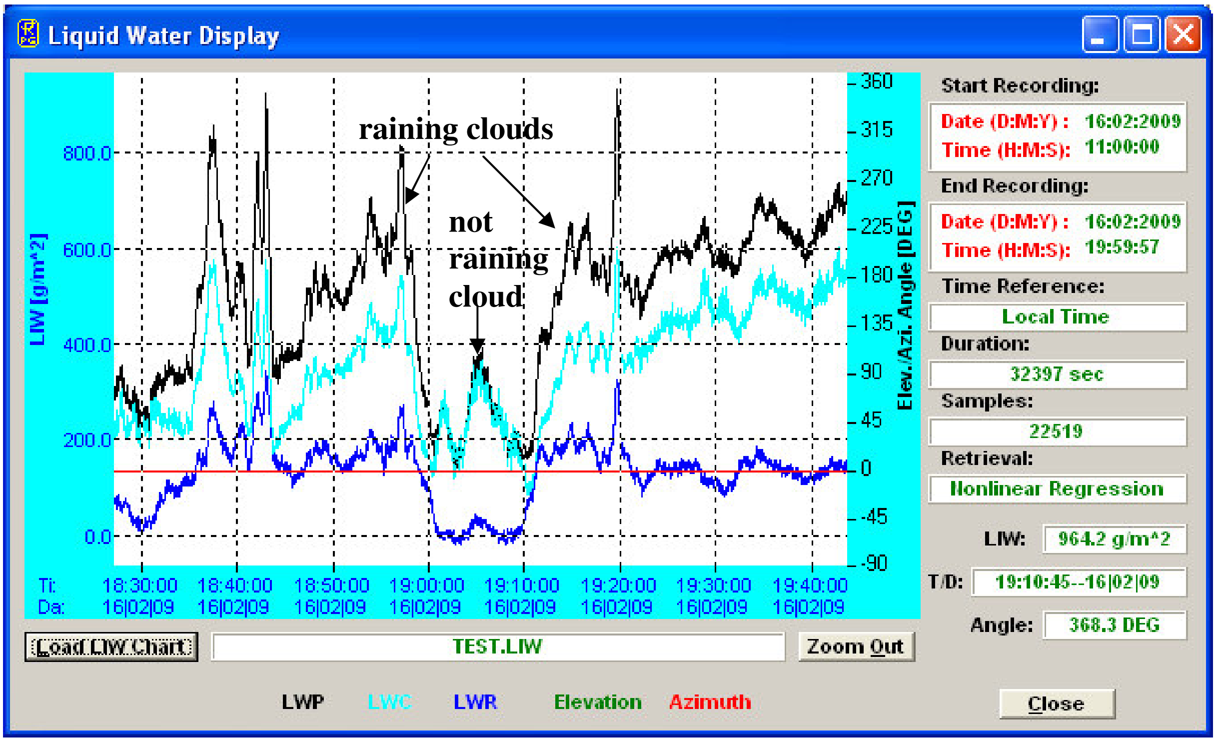

Liquid Water Display
800.0
600.0
400.0
200.0
0.0
LIW [g/m^2]
raining clouds
not raining cloud
Elev./Azi. Angle [DEG]
Ti:
Da:
18:30:00
18:40:00
18:50:00
19:00:00
19:10:00
19:20:00
19:30:00
19:40:00
16|02|09
Start Recording:
Date (D:M:Y): 16:02:2009
Time (H:M:S): 11:00:00
End Recording:
Date (D:M:Y): 16:02:2009
Time (H:M:S): 19:59:57
Time Reference:
Local Time
Duration:
32397 sec
Samples:
22519
Retrieval:
Nonlinear Regression
LIW: 964.2 g/m^2
T/D: 19:10:45--16|02|09
Angle: 368.3 DEG
Load LIW Chart
TEST.LIW
Zoom Out
LWP
LWC
LWR
Elevation
Azimuth
Close

Fig.C.1